IMPACT OF SURFACE CHEMISTRY ON ADSORPTION: TAILORING OF ACTIVATED CARBON

By

MORGANA T. BACH

A DISSERTATION PRESENTED TO THE GRADUATE SCHOOL
OF THE UNIVERSITY OF FLORIDA IN PARTIAL FULFILLMENT
OF THE REQUIREMENTS FOR THE DEGREE OF
DOCTOR OF PHILOSOPHY

UNIVERSITY OF FLORIDA

2007

To my mother and sister

ACKNOWLEDGMENTS

I thank my mom, Teresa Bach, and my sister, Rhiannon Bach, for their love and support over the many years I have pursued my academic career. I would also like to thank Link Charlott for his support and respect of my accomplishments in the academic world.

I thank David Mazyck for his support and advice for the last five years. His tendency to think "outside of the box" and his insight into the academic and business world is admirable. I consider myself lucky to have had him as an advisor and I am surely a better person for it.

TABLE OF CONTENTS

LIST OF TABLES

LIST OF FIGURES

Abstract of Dissertation Presented to the Graduate School
of the University of Florida in Partial Fulfillment of the
Requirements for the Degree of Doctor of Philosophy

IMPACT OF SURFACE CHEMISTRY ON ADSORPTION: TAILORING OF ACTIVATED CARBON

By

Morgana T. Bach

August 2007

Chair: David W. Mazyck
Major: Environmental Engineering Sciences

The present work summarizes research into the impact of the surface chemistry of activated carbon on the water treatment phenomena of pH excursions, the tailoring of activated carbon through manipulation of the dissolved oxygen (DO) content of the water used to create steam for activation, and, most importantly, the impact of these changes in surface chemistry on adsorption.

The increase in total surface acidity and some individual acidic functional groups associated with air treatments of reactivated carbons were reaffirmed as the mechanism by which pH excursions are overcome with air treatments. The proposal that carbon dioxide (CO_2) treatments overcome pH excursions via physisorption, and subsequent desorption, of CO_2 forming carbonic acid upon water immersion was supported through an analysis of mass gained during CO_2 treatment. Both air and CO_2 treatments were not found to suppress the calcium chemistry mechanism responsible for pH excursions. In a comparison of the adsorption performance of the treated carbons for 2-methylisoborneol (MIB), a common taste- and odor-causing compound, the untreated carbon removed less MIB than the air-treated carbon in water containing natural organic matter (NOM) due to decreased adsorption of the competitive NOM with the air-treated carbon related to its increased surface acidity. CO_2 treatment was proven

effective, as shown by its increased removal of MIB, as it deterred water adsorption, which is deleterious to MIB adsorption. In a comparison of adsorption performance for phenol, both the untreated and CO_2-treated carbons performed similarly while the air-treated carbon did not perform as well due to its increased surface acidity.

A novel approach to tailoring activated carbon via varying levels of DO in the water used to create steam for the activation of a wood-based precursor was evaluated using the Box-Behnken design of experiments. The statistical analysis confirmed the impact of changes in DO on the performance of the resulting carbon for adsorption of MIB and supported variation in DO as a possible means of tailoring activated carbon.

CHAPTER 1
INTRODUCTION

Adsorbents have been commonly used to solve environmental issues and researchers have delved into the mechanisms responsible for the success of a particular adsorbent. In the case of activated carbon, although the surface chemistry of activated carbon is as important as its physical properties in water treatment, only the optimization of the latter is well researched. In other words, it is known what physical properties are desired for a contaminant's removal and how to create these physical properties. On the other hand, while there are many methods to alter the surface chemistry (i.e., functional groups) of activated carbon, there are few guidelines available for its optimization, as it is not known what type of functional groups are best for a particular contaminant. Furthermore, it is not clear how to control the quantity, type, and location of these functional groups.

To elucidate the role of surface chemistry in adsorption, the present work summarizes advanced research into the impact of surface chemistry on the water treatment phenomena of pH excursions, the tailoring of the surface chemistry of activated carbon through manipulation of the dissolved oxygen content of the water used to create steam for activation, and, most importantly, the impact of these changes in surface chemistry on adsorption. By investigating not only how changes in surface chemistry are instilled into activated carbon but also the specific groups formed and any effect on adsorption, this research may be a step towards bridging the gap between potential optimization of the physical properties and surface chemistry of adsorbents.

CHAPTER 2
LITERATURE REVIEW

Activation of Activated Carbon

Activated carbon is created when a carbonaceous precursor, generally wood, peat, lignite-coal, bituminous-coal, or other material possessing relatively high carbon content, undergoes a thermal process involving pyrolysis and oxidation to increase the surface area and develop a range of pore sizes within the precursor. Pyrolysis is carried out in an inert environment, or oxygen starved, to ensure that the raw material does not gasify but rather is transformed into char. The oxidation process, or simply activation, is performed in the presence of an oxidizing gas, such as air, steam, carbon dioxide (CO_2), or a combination of these, at temperatures between 973-1173 K in order to oxidize the surface of the carbon pores and further develop the internal pore structure via gasification. In physical activation, the pyrolysis and oxidation steps are separate, while in chemical activation the two processes are combined (Snoeyink and Summers, 1999).

Gasification

Gasification by oxygen proceeds according to the reactions shown in Equations 2-1 to 2-6 (Walker et al., 1959). A free active carbon site is designated by C_f and a surface complex is designated by C(n), where n is the type of complex. The preference of the oxidation reaction for free active sites, associated with high energy edge sites, has been shown by Smith and Polley (1956) and Laine et al. (1963).

$$2C_f + O_2(g) \rightarrow 2C(O) \quad (2\text{-}1)$$

$$C(O) \rightarrow CO(g) \quad (2\text{-}2)$$

$$C_f + O_2(g) \rightarrow C(O_2) \quad (2\text{-}3)$$

$$C(O_2) \rightarrow CO_2(g) \quad (2\text{-}4)$$

$$CO(g) + C(O) \rightarrow CO_2(g) + C_f \quad (2\text{-}5)$$

$$C_f + CO_2(g) \rightarrow 2CO(g) \quad (2\text{-}6)$$

In Equations 2-1 to 2-4, gasification occurs either through evolution of carbon monoxide (CO) or carbon dioxide (CO_2) from the carbon surface. These reaction products may then react with the carbon surface (Equations 2-5, 2-6). The rate of gasification is inhibited by reactions with CO (Equation 2-5), as this causes the concentration of surface oxides available to participate in Equation 2-2 to decrease (Walker et al., 1959). The CO_2 produced may gasify the carbon surface (Equation 2-6). Indeed, CO_2 has been used as an activating agent though it does require a relatively pure quantity of this gas, which may be difficult to obtain in some areas, while air and steam are ubiquitous.

Unlike air activation, steam activation is an endothermic process that is easier to control and better suited for carbons with high surface activity (Hassler, 1974; Kirk-Othmer, 1977). Typical reaction mechanisms for steam activation are found in Equations 2-7 to 2-9 (Walker et al., 1959; Puri, 1970; Lussier et al., 1998).

$$C_f + H_2O \rightarrow C(O) + H_2 \quad (2\text{-}7)$$

$$2C_f + H_2 \rightarrow 2C(H) \quad (2\text{-}8)$$

$$CO(g) + H_2O \rightarrow CO_2(g) + H_2 \quad (2\text{-}9)$$

The initial reaction of the steam with the carbon surface where the oxygen is exchanged from the water molecule to the carbon surface to create a surface oxide (Equation 2-7), which may devolve as CO, produces hydrogen gas (Walker et al., 1959; Puri, 1970; Lussier et al., 1998). As discussed with air oxidation, the CO produced may react to decrease the rate of gasification by reacting with a surface oxide to produce CO_2. The hydrogen produced (Equation 2-7) may also react with the carbon surface to yield a surface hydrogen complex (Equation 2-8),

which inhibits the gasification reaction as this site will not react further as may a C(O) site (Walker et al., 1959; Puri, 1970; Menéndez et al., 1996; Lussier et al., 1998; Bansal et al., 2002). The reverse of Equation 2-7 may also lead to inhibition by hydrogen removing a C(O). The water-gas shift reaction (Equation 2-9) is where the water vapor is broken down to CO_2 and hydrogen gas, the products of which may either activate the surface (Equation 2-6) or inhibit gasification (Equation 2-8).

Creation of Functional Groups

Functional groups (designated here as C(n)) form on the surface of activated carbon due to the presence of heteroatoms, any atom present in the carbon structure that is not carbon or hydrogen, such as oxygen, nitrogen and sulfur. Functional groups are formed from these heteroatoms due to the activation and reactivation scheme used and exposure to the atmosphere and as such these groups are created at a variety of temperatures though there are temperatures for which groups experience optimal formation. Therefore, activation affects both the physical structure of the carbon, via gasification, and also the chemical properties of the carbon through formation of these functional groups.

The thermal stability of oxygen-containing functional groups is such that the functional groups that devolve as CO (e.g., phenolic and quinone groups) are thermally unstable at 973 K and functional groups that devolve as CO_2 (e.g., carboxylic and lactone groups) are thermally unstable at 773 K (Puri, 1970; Otake and Jenkins, 1993). This relative thermal stability is often used as a measurement of the concentration of these functional groups on the carbon surface under a process called temperature programmed desorption (TPD). During TPD, where the temperature is slowly raised to 1223 K in an inert environment, the quantities of CO and CO_2 devolved from the surface are measured and this quantity, and the knowledge of the chemistry behind the creation of the devolved gas (e.g., carboxylic groups devolve as CO_2), yields a

qualitative indicator of the functional groups on the carbon surface (Leon y Leon et al., 1992; Salame and Bandosz, 2001; Bansal et al., 2002). Fourier transform infrared spectroscopy (FTIR), which measures the absorption spectra of the carbon surface to determine individual groups, is also an available "dry" technique of evaluating functional groups. "Wet" methods are also available, such as the Boehm titration method where specific bases or acids are contacted with the carbon's surface then titrated to determine the quantity of base or acid that has reacted with the acidic or basic functional groups on the carbon surface (El-Sayed and Bandosz, 2003; Ania et al., 2004). In a study by Salame and Bandosz (2001) comparing the Boehm titration technique, TPD, and FTIR, it was determined that Boehm titration allows detection of groups of certain strength while omitting other acids and bases such as ketones, esters, and ethers. TPD, found to detect all functional groups present on the carbon surface, was limited to the broad category of CO-producing and CO_2-producing functional groups and thus this method lacks information on individual functional groups. Finally, though the FTIR method provides information on individual functional groups, they found it produced complicated information where mathematical treatments, requiring several approximations, were necessary to clarify the data.

By measuring the oxygen-containing functional groups that desorbed from carbon using TPD it was determined that the optimum temperature for chemisorption of oxygen, using air as the oxidizing agent, occurs around 673 K (Wiegand, 1937; Puri, 1970). Interestingly, the maximum capacity for a carbon to adsorb bases, or its acidic nature, has also been shown to lie close to 673 K (Puri, 1970). The fact that the maximum chemisorption of oxygen and the maximum capacity to adsorb bases occur at the same temperature has led many researchers to

the conclusion that the acidic nature of carbon is closely related to its oxygen content (Puri, 1970; Otake and Jenkins, 1993; Barton, 1997; Ania et al., 2004).

The carboxyl group (COOH) has been suggested as the oxygen-containing functional group responsible for the acidic nature of carbon by several researchers (Kruyt and de Kadt, 1931; Puri, 1970). The temperature at which these carboxyl groups were developed was 673 K in either oxygen or air. More recently, Otake and Jenkins (1993) researched air treated carbons and found a positive linear relationship between the chemisorbed oxygen concentration desorbed as a CO_2 complex, which is indicative of the presence of carboxyl groups on the carbon surface, and total acidity of the carbon. Furthermore, these authors proposed that the oxygen functional groups existing on the air-oxidized char were carboxyl groups and were formed following the mechanism of Figure 2-1.

The importance of these oxygen-containing functional groups on adsorption and their influence on the surface chemistry of activated carbon will be discussed in later sections.

Impact of Activation Parameters

The impact of the activation process on the physical and chemical properties of the carbon has been discussed in general terms but not the effect of the individual activation parameters on these properties. Activation parameters include, but are not limited to, precursor choice, type and flow of oxidant, time of activation, and temperature of activation. The following is a discussion of how and why variation of these parameters, as they are the easiest to control, can affect the resulting carbon's physical and chemical properties.

Type of Precursor

The two main groups of raw material for activated carbon are coal and biomass. Types of coals employed include anthracite, lignite, and bituminous coals (Streat et al., 1995; Zou and Han, 2001). By far the most common precursor for activated carbon used in research is coal;

subsequently, many of the theories on physical and chemical adsorption onto activated carbon are based on coal-based activated carbon and may not hold with biomass-based carbons due to the differing properties of these carbons, as discussed further in this section. Examples of biomass used as raw material for activated carbon include sewage sludge, coconut shells, coconut coir dust, fruits stones (e.g., peaches, plums, and cherries), straw, and nut shells (Gergova et al., 1994; Heschel and Klose, 1995; Streat et al., 1995; Albers et al., 2003; Rio et al., 2005; Souza Macedo et al., 2006). Various types of wood, including pine, oak, and beech have also been investigated (Heschel and Klose, 1995; Streat et al., 1995; Albers et al., 2003; García-García et al., 2003).

The drive to investigate different types of biomass as a precursor for activated carbon does not seem to lie so much in an effort to improve carbon for the removal of a specific compound or water matrix as much as it is an economic or environmental consideration. For example, a study pertaining to the use of pine as a source of activated carbon was prompted by the use of pine as an energy source in the study area, due to the lack of other available energy sources such as coal (García-García et al., 2003). The large supply of char remaining after burning of the pine prompted the investigation into use of this raw material for activated carbon, which could then be sold for an economic benefit. The use of a waste product to create an economically and environmentally useful product is what has prompted the study of sewage sludge, coconut shells (due to local abundance in tropical countries), fly ash from power plants, straw, and used tires, as these wastes would either be incinerated or placed in a land fill in most circumstances (Streat et al., 1995; Rio et al., 2005; Sarkar et al., 2006; Souza Macedo et al., 2006).

A successful carbon in these studies is one that performs as well as traditional carbons in removal of a target compound. These studies employ a number of raw materials and evaluate them based on either adsorption performance or a common method of indicating performance, such as pore size distribution, and they may also analyze the effect of varying activation parameters on the properties of the resulting carbon (Streat et al., 1995; García-García et al., 2003; Rio et al., 2005). For example, Heshel and Klose (1995) employed several agricultural by-products (e.g., fruit stones, nut shells, and wood) to determine the type of raw material that produced the highest quality activated carbon. High quality was defined as a carbon that was abrasion resistant, having low macroporosity (i.e., few large pores), and having high carbon yield, where the latter relates to the quantity of carbon lost during activation. The authors concluded that the highest quality carbon from agricultural by-products was produced from coconut shells, followed by peach stones, plum stones, hazelnut shells, walnut shells, and cherry stones. The authors indicate that a large pore size in the raw material leads to large pores in the carbon. The wood based carbons had higher porosity than either the nut shells or the fruit stones and this led to decreased abrasion resistance.

Heshel and Klose (1995) found that the yield of carbon correlated with the O/C atomic ratio in the carbon. The authors concluded that the morphology of the raw materials determines several important properties of carbon due to the cross-linking cellulose and lignin molecules. A study by Albers et al. (2003) using wood and coconut shells as the raw material demonstrated from scanning electron microscope (SEM) pictures that the inherent structure of the raw material is present even after pyrolysis. Gergova et al. (1994) and Khezami et al. (2005) observed the same phenomenon of a woody structure that is preserved and becomes visible after the high temperatures employed in pyrolysis. Even at the atomic level, differences in the graphite

structure of activated carbons are apparent based on the raw material employed (Albers et al., 2003).

Gergova et al. (1994) also note that lignin and cellulose in the raw materials of agricultural waste may affect porosity development which may relate to the finding of Hershel and Klose (1995) that the O/C atomic ratio plays a role in char yield. Heschel and Klose (1995) and Khezami et al. (2005) note that lignin as a source of activated carbon produces the highest char yield, which may relate to porosity and the fact that lignin has a lower oxygen content than cellulose. These studies highlight the importance of the choice of raw material when creating activated carbon.

Type of Oxidant

Examples of oxidants that may be used in the thermal activation process include air (C-O_2), steam (C-H_2O), carbon dioxide (C-CO_2), or a combination of these. While use of either oxidant to oxidize the surface of carbon, and thereby improve its surface area, will produce an acceptable activated carbon, there are advantages and disadvantages to each oxidant.

Walker et al. (1959) indicates that the activation energy for C-O_2 is less than C-H_2O which is in turn less than C-CO_2. This is due to the activation energy being determined by either the adsorption (e.g., creation of C(O)) or desorption (e.g., evolution of CO(g)) step. The C-O_2 adsorption step is much more exothermic than the C-H_2O adsorption step and due to this exothermic reaction the lifetime of the functional groups on the C-O_2 reacted carbon may be short. Given that the desorption of the surface oxide created by the C-O_2 reaction occurs relatively quickly, the activation energy for C-O_2 is determined by the adsorption step. The C-H_2O and C-CO_2 adsorption step, having a lower exothermic nature, may have a longer lifetime for its adsorbed group so that desorption is the rate limiting step. However, while C-O_2 may require lower activation energy, energy is released during the reaction of air with the carbon such

that control of the process may be difficult and generally is better suited for low activity carbons (Walker et al., 1959; Kirk-Othmer, 1977).

The literature is rife with comparisons of C-CO_2 versus C-H_2O activations. Tomków et al. (1977) investigated the porous structures of carbons resulting from C-O_2, C-H_2O, and C-CO_2 and concluded that C-H_2O created a higher distribution of pores of different sizes due to the progressive widening of pores once they are formed. C-CO_2 activations yielded mainly micropores (i.e., pore openings smaller than 2 nm) suggesting a higher occurrence of pore creation rather than pore widening. These findings were supported by Ryu et al. (1993). However, Wigmans (1989) found the opposite trend to Tomków et al. (1977) where C-CO_2 produced widening of micropores to mesopores (i.e., pore openings between 2-50 nm). Alcaniz-Monge et al. (1994) and Rodríguez-Reinoso et al. (1995) worked to clarify this apparent contradiction by investigating the difference in the gases' diffusion and accessibility to the pores. Interestingly, at low burnoffs (e.g., low levels of gasification) the results of Wigmans (1989) were confirmed by Alcaniz-Monge et al. (1994), where the C-H_2O showed a higher production of micropores, though at higher burnoffs the C-CO_2 had a higher concentration of micropores confirming the results of Tomków et al. (1977). Overall, however, the authors surmised that Tomków et al.'s (1977) view of pore formation dominated and this was attributed to the difference in diffusion of the CO_2 and steam molecules.

Walker et al. (1954) found that the order of reaction rates were such that the rate of C-H_2O progressed at approximately three times the rate of C-CO_2 and the rate of C-O_2 progressed at several orders of magnitude faster than both C-H_2O and C-CO_2. Later studies further confirmed that C-CO_2 gasification is slower than that of steam gasification likely due to the faster diffusion rate of the H_2O molecule (Ryu et al., 1993; Alcaniz-Monge et al., 1994; Walker

et al., 1996). Rodríguez-Reinoso et al. (1995) used the relative reaction rates of C-H_2O and C-CO_2 to clarify the impact of burnoff on the development of pores with steam and carbon dioxide. Carbon dioxide reacts first to create and widen narrow micropores so that at low burnoff the micropores will dominate. Given further burnoff (i.e., further opportunity for the CO_2 to react with the carbon), the narrow micropores will become mesopores and macropores (i.e., pores greater than 50 nm) which yields a more diverse pore structure. Steam, on the other hand, reacts to continually create and then expand micropores so that micropores do not remain intact very long due to the higher reaction rate of C-H_2O.

Another possible explanation proposed by Rodríguez-Reinoso et al. (1995) was that C-CO_2 created a higher number of oxygen containing functional groups, located on the openings of the pores, and that these groups, being more thermally stable than those produced by steam activation, would close the pores to further diffusion of carbon dioxide which would have allowed for pore widening. Later work by these authors (Molina-Sabio et al., 1996) supported this hypothesis. Walker et al. (1996) also suggests that hydrogen is a greater inhibitor in the steam reaction (Equation 2-7) which limits the creation of pores and would explain the decrease in micropore formation. Regardless of the explanation, the conclusion is that steam activation yielded a wider pore size distribution than activation with carbon dioxide (Tomków et al., 1977; Alcaniz-Monge et al., 1994; Rodríguez-Reinoso et al., 1995; Molina-Sabio et al., 1996; Walker et al., 1996). While micropores are preferred for the adsorption of some small molecules, it is generally considered advantageous to have a wide pore size distribution as the larger pore sizes act as "roadways" by which the target molecule can travel to its final adsorption site (Tennant and Mazyck, 2003). To this end, steam activation is often employed.

In terms of activation with oxygen, Tomków et al. (1977) determined that these carbons have a high development of pores but only at low burnoff and this was related to the blocking of the pores due to creation of functional groups at the edge of the pore openings. All carbons activated with oxygen in this study were found to have a higher concentration of polar centers than either the C-H_2O or C-CO_2 carbons, which is related to the influence of oxygen-containing functional groups on polarity. In addition, at higher temperatures, where these oxygen-functional groups would be expected to devolve (i.e., be removed from the carbon surface), the pore structure resulting from C-O_2 is improved.

Time, Temperature, and Oxidant Flow

Gergova et al. (1993) evaluated the effect of activation temperature and activation time on the functional groups created during steam activation of several different types of agricultural precursors. The trends indicate an increase in the quantity of oxygen-containing functional groups with treatment time, from 1 to 3 hrs, at lower temperatures (873 K) and a decrease in these groups with an increase in treatment time at higher temperatures (973 K), though this trend was not true of all precursors. This relates to the degradation of functional groups at higher temperatures and the limited creation of new functional groups to replace the ones lost, a finding supported by Arriagada et al. (1997).

All carbons in Gergova et al.'s (1993) study showed a decrease in solid yield, the mass of carbon remaining after activation, with an increase in activation time and temperature. Given the nature of the gasification reaction, it is anticipated that with higher temperature, which would speed gasification reactions, and longer treatment time, which would allow more gasification to occur, that the solid yield would decrease and this is supported in many studies (Gergova et al., 1993; Gonzalez et al., 1994; Rodríguez-Reinoso et al., 1995; Gergova et al., 1996; Martin-Gullon et al., 1996; Tennant and Mazyck, 2003). As the degree of gasification increases with an

increase in temperature and treatment time, there is also generally an increase in the volume of pores and also the surface area within the carbon due to the removal of carbon atoms from the carbon surface to create new pores and higher surface area (Gergova et al., 1994; Centeno and Stoeckli, 1995; Rodríguez-Reinoso et al., 1995; Gergova et al., 1996; Mazyck and Cannon, 2002; Zhang et al., 2003). However, overactivation can occur at high temperatures and or treatment time as external mass loss exceeds internal mass loss, where pores are developed, and/or the walls of pores begin to collapse (Gergova et al., 1994; Tennant and Mazyck, 2003; Mackenzie et al., 2005).

Gonzalez et al. (1994) found that the rate of steam flow did not significantly affect the resulting micropore and mesopore formation in activated carbon and that low temperatures favored the widening of narrow micropores. Mazyck and Cannon (2002) also observed that steam flow had no impact on pore size distribution. Gonzalez et al. (1994) indicate that, though an increase in gasification rate has been observed with an increase in the flow of carbon dioxide due to the presence of a concentration gradient which compels the oxidant to enter the pores at a faster rate (i.e., bulk diffusion), the increase in steam flow yields more water vapor on the particles' outer surface resulting in mass loss and/or the creation of macropores. Martin-Gullon et al. (1996) further this theory by suggesting that the inhibiting factors produced by gasification (CO and H_2) (Equation 2-5 and 2-7, respectively) would dilute the steam on the internal portions of the carbon thus leaving the highest concentrations of pure steam on the external surface of the particle which would lead to external gasification rather than internal. The dilution theory was supported by Arriagada et al. (1997).

Rodríguez-Reinoso et al. (1995), however, found that at lower temperatures the steam flow had no effect while at higher temperatures the rate of steam flow yielded an increase in

gasification. An increase in the volume of mesopores with an increase in steam flow was also observed by Martin-Gullon et al. (1996). Rodríguez-Reinoso et al. (1995) clarified this contradiction by noting that at higher temperatures the inhibiting effect of the hydrogen formed during gasification (Equation 2-7) is less effective. As steam flow is increased one would anticipate that more oxidant will react with the carbon; however, at lower temperatures, the increase in steam flow yields a corresponding increase in the amount of hydrogen produced by the reaction of Equation 2-7 which would inhibit reactions so that similar quantities of gasification would occur regardless of the increase in oxidant. At higher temperatures, where the gas-water shift is less efficient, an increase in oxidant would indeed yield an increase in oxidation without as significant an affect of hydrogen inhibition.

Adsorption

Physical Adsorption

Adsorption of a substance onto activated carbon in water occurs when the substance is concentrated more on the surface of the activated carbon than it is in the bulk solution. The substance that accumulates is called the adsorbate and the activated carbon is termed the adsorbent. Physisorption, or physical adsorption, occurs when the accumulation results from dispersion forces while chemisorption, or chemical adsorption, results from an exchange or sharing of electrons between the adsorbate and the surface of the activated carbon. The properties of activated carbon that make it ideal as an adsorbent are a significant surface area to which the adsorbate may accumulate and an extensive internal pore structure in which the adsorbate may become trapped, thus encouraging its accumulation.

The rate of removal, or adsorption kinetics, is governed by the rates of the four steps composing physical adsorption. The first step, bulk transport, where the adsorbate moves from the bulk solution to the boundary layer of the adsorbate, is encouraged by the turbulent flow

surrounding the activated carbon. Film resistance to transport follows bulk transport and involves the transport of the adsorbate through the stationary layer of water surrounding the adsorbent. Film resistance may also be minimized by increased flow rate past the adsorbent. The third step is internal pore transfer where the adsorbate travels through the adsorbent's pores via surface or pore diffusion to existing adsorption sites. Internal pore transfer is often the rate-limiting step as the final step, physical adsorption, occurs almost instantaneously, so it has little effect on the rate of the overall reaction (Snoeyink and Summers, 1999). The rate of adsorption, therefore, is influenced by the same variables affecting diffusion rate, including the concentration gradient and the temperature of the system (Bansal et al., 1988).

The relative hydrophobicity of the adsorbate can be a driving force for its accumulation on the adsorbent. Thus, the adsorption of a substance generally decreases with increased contaminant solubility in water (Snoeyink and Summers, 1999). The pore size of the activated carbon also plays a major role in adsorption as, for example, a large natural organic matter (NOM) molecule will be unable to fit into small pores (i.e, micropores). An activated carbon with a large volume of mesopores and macropores would be better suited for NOM removal (Newcombe, 1999). Conversely, a larger microporous volume is generally preferred when the target compound is a small molecule. However, an increase in mesopores can be associated with an increase in adsorption of small molecules (Tennant and Mazyck, 2003, Nowack et al., 2004; Rangel-Mendez and Cannon, 2005) though the mesopores may not be the final adsorption sites for the compound (for example 2-methylisoborneol (MIB)). The mesopores simply serve to aid in diffusion of the target compound through the pores to their final adsorption sites, likely micropores. It is common knowledge that mesopores aid in diffusion particularly in fine powders and that the adsorption of small molecules is most effective in micropores due to the

greater number of contact points between the molecule and the adsorbent (Suzuki, 1990; Pelekani and Snoeyink, 1999; Quinlivin et al., 2005; Rangel-Mendez and Cannon, 2005).

Effect of Surface Chemistry on Adsorption

While general trends related to strictly physical adsorption have been discussed, the impacts of surface chemistry on adsorption must also be discussed, as there are cases where it is the chemical properties of the activated carbon that dominate adsorption rather than its physical properties.

The addition of oxygen to the surface of an activated carbon has been shown to alter its wettability, catalytic and electronic properties, as well its adsorption capabilities (Puri, 1970; Bansal et al., 2002; Szymański, 2002). Acidic oxygen-containing functional groups are mainly present on the outer surface or edge of the basal plane due to limited diffusion into the micropores (Puri, 1970; Menendez et al., 1996; Ania et al., 2004). As these outer sites constitute the majority of the adsorption surface, the concentration of oxygen on the surface has a great impact on the adsorption capabilities of the carbon (Puri, 1970).

The presence of oxygen imparts a polar nature to the activated carbon, which results in a preference for removal of the more polar component of a solution, e.g., H_2O (Kipling and Gasser, 1960). El-Sayed et al. (2003) found that the adsorption of valeric acid onto activated carbon decreased as the density of acid groups on the surface increased. These authors suggested that the polar nature of the activated carbon surface, associated with its high surface oxygen group content, resulted in the preferential adsorption of water molecules. In addition, the presence of carboxylic groups acted as physical obstacles to the interaction of the valeric acid and the activated carbon surface. Bansal et al. (2002) also attributed the decrease in phenol adsorption with increased oxidation of activated carbon to the increasing hydrophilic character of

the oxidized carbons. Ania et al. (2004) found a decrease in the adsorption of salicylic acid as the oxygen-containing functional groups increased at low adsorbate concentrations. At high levels of salicylic acid, however, the study found that the adsorption capacity of the carbon was similar to an activated carbon that had not been oxidized and these authors proposed that the higher concentration of valeric acid allowed the water molecules adsorbed onto the hydrophilic carbon sites to be displaced.

Pendleton et al. (1997) researched the effects of surface chemistry on the adsorption of MIB and linked decreased adsorption with an increase in the hydrophilic nature of the oxidized carbon. They also found a strong correlation (R^2=0.99) between oxygen content and the number of hydrophilic sites. A subsequent study by the same research team (Considine et al., 2001) further supported the link between oxygen content and decreased adsorption of MIB. In this study, the adsorption of MIB in a dichloromethane solvent, a non-polar solvent, was investigated as opposed to previous experiments in water. The results showed that adsorption of MIB was independent of oxygen content in this solvent, further supporting the contention that adsorption of water as a result of surface oxidation impedes MIB adsorption.

Karanfil and Kitis (1999) found that surface oxidation, and the resulting density of strong acid functionalities, decreased the adsorption of dissolved organic matter (DOC) (the dissolved portion of NOM). Water clusters forming around the polar (hydrophilic) functional groups on the surface reduced the ability of the DOC to reach the smaller pore sizes needed for its adsorption.

The chemisorption of oxygen and the resulting functional groups have also been found to destroy delocalized π-electrons due to electron localization (Leon y Leon et al., 1992; Ania et al., 2004). The adsorption of phenol has been attributed to the electron-donor acceptor complexes

formed between the delocalized electrons on the basal planes on the surface of the carbon and the aromatic ring of the phenol (Bansal et al., 2002; Ania et al., 2004). A decrease in phenol adsorption on oxidized samples has been shown by a number of researchers (Bansal et al., 2002; Ania et al., 2004). As the bonding sites are destroyed through chemisorption of oxygen, the adsorption of phenol decreases (Ania et al., 2004). Pereira et al. (2003) performed a study on an acidic anionic dye, where the presumed adsorption mechanism involved the delocalized π-electrons of the carbon surface and the free electrons of the dye molecule, and found that the adsorption of the anionic dye was hindered by the presence of acidic oxygen-containing functional groups on the surface of the activated carbon. It should be noted that, in addition to both the increased hydrophilicity and the destruction of π-bonds, the formation of acidic-oxygen containing functional groups create a weakening in the donor-acceptor (acid/base) adsorption mechanism (Ania et al., 2004).

Current Uses of Activated Carbon

Following activation, the carbon may be distributed as either powdered activated carbon (PAC) or granular activated carbon (GAC). PAC is activated carbon ground in various types of mills so that 65-90% passes through a number 325 mesh (45μm) sieve while GAC consists of any larger activated carbon particles and is the portion of activated carbon used in the packed bed contact basins of water treatment plants. GAC can be used as a substitute for typical granular filter media, in that it removes suspended matter, though through adsorption GAC is also capable of removing organic compounds such as synthetic organic chemicals (SOCs), NOM, and taste and odor causing compounds (Gerber, 1968; Frederick et al., 2001a; Bansal et al., 2002).

SOCs, such as most pesticides, may be contaminants in both ground and surface water. SOCs at chronic exposure levels may cause neurological and kidney effects and, for some pesticides, cancer (Hammer and Hammer, 2001). One common organic compound that is

targeted for removal by activated carbon is phenol which can be both manufactured and naturally occurring and is relatively common in the environment due to discharge from industries such as those producing plastics (Jung et al., 2001; Bansal et al. 2002).

NOM, a mixture of fulvic, humic acids, hydrophilic acids, and carbohydrates, can impart color to water and may also react with chlorine, added for disinfection purposes, to create disinfection by-products (DBPs). DBPs, such as chloroform, a trihalomethane, are considered carcinogenic (Bull et al., 1982). It is, therefore, important to reduce the NOM concentration in the water before disinfection with chlorine occurs. Adsorption of NOM onto GAC is enhanced if calcium complexes with the NOM prior to adsorption by activated carbon (Frederick et al., 2001a).

Taste and odor causing compounds, the removal of which constitutes the primary reason water treatment utilities use activated carbon, may result from biological growth or industrial activities. An example of a taste and odor causing compound resulting from biological growth is 2-methylisoborneol (MIB), which can be produced by cyano-bacteria, or blue-green algae (Gerber, 1968). MIB, described as having an earthy-musty odor, enters a water treatment plant when the source water is surface water experiencing a bloom in the growth of the MIB producing organism. If occurrences of MIB are relatively short in duration PAC may be used as an additive during water treatment rather than a permanent GAC filter.

Reactivation of Activated Carbon

During normal use, activated carbon will eventually become saturated with adsorbates so that the treated water exceeds the desired level of adsorbate removal, or reaches breakthrough. At this point, the spent activated carbon can be reactivated to restore the adsorption capacity of the GAC so that it can be reused rather than simply disposed of and replaced with virgin GAC.

The time to breakthrough for a GAC bed can range from about 6 months to 5 years, depending on the type of adsorbate, the influent concentration, and the desired treatment level (Kawamura, 2000).

Thermal or chemical regeneration may be employed, though thermal reactivation is the most commonly employed scheme. Thermal reactivation consists of four steps: drying, desorption, pyrolysis, and gasification. The drying process removes water and some highly volatile adsorbates. At higher temperatures, thermal desorption occurs with vaporization of volatile adsorbates and decomposition of unstable adsorbates to more volatile components. A pyrolytic process follows using high temperatures, between 923-1123 K, in an inert environment that converts heavy or non-volatile adsorbates to char. The final step, gasification at temperatures above 973 K in steam, CO_2, or a combination of both, involves desorption of the vapors and gaseous products of char and their exit from the pores of the reactivated carbon (Clark and Lykins, 1989; Cannon et al., 1993; Snoeyink and Summers, 1999).

Reactivation has several effects on the activated carbon, aside from the intended effect of, ideally, restored adsorption capacity. Mass loss during the activation process may range from 10-15% of the original GAC and is the result of loss through the transfer of GAC from the treatment site to the regeneration site and/or burning of the GAC during reactivation (Clark and Lykins, 1989). The loss is compensated for by the addition of virgin GAC before the reactivated GAC is returned to service. The surface chemistry of the activated carbon is also affected by reactivation as most oxygen-containing functional groups are stripped during reactivation at temperatures greater than 973 K and in an inert environment (Menendez et al., 1996; Pereira et al., 2003).

Inorganic molecules, such as calcium, may be adsorbed during normal operation of a GAC filter and are not removed during the activation or reactivation processes. The inorganic molecules remaining on the surface of the reactivated carbon prevent these adsorption sites from being freed for further adsorption and thus compromise the ability of the reactivation process to restore the adsorption capacity of the carbon (Clark and Lykins, 1989). One well-documented effect of calcium presence in the reactivation process is calcium catalysis (Knappe et al., 1992; Cannon et al., 1993; Mazyck and Cannon, 2000, 2002). Calcium catalysis increases the number of active sites on the surface of the carbon rather than, in the traditional sense of a catalyst, reducing the activation energy. Calcium catalyzes the gasification step of reactivation and is characterized by increased mass losses during the reaction process and pore enlargement (Knappe et al., 1992). As discussed previously, the pore size of the activated carbon can affect its ability to adsorb certain compounds, and an increase in pore size may make it unsuitable for certain applications. There is also cost associated with the addition of virgin GAC to replace the increased mass lost during the reactivation process.

Another result of reactivation is the incidence of pH excursions, an increase in the pH of treated water when reactivated carbon is returned to service (Farmer et al., 1996; Farmer et al., 1998). The duration and extent of the pH excursion will determine its impact on the system.

pH Excursions in Water Treatment

Many water and wastewater utilities have found that when thermally reactivated GAC is returned to service, the pH of the subsequently treated water is elevated (e.g., pH > 9) for days or even weeks (Mazyck et al., 2005). Water with high pH levels is unfit for distribution to customers, as it exceeds the United States Environmental Protection Agency secondary standards of the National Secondary Drinking Water Regulations ($6.5 < pH < 8.5$) and could also bring about calcium carbonate ($CaCO_3$) precipitation problems in distribution systems.

A water utility in the Virginia-American Water Company, under the umbrella of the American Water Works Company, measured increases in pH in their backwash water when a reactivated GAC was placed back in service (Figure 2-2). These data are representative of a full-scale GAC filter bed adsorber. As shown, the reactivated GAC posed an adverse effect on water quality in that it elevated the filter bed adsorber's effluent pH to greater than 11. Even after 6 days, the pH was still above 8.5. Note that the pH of natural water is approximately 7.

In addition to the pH, the water utility also measured the concentration of calcium in the effluent for two days. As shown in Figure 2-2, as the calcium concentration decreased, the water pH likewise decreased. The influent calcium concentration in their backwash water was relatively constant over the two days. No other operational changes could have contributed to the higher Ca^{2+} and OH^- levels; these results are fairly typical, as reported by American Water Works Company personnel. These results led to the hypothesis of a calcium chemistry mechanism proposed by Mazyck et al. (2005) and discussed further below.

pH Excursion Mechanisms for Activated Carbons

A mechanism involving anion exchange with hydroxide ions following carbon protonation has been proposed by Farmer and coworkers to explain pH excursions (Carr and Farmer, 1995; Dussert et al., 1995; Farmer et al., 1996). These authors suggested that pH excursions are a function of the carbon surface that is altered during high temperature activation or reactivation. Activated carbons exposed to high temperatures in a reducing atmosphere during manufacturing and reactivation tend to adsorb strong acids in water. Garten and Weiss (1957) classified these as H-type carbons. In contrast, L-type carbons are those produced by surface oxidation; these are known to adsorb strong bases in water. Farmer et al. (1996) argued that this acid adsorption during water treatment might involve the protonation of pyrone-type surface groups or other similar functionalities on the carbon surface, in agreement with Leon y Leon et

al. (1992). In addition, they suggested that loading the carbon with sulfate, chloride, or other anions that are present in water could neutralize the positive charge on the carbon surface. Furthermore, they proposed that this charge neutralization could also occur through an anion exchange process involving sulfates and hydroxides on the carbon surface. In other words, they surmised that the carbon could adsorb sulfates or other anions from water while releasing hydroxyls, and that this ion exchange process could cause the pH to rise. Farmer et al. (1996) did acknowledge that this anion exchange mechanism requires additional testing and confirmation. To date, however, there has been no further evaluation by these authors presented in the literature that would either prove or disprove their hypothesis.

Dussert et al. (1995) supported this anion exchange mechanism because they found no significant pH excursion when virgin GAC was immersed in Milli-Q (anion-free) water, and they concurred that anions were required to trigger a pH effect. These authors came to their conclusions after studying virgin GACs that removed 2 to 9 mg of sulfate/g GAC. In Milli-Q water spiked with 80 mg sulfate/L, they measured the water pH and sulfate capacity for several virgin carbons. Not only did they find that pH excursions only occurred when anions such as sulfate were present, but they also reported that, as the sulfate capacity increased, pH also increased. In their study, the carbons that did not exhibit pH excursions also did not significantly remove sulfate ions from solution (< 0.7 mg/g). They also found that sulfate (SO_4^{2-}) removal was greater than nitrate (NO_3^-) or chloride (Cl^-) removal. They did not measure calcium concentrations for their carbons; however, they did find that the ash content of the carbon could not be correlated with pH excursions.

To discern if an anion exchange mechanism was also valid in describing pH excursions with reactivated GAC, Mazyck et al. (2005) tested reactivated carbons under conditions similar

to those used by Dussert et al. (1995) to support an anion exchange mechanism. According to the anion exchange mechanism supported by Dussert et al. (1995), the sulfate uptake should be highest when there is a high pH excursion. The data of Mazyck et al. (2005) demonstrated an opposite trend where, as the pH excursions of the reactivated GAC increased, the sulfate uptake decreased. For example, at a water contact pH, a predictor of pH excursions, of 8.75 the sulfate uptake was 1.4 mg sulfate/g GAC while at a water contact pH of 10.6 there was no measurable sulfate uptake. In addition, pH excursions were found to occur even in Milli-Q water, where sulfate ions were not present suggesting that anions are not responsible for the observed pH excursions with reactivated GAC. In light of these results, Mazyck et al. (2005) concluded that the uptake of sulfate and the subsequent release of hydroxyl ions (i.e., an anion exchange mechanism) was not responsible for the observed pH excursions with reactivated GACs.

The observation of a relationship between calcium and pH excursions, shown in Figure 2-2, led to a hypothesis by Mazyck et al. (2005) of a calcium chemistry mechanism behind pH excursions. During potable water treatment, water-soluble calcium can adsorb onto GAC as a complex with NOM (Nowak and Cannon, 1997; Nowak et al., 1999; Frederick and Cannon, 2001; Frederick et al., 2001a, 2001b). Moreover, calcium is abundant in many coal-based carbons. Thermal reactivation of spent GAC at temperatures above 1123 K decomposes the oxygenated functionality of the NOM that complexes with calcium. This process results in the formation of CaO, which is thermodynamically the most stable species at these high temperatures (Mazyck and Cannon, 2000). When the reactivated carbon is returned to service, the calcined CaO can react with water to form $Ca(OH)_2$ (Equation 2-10). Furthermore, $Ca(OH)_2$ can dissolve and subsequently dissociate as Ca^{2+} and $2OH^-$ (Equation 2-11). The release of OH^- would elevate the pH of the subsequently treated water.

$$CaO + H_2O \rightarrow Ca(OH)_2 \quad (2\text{-}10)$$

$$Ca(OH)_2 \rightarrow Ca^{2+} + 2OH^- \quad (2\text{-}11)$$

Calcium chemistry and thermodynamics as related to GAC and thermal reactivation have been previously discussed in the literature at length (Cannon et al., 1994; Mazyck and Cannon, 2000, 2002). Therefore, it was proposed that the manner by which the reactivated GAC was contributing both calcium and hydroxyl ions to the water was via the mechanisms described in Equations 2-10 and 2-11 above. Furthermore, it was rationalized that the deviation from a $[OH^-]$ (molar concentration of hydroxyl ions) to $[Ca^{2+}]$ (molar concentration of calcium ions) ratio of 2, is caused by the OH^- that originated from $Ca(OH)_2$ being consumed to some extent by the natural buffering capacity of the water. Thus, the data from the Virginia-American Water Company (Figure 2-2) could be taken as a semi-quantitative example of the mechanisms described in Equations 2-10 and 2-11.

In further support of the calcium chemistry mechanism, a significant correlation was found between pH and calcium present in solution and altering the reactivation process to avoid the creation of calcium species that will participate in the proposed calcium chemistry, using a reactivation scheme proposed by Mazyck and Cannon (2000, 2002), was found successful in overcoming pH excursions (Mazyck et al., 2005). Both of these finding supported the hypothesis of the calcium chemistry mechanism dominating pH excursions with reactivated carbons.

Methods to Overcome pH Excursions

The three broad categories of methods to overcome pH excursions are on-site treatments, tailoring of the reactivation process, and post-reactivation treatments performed before the reactivated GAC is returned to service.

One on-site method that would occur prior to reactivation is the reduction of the calcium adsorbed onto the activated carbon during water treatment. To achieve this, either the NOM complexes with a stronger cation, thus out-competing calcium, or the calcium-NOM complex is removed before it comes into contact with the GAC. The use of an iron coagulant would be ideal as it could facilitate both of the above goals. Iron (Fe^{3+}) is a stronger cation than calcium and would displace the calcium from the NOM though competition with NOM by hydroxyl species may hinder the process near a neutral pH. Nowack et al. (1999) proposed that, at near neutral pH, soluble iron hydroxide would precipitate depleting the amount of iron available for further reactions with NOM. The iron would also coagulate the calcium-NOM complexes already formed and this floc would be allowed to settle out before reaching the GAC. Nowack et al. (1999) and Frederick et al. (2001) have shown that the addition of iron coagulant to a system containing both calcium and NOM yielded a decrease in the amount of calcium-NOM complexes adsorbed to the carbon as well as a relatively level iron loading onto the GAC. These results indicate that, not only is iron addition successful in decreasing calcium loading, but that the primary mechanism responsible for this is coagulation of the iron-NOM and/or calcium-NOM complexes. The accumulation of iron is not detrimental to the reactivation process as iron catalysis is suppressed by the presence of sulfur, which is ubiquitous in coal-based carbons (Nowack et al., 1999). A near neutral pH was indeed found to hinder iron-NOM formation as the hydroxide species out-competed the NOM for complexation with the iron ions. Therefore, Nowack et al. (1999) and Frederick et al. (2001) concluded that a combination of pH adjustment to approximately 6.0 pH and iron addition, on the order of 5 mg/L, are the most effective in reducing calcium loading. Water treatment facilities that operate above this range of pH are expected to accumulate higher levels of calcium onto their GAC.

Other on-site treatments to overcome pH excursions after the reactivated carbon is returned to service include backwashing, recycling of the high pH water, and pH adjustments before the treated water is discharged. Both backwashing and recycling involve running water through the GAC until the pH reaches acceptable levels, which reduces the yield of treated water through the system (Farmer et al., 1998). In addition, backwashing may require a holding tank, as the high pH water cannot be discharged, which will restrict the allowable backwashing time (Carr and Farmer, 1995). Acid treatment of the high pH water prior to discharge to stabilize the pH can be time-consuming and expensive, due to additional monitoring equipment.

Acid-washing a traditionally reactivated carbon prior to use, aside from being time-consuming and expensive, may not even produce a pH stable carbon (Dussert et al., 1995). In addition, oxygen surface complexes are introduced to the surface of the carbon if an oxidizing acid is used and this can impact the adsorption capabilities of the reactivated carbon, as discussed previously. Depending on the acid, the micropore volume may also decrease as a result of treatment.

A reactivation protocol proposed by Mazyck et al. (2005) was discussed that can overcome calcium catalysis and the resulting pH excursions by reactivating the carbons at temperatures below that at which CaO is formed, 1123 K. It is the CaO form that participates in the calcium chemistry mechanism. A decrease in the amount of CaO available to participate in the calcium chemistry reactions will result in a decreased pH excursion.

Oxidizing the reactivated carbon, outlined in a patent by Dussert et al. (1995), or treating the reactivated carbon with carbon dioxide (CO_2), outlined in a patent by Farmer et al. (1998), have been offered as means to create a pH stable carbon. Both patents propose that oxidation or CO_2 treatment, depending on the patent, neutralizes the surface of the reactivated carbon, thus

inhibiting any anion-exchange during water treatment. As the focus of a previous study (Mazyck et al., 2005) was the role of calcium in pH excursions and the result was that the anion-exchange mechanism does not fully explain the excursions found in reactivated carbons, there must be an additional explanation for why these treatments are able to create pH stable carbons.

Previous work by this author (Bach, 2004) determined that air treatments of reactivated carbons create pH stable carbons (i.e., pH < 8.5) through the formation of acidic oxygen-containing functional groups on the carbon surface which balance out the hydroxyl ions added by the calcium chemistry mechanism. This was supported by an evaluation of the total surface acidity of the air-treated versus untreated carbon. However, given the discussion of the role of individual functional groups on surface acidity, specifically the carboxyl group, an evaluation of individual functional groups would be required to further substantiate this proposal. CO_2 treatment was also found to create a pH stable carbon and it was proposed that CO_2 treatments form pH stable reactivated carbons via physisorption, and subsequent desorption, of CO_2 forming H_2CO_3 and then HCO_3^- upon water immersion which also balances out the hydroxyl addition by the calcium chemistry mechanism. This hypothesis was supported by similar total surface acidity found between an untreated and a CO_2 treated carbon, though an analysis of individual functional groups rather than total acidity would further support this theory. The literature also demonstrates that there would be no chemisorption of CO_2 onto CaO to form $CaCO_3$ which would not participate in the proposed calcium chemistry mechanism of Equations 2-10 and 2-11 (Mazyck and Cannon, 2000).

Following the treatments to overcome pH excursions and after evaluating their success, an air treated, a CO_2 treated and an untreated reactivated carbon were evaluated for their performance in the removal of a common taste and odor causing compound, MIB (Bach, 2004).

The results demonstrated that the untreated reactivated GAC removed more MIB than the air treated reactivated GAC in organic free water, due to an increase in the effects of surface acidity with the air-treated carbon, while this trend was reversed when NOM was present. The hypothesis behind the improved performance of the air treated carbon in water containing NOM was that the air treated carbon's surface charge, related to its surface acidity, made it less attractive to the negatively charged NOM leaving more adsorption sites available for MIB. In both waters, the CO_2 treated reactivated GAC removed the greatest quantity of MIB. The CO_2 treated reactivated GAC was shown to adsorb slightly less water in a study of water vapor removal from air, suggesting that the CO_2 treated carbon deterred water adsorption, which is deleterious to MIB adsorption. These findings highlight the importance of investigating changes in adsorption performance following deliberate changes in surface chemistry, as was done in order to overcome pH excursions.

Influence of Dissolved Oxygen in Water used to Create Steam

To this point, the impacts of surface chemistry on activated carbon, including its role in adsorption, as well as methods to tailor this surface chemistry for a specific goal (e.g., overcoming pH excursions) have been discussed. Rather than tailor surface chemistry following reactivation, a method to tailor reactivated carbon's surface chemistry during the reactivation process has also been explored, namely altering the dissolved oxygen (DO) content of the water used to create steam for steam reactivation (Chestnutt et al., 2007).

Water may be converted to steam for several industrial applications including laundry services, locomotion (i.e., steam engines), food manufacturing, wood pulp products, and activated carbon creation. When water is heated at sufficient temperatures to convert it to steam, any DO present in the system will devolve as gaseous oxygen (O_2). The devolution of oxygen in boiler systems has been documented as creating corrosion and pitting within the piping systems

employed in these facilities (Bizot and Bailey, 1997). First, the metal iron in the pipe dissolves to iron (II) in an anodic reaction followed by water's reaction with hydroxide ions to form ferrous hydroxide ($Fe(OH)_2$) (Equation 2-12). The ferrous hydroxide then reacts with oxygen to form iron (III) hydroxide (Equation 2-13), the dehydration of which forms iron (III) oxide more commonly known as rust (Bizot and Bailey, 1997).

$$Fe^{2+} + 2OH^- \rightarrow 4\ Fe(OH)_2\ (s) \quad (2\text{-}12)$$

$$4Fe(OH)_2 + O_2 + 2H_2O \rightarrow 4Fe(OH)_3(s) \quad (2\text{-}13)$$

This reaction demonstrates the impact that the DO present in water used to create steam may have on materials with which it comes into contact. With the impact of DO in mind, Chestnutt et al. (2007) studied the effect of DO in the water used to create steam on the reactivation of carbon. While several reactivation scenarios (i.e., different time, temperature regiments, etc.) were evaluated, Figure 2-3 shows an analysis of the performance of three reactivated carbons exposed to the same reactivation scenario only with differing DO values in the water used to create the steam. The performance in this study was evaluated using a column study where the effluent concentration of the target compound, MIB, was evaluated versus the volume of water treated, or bed volumes (BV). As demonstrated by Figure 2-3, the change in the DO content of the water used to create steam yielded a difference in the performance of the resulting reactivated carbon. Namely, the reactivated carbon exposed to steam resulting from water with high DO treated fewer bed volumes to breakthrough than a reactivated carbon exposed to steam created from low DO water. Here, breakthrough is defined as the number of bed volumes treated before the effluent exceeds the odor threshold concentration (OTC) of MIB (i.e., the concentration of MIB above which it is generally noted by the human palate) of 10 ng/L (Rashash et al., 1997). The impact of DO on the adsorption performance of the resulting carbons

was related to an increase in surface acidity of the carbons as the level of DO in the water used to make steam increased. The impact of surface acidity on MIB adsorption has been discussed at length.

While the mechanism behind the creation of increased acidity with an increase in the DO content of the water was not investigated in the work of Chestnutt et al. (2007), the results of this work do indicate that altering the DO of the water used to create steam for reactivation of carbon is a plausible means by which to alter surface chemistry and thereby influence the adsorption properties of reactivated carbon.

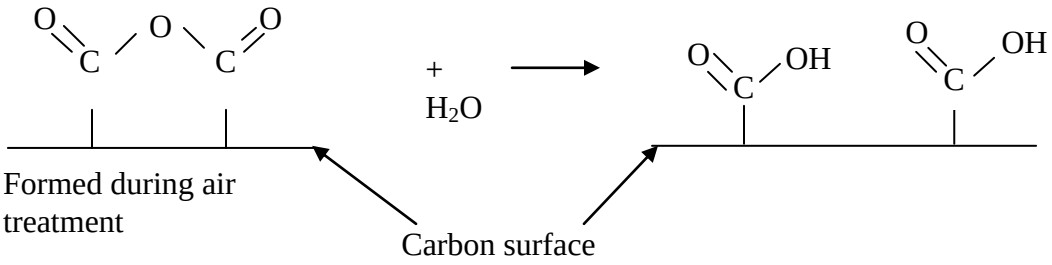

Figure 2-1. Proposed mechanism for the formation of COOH on an activated carbon surface.

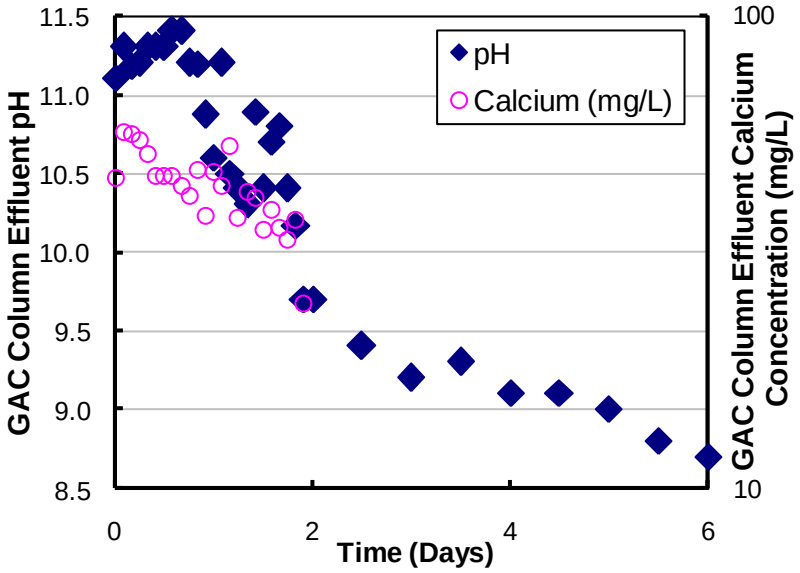

Figure 2-2. Full-scale water treatment plant effluent pH and calcium concentration data after reactivated GAC was returned to service (Mazyck et al., 2005).

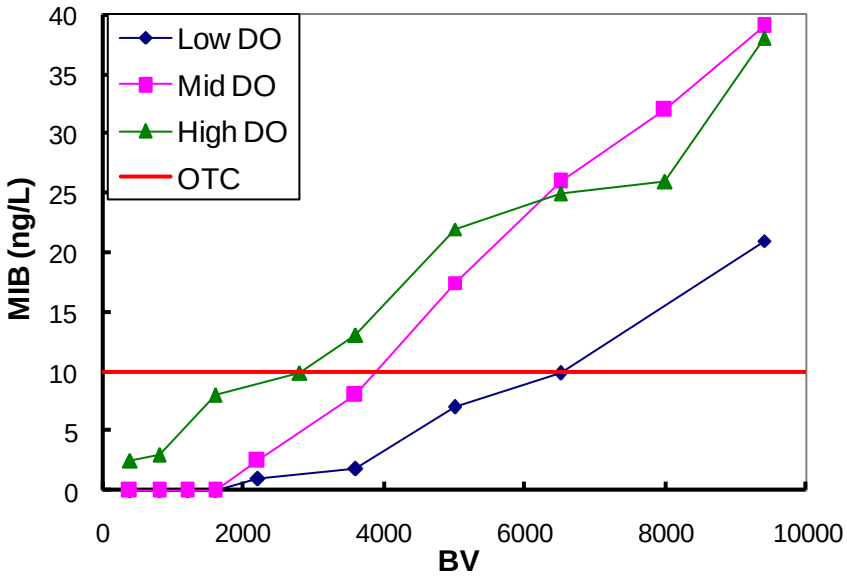

Figure 2-3. Comparison of performance in the removal of MIB for reactivated carbons created with varying DO content in the water used to create steam (Chestnutt et al., 2007).

CHAPTER 3
HYPOTHESIS AND OBJECTIVES

The objectives of the current work can be divided into two main categories: research related to overcoming pH excursions and research related to tailoring activated carbon using the DO content of the water used to create steam.

pH Excursions

Hypothesis

- Air treatments overcome pH excursions via increased surface acidity, specifically the carboxyl group and not via suppression of the calcium chemistry mechanism.
- CO_2 treatments overcome pH excursions via physisorption of CO_2 to the carbon surface and subsequent desorption to form carbonic acid and not via suppression of the calcium chemistry mechanism.
- Performance of a CO_2 treated carbon for removal of MIB is higher than both air treated and untreated carbon due to a decreased wetting time associated with the CO_2 treated carbon.
- Performance of an air treated carbon for MIB removal in water containing NOM is better than that of an untreated carbon due to the preference of the untreated carbon for NOM adsorption.
- Methods to overcome pH excursions, namely air and CO_2 treatments, will adversely affect the removal of phenol using a granular activated carbon column as increases in surface acidity are known to be deleterious to the adsorption of phenol and the surface chemistry of carbon can affect adsorption in both batch and column systems.

Objectives

- Investigate individual acidic functional groups on the air-treated, CO_2-treated, and untreated carbons versus the ability of these treatments to overcome pH excursions.
- Investigate mass change of carbon, indicative of CO_2 adsorption, during CO_2 treatment.
- Evaluate calcium in solution after contact with air- and CO_2- treated carbons to determine relative progression of the calcium chemistry mechanism as compared to an untreated carbon.
- Determine relative adsorption of MIB for a CO_2-treated and an untreated carbon after contact with only water for various lengths of time to confirm a difference in wetting time.

- Measure concentration of NOM remaining in solution after contact with MIB and an air-treated, CO_2-treated, and an untreated carbon to support hypothesis of competitive adsorption between MIB and NOM.

- Compare the performance of an air-treated, CO_2-treated, and untreated carbon for the removal of phenol in a column study.

Tailoring of Activated Carbon Using Dissolved Oxygen (DO)

Hypothesis

Altering the DO content of the water used to create steam during steam activation of a wood-based precursor will alter the surface chemistry/physical structure of the activated carbon affecting adsorption performance.

Objectives

- Evaluate the impacts of four different activation parameters (time, temperature, steam flow, and DO content of the water used to created steam) at three different levels (low, medium, and high) on the adsorption performance, physical properties, and chemical properties of the resulting activated carbon.

- Evaluate different methods of altering DO in the water used to create steam for activation and their impact on removal of MIB.

CHAPTER 4
EXPERIMENTAL METHODS

Reactivated Carbon Samples for Overcoming pH Excursions

Ten coal-based reactivated GAC samples, designed for adsorption from an aqueous solution, were received from the NORIT Americas, Inc. plant in Pryor, OK. These carbons had been used in potable water treatment, had become spent, and had been subsequently reactivated using traditional methods in Pryor, OK. A composite of three of these samples (i.e., these samples were commingled) having the highest calcium content (5.6-7.8 g Ca/kg carbon) and also exhibiting the highest pH excursion was used throughout the research into pH excursions. The BET surface area of the composite was 896 m^2/g with a micropore (< 2 nm) volume of 0.35 cm^3/g and a mesopore/macropore (>2 nm) volume of 0.13 cm^3/g.

Carbon Precursor for Activations

A wood-based fly ash was used as the carbonaceous precursor in this study. Fly ash from wood-combustion has been investigated as an addition to composts to aid in adsorbing odors, controlling pH and moisture content, and nutrient addition (Campbell et al., 1997; Rosenfeld and Henry, 2000; Das et al., 2003). Wood-based fly ash also outperformed a coal fly ash in the catalytic oxidation of H_2S and methanethiol, due to the higher surface area of the wood-based fly ash, in a study of sulfur compound removal from gaseous waste streams (Kastner et al., 2003). The fly ash used in this study was a side product of combustion taking place at a wood processing facility in Florida. By utilizing a wood-based fly ash, the activation uses a renewable resource as well as recycling a waste stream which enhances the environmental impetus to use such a material.

Air Treatments and CO_2 Treatments of Reactivated Carbons

Air treatments were conducted in ambient air using a muffle furnace. Three grams of carbon were placed in crucibles at the desired temperature inside a muffle furnace where they were continuously exposed to 52.5 mmol O_2/g GAC for 15, 30, or 60-minutes. The air treatment temperatures used were 623 K, 673 K, and 723 K based on Dussert et al.'s (1995) preferred temperature range for the air treatments of between 623 K and 773K. After treatment, the samples were allowed to cool in a dessicator and were stored until further use.

A clamshell furnace similar to that used by Mazyck and Cannon (2000, 2002) held a quartz-fluidized bed wherein CO_2 treatments were carried out at ambient temperatures. A porous plate near the center of the quartz-fluidized bed allowed a flow of 0.9 L/min of CO_2 to contact three grams of sample for 20 minutes for an exposure of 281 mmol CO_2/g carbon. The treatment is similar to that employed by Farmer et al. (1996) with the exception that dry GAC was exposed to CO_2 instead of wet GAC.

Activations with Varying DO Content in Water

Using the same clamshell furnace used for CO_2 treatments, activations involved exposing five grams of sample, resting on a porous plate near the center of the quartz-fluidized bed, to a steam flow under the desired conditions. Steam flow is reported as g H_2O/g carbon which is the mass of water, determined by the flow of steam as measured with a flow gauge multiplied by the given period of activation, divided by the mass of carbon with which the steam comes into contact. Activations were preceded by a pyrolysis step where the five grams of sample were exposed to the activation temperature in a flow of pure nitrogen gas for a time equal to the steam exposure (i.e., activation time).

Henry's law was used to calculate the theoretical DO level in the deionized water used to create steam under varying experimental conditions, as well as the concentration of other

dissolved gases, in order to compare these theoretical values to the measured DO concentrations. Henry's law (Equation 4-1) relates the concentration of gas in solution to the partial pressure of the gas above the solution. Partial pressure (P_x), according to Dalton's Law, is defined as the pressure exerted by a single gas in a gaseous mixture where the total pressure equals the sum of the partial pressures of each gas in the mixture (Petrucci and Harwood, 1997). C equals the concentration of gas X in solution (mol/L); k_H is Henry's constant for gas X (mol/L/atm); and P_x is the partial pressure of gas X (atm).

$$C_x = k_H * P_x \quad (4\text{-}1)$$

The DO content of the water was manipulated based on the gas (e.g., pure nitrogen, air, or pure oxygen) used to pressurize a water vessel set at 10 psi (gauge), which then delivered the water to a preheater set at approximately 723 K which then sent steam to the fluidized bed reactor. Nitrogen gas pressurization yielded a DO concentration of less than 4 mg/L, air pressurization yielded a DO of approximately 7.5 mg/L, and pure oxygen pressurization created a DO concentration of greater than 10 mg/L. The DO concentration was measured inline using a Mettler Toledo inline DO probe placed just prior to a water gauge which measured water flow into the preheater. Following activation, the carbon samples were cooled to ambient temperatures in the furnace under a nitrogen flow to prevent interactions with the atmosphere at high temperatures.

Water Contact pH

The water contact pH of the carbons was determined by mixing approximately 2 grams of as-received GAC with 80 mL of Milli-Q water for 30 minutes, then measuring the pH. This ratio of GAC to solution was the same used by Dussert et al. (1995) and Farmer et al. (1996). In initial exploratory experiments, pH measurements were taken every five minutes, and it was observed that after 20 or 30 minutes the pH reached a pseudo-equilibrium level (less than 0.1

change in pH over 5 minutes). Dussert et al. (1995) used a similar technique and concluded that this protocol provides a good prediction of the pH that would be measured during water treatment service. For the experiments described herein, each reactivated carbon was sampled twice and the pH for these two samples was within ± 0.4 pH units.

Calcium Solution Concentration

Following the water contact pH experiments, the GAC was separated from the solution utilizing a vacuum filtration apparatus (0.45 μm Whatman filter paper). The calcium levels leached out of the GAC during the 30-minute water contact pH experiment were analyzed by inductively coupled plasma (ICP) emission spectroscopy (Perkin Elmer, Optima 3200RL). The measured concentrations of the replicas were within ± 3.5% of one another.

Adsorption Experiments (Batch)

For batch equilibrium studies, PAC was created by grinding the carbons in a crucible and sieving the resulting particles through a 325 mesh (45 μm). Then, a 0.5 L stock solution of 153 ng radiolabeled C^{14}-MIB/L was created by blending 95.7 μL of an 800,000 ng MIB/L-methanol stock solution with 500 mL of either deionized (DI) water or natural water influent to the Manatee County Water Treatment Plant (Bradenton, Florida) (Total organic carbon=10.0 mg/L; Specific UV Absorbance=4.78 L/mg-m; pH=7). Note, MIB (1,2,7,7-tetramethyl-exo-bicyclo(2.21)heptan-2-ol) is a moderately hydrophobic compound of low molecular weight with a molecular size of approximately 6 Å (Newcombe et al., 2002; Rangel-Mendez and Cannon, 2005). From the 153 ng radiolabeled C^{14}-MIB/L solution, 50 mL allotments were added to separate gas tight syringes followed by addition of 10 ppm carbon. The syringes were then sealed, permitting a small amount of headspace, and allowed to mix on a rotisserie style mixer. After 24 hours, a 0.45 μm luer-lock nylon filter, attached to each syringe, was used to separate

the carbon from 9 mL of the solution, which was then tested according to previous studies using radiolabeled C^{14}-MIB (Gillogly et al., 1998; Tennant and Mazyck, 2003). Each sample was measured twice for MIB and the mean of these two runs was used for the final value. Typical reproducibility was within ±1%. The entire process, starting with 50 mL samples of either DI or natural water, was repeated for each carbon. Each dose experiment was run in replicate and the error bars shown in the figures represent one standard deviation from the mean of these replicate runs.

Select samples were analyzed for NOM remaining in solution using a Tekmar Dohrmann Apollo HS 9000 with an autosampler to measure nonpurgeable dissolved organic carbon (DOC). Error is represented as plus or minus one standard deviation from the mean of triplicate analyses.

For batch studies with phenol, 30 mL of 5 mg/L phenol where mixed in vials containing 50 ppm carbon for 24 hours. The PAC was then separated from the solution utilizing a vacuum filtration apparatus (0.45 μm Whatman filter paper). The samples were stored at 277 K under low light conditions until they were ready to be measured at which point dilutions were employed to ensure detection on a gas chromatography-mass spectroscopy instrument (Varian, Saturn 2100P). The averages of replicate experiments are reported with error bars representing one standard deviation from the mean.

Rapid Small-Scale Column Tests (RSSCTs)

For column studies with phenol as the target compound, a commercially available activated carbon (F400) was exposed to the same air and CO_2 treatments used to overcome pH excursions and then these carbons were evaluated using RSSCTs. Details pertaining to the RSSCT design are listed in Table 4-1. The advantages of RSSCTs are that: (1) they can provide a breakthrough profile in a fraction of the time compared to full- or pilot-scale studies; (2) a

smaller volume of water is required for testing; and (3) extensive isotherm studies are not required to predict full-scale performance (Crittenden et al., 1986; Crittenden et al., 1991). Although the RSSCT can significantly reduce the time and cost of the study, the limitation of the RSSCT is that it can over-predict full-scale GAC performance (Summers et al., 1989; Crittenden et al., 1991); nevertheless, it is not expected that the relative comparison between carbons would change.

The RSSCTs employed in this study were designed using full-scale design parameters and scaling equations available in the literature (Crittenden et al., 1991). The RSSCT column was manufactured from acrylic (1.5 cm x 0.41 cm) (0.59 in. x 0.16 in.) with Teflon inserts to prevent the sorption of compounds. Similarly, a Masterflex L/S rigid PTFE pump head, PTFE tubing, and PTFE fittings were used throughout the system to avoid sorption of compounds. Throughout the entire experiment, a flow meter monitored water throughput (4.4 mL/min), and all experiments were performed in duplicate.

The various reactivated carbons were evaluated using the RSSCT by spiking aliquots of deinoized water with a phenol concentration of 5 mg/L. At the time of sampling, a 20 mL vial was placed at the discharge tube where 13 mL of sample were collected over 3 minutes. The samples were stored at 277 K under low light conditions until they were ready to be measured at which point dilutions were employed to ensure detection on a gas chromatography-mass spectroscopy instrument. The averages of replicate experiments are reported with error bars representing one standard deviation from the mean.

BET Surface Area Measurements

To determine surface area, the carbon samples were first outgassed at 383 K for 24 hours. Then, an N_2 adsorption isotherm was carried out at relative pressures between 0.05 and 0.35 in a NOVA 1200 (Quantachrome) gas sorption analyzer. The resulting data was then analyzed using

the BET model to determine the surface area of each sample. Duplicate samples were analyzed with average error less than 5%.

Pore Size Distribution Measurement

Pore size distributions (PSDs) were performed using a Quantachrome Autosorb I. Each carbon sample was first outgassed at 383 K for 24 hours. The sample cell was then placed in a liquid nitrogen bath which created an analysis temperature of approximately 77 K with nitrogen gas used as the adsorbate. The density functional theory (DFT) was used to develop the pore size distribution data in the micropores (< 2 nm) from the nitrogen isotherm with a relative pressure range from 10^{-6} to 1, while the Barrett, Joyner, Halenda (BJH) model was used for all pores greater than 2 nm.

pH at the Point of Zero Charge

To determine the pH at the point of zero charge (pH_{pzc}), where the point of zero charge is defined as the condition where the charge on the surface of the carbon is neutral or zero, an aqueous system where the carbon sample dominates the pH of the system was evaluated. To this end, 0.5 g of carbon sample was mixed with 5 mL of nanopure water which was previously bubbled with nitrogen gas for 20 minutes to remove any carbon dioxide from the system that may interfere with the influence of the carbon sample on the water pH. The headspace above the solution was also purged with nitrogen gas. The vial was then covered with parafilm to eliminate mixing with the atmosphere and the sample was allowed to mix for 24 hours in order for the carbon to reach equilibrium with the solution. After 24 hours, the pH of the sample was determined using a standard pH electrode and this pH measurement was recorded as the pH_{pzc}. Each pH_{pzc} measurement was performed in duplicate with each experiment performed in replicate. The replicates were within ±1%.

Boehm Titration

The concentration of acidic oxygen complexes created on the surface of the carbon samples was determined according to the Boehm titration method (Boehm, 1966). An allotment of 0.5 g of carbon and 25 mL of either 0.05 N NaOH, 0.25 N NaOH, 0.05 N $NaHCO_3$, or 0.05 N Na_2CO_3 were shaken in sealed vials for three days. The suspensions were then filtered using a 0.45 μm filter and 20 mL of the filtrate was titrated with 0.1 N H_2SO_4 to a pH of 4.5. The amount of base consumed by each sample was determined by comparing each titration to that of a blank. Any base consumed by the sample results from the neutralization of acidic functional groups and is dependant on the type of base used. Carboxyl groups react with $NaHCO_3$; lactone groups are measured with the difference between the reaction with Na_2CO_2 and $NaHCO_3$; phenolic groups are measured with the difference between reactions with 0.05 NaOH and Na_2CO_2; the difference between 0.25 NaOH and 0.05 NaOH measures carbonyl groups; total acidity is measured with 0.05 NaOH. The error in the measure of functional groups represents the highest and lowest values found in repeated experiments.

Statistical Design of Experiments: Box Behnken

Traditionally, the evaluation of the effect of several variables on a result is made using a full factorial, one-factor-at-a-time, or the fractional factorial approach to obtaining data. The full factorial approach involves the collection of data relating to all possible combinations of the factors (variables). With four factors under investigation in this research and a proposed three levels (settings) for each factor, the full factorial method corresponds to 81 experiments. The benefit of such an approach is that the choice of optimum conditions will be clear when the data are analyzed; the optimum experimental conditions will be run as one of the experiments. However, performing at least 81 experiments, as this number does not take into account replicate experiments, can be expensive in terms of both cost and time.

Given the drawbacks of a full factorial approach, many researchers revert to the one-factor-at-a-time approach, which evaluates the effect of varying one factor while holding all other factors constant. Once the level that produces the best result has been determined for this factor, the level is fixed while another factor is evaluated with the remaining factors constant. The one-factor-at-a-time approach used in this research would yield nine experiments. Clearly, this approach would be tempting to a researcher when compared with the 81 runs required for a full factorial approach. However, the one-factor-at-a-time approach has significant drawbacks when considering the validity of the final optimum conditions, as it does not take into account interactions. An interaction between factors occurs when two or more factors acting together have an effect on the result greater than the factors acting alone.

The fractional factorial approach mediates the cost and result validity issue by utilizing the principles of the design of experiments (DOE). DOE is defined as the evaluation of the simultaneous effect of changing variables on the final product in order to gain the maximum amount of definitive information with the minimal amount of expended resources. The fractional factorial approach uses only a predetermined set of experiments chosen from the full factorial. Unlike the one-factor-at-a-time approach, there is a logical plan behind the choice of experiments run from the full factorial and statistical analysis yields a final result with a specific associated value of certainty, without the requirement to run each combination in the full factorial. Therefore, fractional factorials, specifically a Box-Behnken design (Box and Behnken, 1960), will be used in this research with 29 runs required.

The proposed Box-Behnken design is formed by combining a 2^k factorial design, where 2 is the number of levels and there are k variables being studied, with incomplete block designs to

produce a 3^k fractional factorial (Montgomery, 1991). A 2^2 full factorial design is shown in Table 4-2.

In a Box-Behnken design, each pair of factors being studied is linked to a 2^2 factorial where the two factors are varied at two levels (high and low) while the third factor is fixed at its center level (middle). The combination of factorials in this fashion for a Box-Behnken 3^3 design is shown in Table 4-3.

A visual representation of the Box-Behnken design of 3^3 is shown in Figure 4-1, where each dot represents experiments and the vertices represent the three factors. It should be noted from the 3^3 design that, although 12 experiments are required to complete the combination of factorials, there is also an additional point at the center.

A 3^4 design, which is the suggested Box-Behnken design for this experiment, requires four axis for which the visual representation is less simple but the same theory applies. This design would contain 24 design points plus a certain number of runs at the center point. It is from this replication of center points that analysis of error can be made. Myers (1995) recommends 3-5 replicates of the center points and the upper limit of this will be used in this Box-Behnken design for a total of 29 runs (i.e., 24 runs plus five runs at the center point).

The center point is replicated to obtain the pure error associated with the experiment. Pure error in an experiment accounts for any random error in experimentation that is not accounted for by the lack of the data's fit to the proposed model. By utilizing the five replicate experiments at the center point, pure error has four degrees of freedom (five replicate experiments at the center point minus one) and there are 10 degrees of freedom for lack of fit. In this way, the Box-Behnken is able to incorporate a level of significance in the final result without the need to repeat every experiment. To ensure that the error is random, the required 29 runs are

performed in a computer generated random order. The pure error is then used to analyze the lack of fit, while the total residual error (i.e., pure error plus lack of fit) is used to determine the significance of each factor evaluated according to the common evaluation method known as the F-value. Equation 4-1 shows how to calculate the F-value to determine the significance of the model's lack of fit. It is desired that the models lack of fit be insignificant (i.e., it is desired that the generated model to predict results fits well with the data).

$$\text{F-value} = \frac{\text{Sum of Squares Lack of fit/degree of freedom lack of fit}}{\text{Sum of Squares Pure Error/degree of freedom pure error}} \quad (4\text{-}1)$$

To determine whether an F-value is significant to a 0.05 level of significance, or a 95% confidence interval, as used in this study, the P-value (Prob > F) was employed. The P-value gives the probability of obtaining an F-value at least that high due solely to random error, where a P-value less than 0.05 would indicate a significant parameter such that there is less than a 5% chance that an F-value that large could be due solely to random error. Equation 4-2 shows how to calculate the F-value to determine the significance of a factor.

$$\text{F-value} = \frac{\text{Sum of Squares Factor/degree of freedom factor}}{\text{Sum of Squares Residual/degree of freedom residual}} \quad (4\text{-}2)$$

For this study, the Box-Benken approach was evaluated using Design-Expert software, version 6.0.5, distributed by Stat-Ease, Inc. in 2001.

Table 4-1. RSSCT and full-scale design parameters

Parameter	Full-scale	RSSCT*
Grain Size (U.S. mesh)	12 x 40	170 x 200
EBCT (min)	7.5	0.045
Hydraulic loading rate (mm/min)	167.5	335.1
Time to process 1000 BV	5.2 d	0.74 hr

*Constant diffusivity conditions based on Speitel et al. (2001)

Table 4-2. 2^2 full factorial

Experiment	Variable A	Variable B
1	Low	Low
2	Low	High
3	High	Low
4	High	High

Table 4-3. Box-Behnken 3^3 fractional factorial

Experiment	Variable A	Variable B	Variable C
1	Low	Low	Middle
2	Low	High	Middle
3	High	Low	Middle
4	High	High	Middle
5	Low	Middle	Low
6	Low	Middle	High
7	High	Middle	Low
8	High	Middle	High
9	Middle	Low	Low
10	Middle	Low	High
11	Middle	High	Low
12	Middle	High	High
Center run	Middle	Middle	Middle

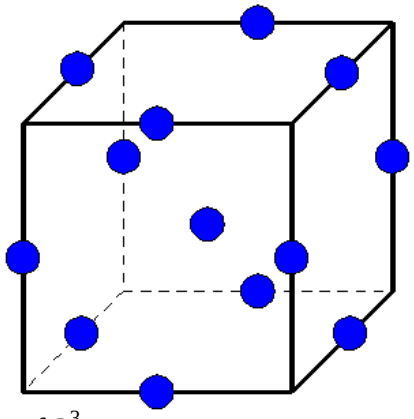

Figure 4-1. Box-Behnken design of 3^3

CHAPTER 5
STRATEGIES FOR OVERCOMING pH EXCURSIONS FOR REACTIVATED GRANULAR ACTIVATED CARBON: AIR AND CARBON DIOXIDE TREATMENTS

Previous research into the mechanisms behind pH excursions have demonstrated the plausibility of a calcium chemistry mechanism behind pH excursions experienced with reactivated carbons (Mazyck et al., 2005). Further research has suggested that mechanisms to overcome pH excursions, namely air and carbon dioxide (CO_2) treatments, are effective in overcoming pH excursions due to addition of acidity to solution either by increased total surface acidity, as with air treatments, or physisorption of carbon dioxide and subsequent desorption to form carbonic acid, as with CO_2 treatments (Bach, 2004). However, additional research needs to be done to support these mechanisms and, therefore, the intent of the current work is to bolster the hypothesis made in the previous work via additional experiments. Due to the fact that the current work builds directly from previous work, certain figures have been reproduced for the reader's benefit and are marked as "(Bach, 2004)" to differentiate the previous work from new work done in this study.

Creation of a pH Stable Carbon

Air treatments of a coal-based reactivated carbon were conducted according to the patent of Farmer et al. (1998) to investigate the creation of a pH stable reactivated GAC which has a water contact pH less than 8.5 pH units, as this pH falls between the NPDES permitted discharge pH of 6 to 9 while still allowing for a small safety factor (Bach, 2004). A pH stable carbon is not expected to exhibit a pH excursion upon return to service (Dussert et al., 1995; Farmer et al., 1998; Mazyck et al., 2005). The resulting water contact pH of the air treated carbons, treated at three different temperatures and treatment times, measured in deionized (DI) water, is shown in Figure 5-1. Dashed lines at a water contact pH of 8.5 and 6.5 highlight the cutoff between an

acceptable and unacceptable water contact pH incorporating a safety factor. The first data bar, at time zero, represents the water contact pH of the untreated carbon (i.e., reactivated GAC).

While a pH stable carbon is not created at any of the three treatment times when the temperatures is 623 K, after 60-minutes of air treatment at 673 K and after only 30-minutes of treatment at 723 K a pH stable carbon is created. These results indicate that treatments to overcome pH excursions with virgin carbons are also successful in overcoming pH excursions with reactivated carbon in DI water.

The CO_2 treatment scenario, wherein the composite sample was exposed to a CO_2 flow of 0.9 L/min for 20 minutes (281 mmol CO_2/g) at ambient temperature, also created a pH stable carbon (pH=8.3) (Bach, 2004). The CO_2 flow rate and contact time were chosen based on preliminary experiments demonstrating that this time and flow rate were sufficient to create a pH stable carbon (Figure 5-2). At 20 minutes, a pH stable carbon was created at the lowest carbon dioxide flow (i.e., 0.9 L/min) and, therefore, this treatment time and flow were used in all subsequent analyses. Again, the proposed method to overcome pH excursions experienced with virgin carbons in water containing anions is also successful in overcoming pH excursions with reactivated GAC in DI water.

Surface Acidity of Air-Treated Carbons

The air treatments tested herein bound the ideal temperature for production of acidic functional groups, specifically carboxyl groups, which leads to the hypothesis that air treatments overcome pH excursions by creating acidic functional groups on the GAC surface which balance out the hydroxyl ions imparted to the water via the calcium chemistry mechanism. The quantity of individual functional groups on the surface of air treated carbons with a treatment time of 60-minutes and the untreated carbon is shown in Figure 5-3.

As expected, the air treatments that created pH stable carbons (i.e., treatments at 673 K and 723 K) show an increase in total acidity compared to the untreated carbon. The 623 K treatment, which did not create a pH stable carbon, had a similar quantity of oxygen-containing functional groups as the untreated carbon except for lactone groups, which were slightly more prevalent in the air treated carbon. Interestingly, though 60–minute air treatments at 673 and 723 K yielded pH stable carbons, only the treatment at 723 K showed an increase in the quantity of carboxyl groups compared to the untreated carbon. This result suggests that several acidic functional groups are responsible for creating pH stable carbons, as the 673 K treatment yielded a pH stable carbon without a significant increase in carboxyl groups. The 723 K air treated carbon also showed an increase in the lactone and phenolic groups compared to all other samples. The carbonyl functional group was found to form to a significant extent in the 673 K sample compared to all other samples and, like the 723 K sample, it showed an increase in the lactone and phenolic groups compared to the untreated sample. Given this information, it seems likely that the lactone and phenolic groups play a role in creating a pH stable carbon at these temperatures.

Surface Acidity of CO_2 Treated Carbons

The CO_2 treated and the untreated carbon yielded similar quantities of acidic functional groups on the carbon surfaces (Figure 5-4), indicating that addition of surface acidity is not responsible for overcoming pH excursions with CO_2 treatment.

Here, the mechanism that creates a pH stable carbon is likely physisorption of CO_2 to the carbon surface. Upon immersion into water, the CO_2 desorbs and reacts with water to form carbonic acid (H_2CO_3) and then bicarbonate (HCO_3^-) after deprotonation at the pH typically observed in water treatment. Based on calculations predicting the pH of a system where only the

dissolution of CO_2 from the atmosphere and the calcium chemistry mechanism influences pH, the theoretical equilibrium pH is approximately 8.6 compared to the measured water contact pH of 8.3 with the CO_2 treated carbon. The theoretical equilibrium pH for the untreated carbon is also approximately 8.5 though the measured water contact pH is 10.7. It is possible that the additional CO_2, which is expected to dissolve upon contact with water, on the CO_2 treated carbon's surface allows the system to reach its equilibrium pH at a faster rate than the untreated carbon. An analysis of the weight gain following CO_2 treatment showed a slight increase in weight which, assuming the mass gain is due solely to CO_2 physisorption, corresponds to an addition of $1.1*10^{-5}$ M CO_2. The equilibrium concentration of CO_2 dissolved into solution from the atmosphere at room temperature is $0.9*10^{-5}$ M CO_2/L, which may support the hypothesis that CO_2 treatment increases the rate at which the solution reaches equilibrium with the atmosphere. For example calculations of CO_2 in solution, see Appendix A.

As with air treatment, it is proposed that the CO_2 treatment balances out the basic effects of the calcium chemistry mechanism, for the bicarbonate buffers the hydroxyl ions released from the calcium hydrolysis, thus depressing the magnitude of the pH excursion. It is not anticipated that CO_2 treatment forms $CaCO_3$ to any great extent, which would not participate in the pH excursion mechanism, because the optimum chemisorption temperature of CO_2 to CaO, to form $CaCO_3$, is near 573 K and the CO_2 treatments used herein occurred at ambient temperatures (295 K) (Mazyck and Cannon, 2000).

Verification of Mechanisms

To support the hypothesis that neither air treatments nor CO_2 treatments inhibit the calcium chemistry mechanism from progressing, an examination of the calcium that dissolved from the carbons shown in Figure 5-3 and Figure 5-4 was performed (Table 5-1).

An analysis of the calcium in solution after CO_2 treatment showed that the untreated carbon yielded 34 mg/L Ca^{2+} and the CO_2 treated carbon created approximately 30 mg/L Ca^{2+}. These findings suggest that CO_2 treatment results in a slight decrease in dissolved calcium, though it is not significant enough to fully account for the creation of a pH stable carbon as this change of 4 mg/L Ca^{2+} would only be expected to decrease the pH by 0.7 versus the observed decrease in pH of 2.1.

Table 5-1 also shows an unexpected increase in dissolved calcium present in solution at air treatment temperatures of 673 and 723 K (60 and 69 mg/L, respectively). An increase in the concentration of calcium in solution suggests that there is more calcium involved in the proposed calcium chemistry mechanism responsible for the pH excursion. A plausible explanation is that not all of the calcium adsorbed to the activated carbon during service reacted to form CaO during reactivation. During the subsequent air treatment to create a pH stable carbon, the calcium not already present as CaO (e.g., $CaCO_3$) reacted to form CaO, the thermodynamically stable species at the temperatures and partial pressure of oxygen used during air treatments herein (Mazyck and Cannon, 2000). Conversely, a portion of the original adsorbed calcium-NOM complex may have remained through reactivation and was subsequently converted to CaO by the air treatments employed herein. To determine if air treatments act to create more CaO on the carbon surface, which then participate in the proposed calcium chemistry mechanism, treatments at the same temperature but in a nitrogen environment were performed and the resulting calcium in solution evaluated. The nitrogen treatments resulted in approximately half the concentration of calcium in solution (32 and 34 mg/L at 673 and 723 K, respectively) that was obtained with air treatments at the same temperature, supporting the hypothesis presented above. This suggests interplay between the addition of increased basicity (as demonstrated by an increase in dissolved calcium

and thus more hydroxyl ions) and increased acidity (as demonstrated by Figure 5-3) with air treatments.

Summary and Conclusions

Air treatments and CO_2 treatments designed to create pH stable carbons from virgin carbons in anion-containing water were successful at creating pH stable reactivated carbons in deionized (ion-free) water. These findings support the work of Mazyck et al. (2005) which questioned the plausibility of an anion-exchange mechanism and the suppression thereof as an explanation for the creation of a pH stable carbon. In other words, the treatments created pH stable carbons even in anion-free water.

Air treatments of reactivated carbons at 673 K and 60-minutes or 723 K for 30- or 60-minutes were found to create pH stable carbons through the formation of acidic oxygen-containing functional groups on the carbon surface. It is proposed that CO_2 treatments form pH stable reactivated carbons via physisorption, and subsequent desorption, of CO_2 forming H_2CO_3 and subsequently HCO_3^- upon water immersion. While an increase in the mass of the carbon due to CO_2 physisorption was observed, additional experiments would need to be performed to confirm this hypothesized mechanism. However, an analysis of the functional groups on the CO_2 treated carbons' surface and an analysis of the calcium in solution following contact with the treated carbons ruled out both increased acidity and calcium chemistry suppression as plausible mechanisms behind the creation of a pH stable carbon with CO_2 treatment.

Table 5-1. Calcium in solution with treatments

Temperature (K)	Calcium in solution (± 1mg/L)
Ambient (Untreated)	34
Ambient (CO_2)	30
623 (Air)	37
673 (Air)	60
723 (Air)	69
673 (Nitrogen)	32
723 (Nitrogen)	34

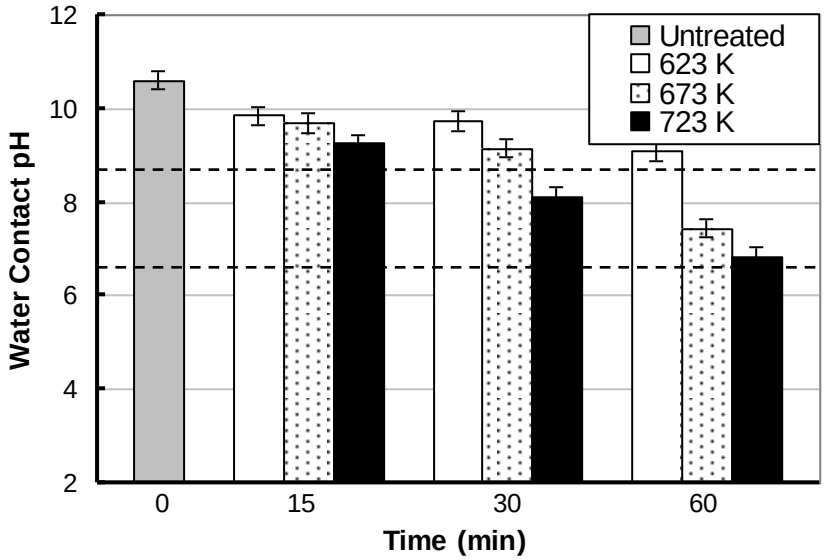

Figure 5-1. Effect of air exposure time and temperature on water contact pH of reactivated carbon. Dashed lines represent a pH of 8.5 and 6.5, respectively (Bach, 2004).

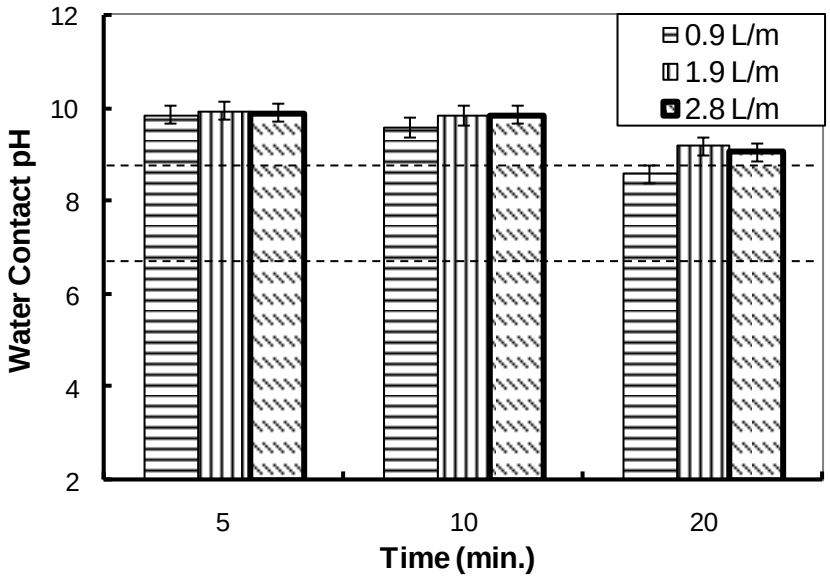

Figure 5-2. Effect of treatment time and gas flow on resulting water contact pH of CO_2 treated carbon.

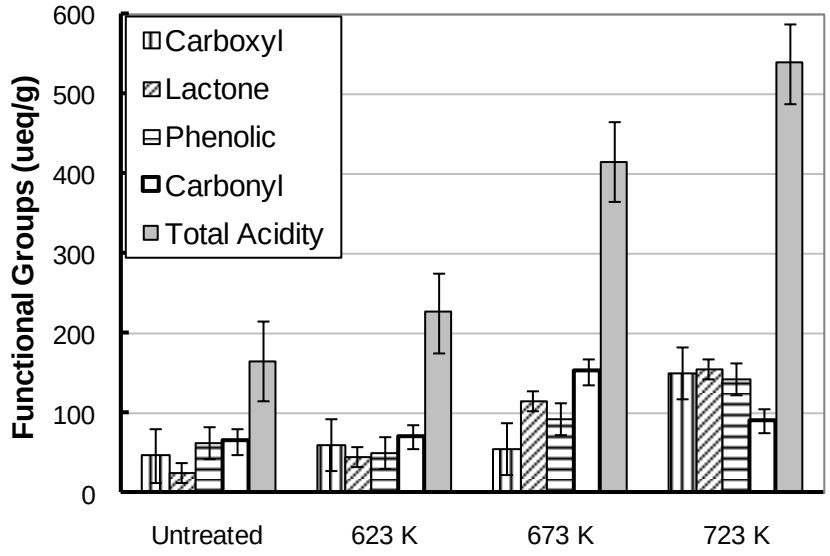

Figure 5-3. Effect of air treatments after 60-minute contact time at varying temperature on individual acidic functional groups.

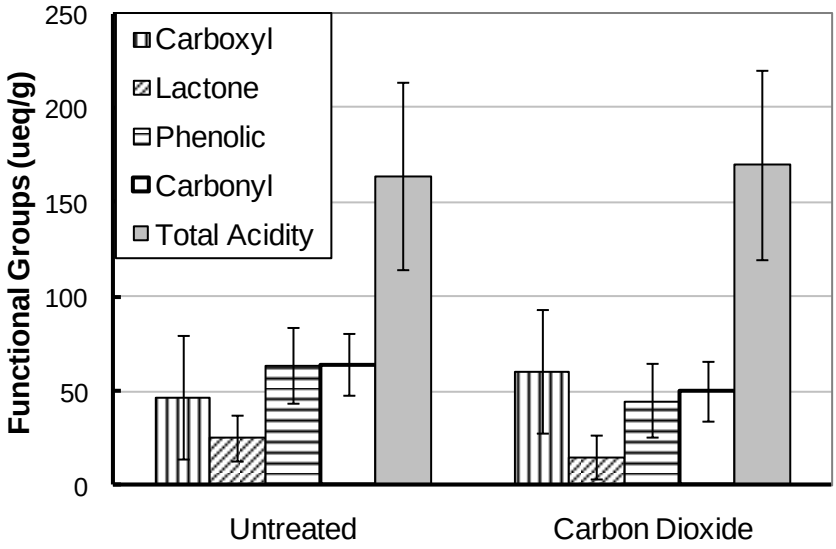

Figure 5-4. Effect of CO_2 treatments on individual functional groups.

CHAPTER 6
METHODOLOGIES FOR OVERCOMING pH EXCURSIONS FOR REACTIVATED GRANULAR ACTIVATED CARBON: EFFECT ON ADSORPTION PERFORMANCE

The work discussed in Chapter 5 supported the hypothesis that air treatments of reactivated carbons create pH stable carbons (i.e., pH < 8.5) through the formation of acidic oxygen-containing functional groups on the carbon surface which balance out hydroxyl ions added by the calcium chemistry mechanism. The hypothesis that CO_2 treatments form pH stable reactivated carbons via physisorption, and subsequent desorption, of CO_2 forming H_2CO_3 and then HCO_3^- upon water immersion which again balances out the hydroxyl addition by the calcium chemistry mechanism was also supported. The addition of oxygen to the surface of an activated carbon and its effect on adsorption is well-known and therefore a follow-up study by Bach (2004) evaluated the removal of the target compound MIB using the treated carbons.

To determine the effect that the treatments designed to create pH stable carbons have on adsorption, a pH stable air treated carbon (673 K, 60-minute treatment), a CO_2 treated carbon, and an untreated carbon were evaluated for their removal of MIB in both deionized (DI) water (i.e., organic free) and natural water (containing 10 mg/L natural organic matter (NOM) measured as total organic carbon (TOC)). The characteristics of the pH stable carbons and an untreated carbon are shown for comparison in Table 6-1. Note that the BET surface area of the carbons can be considered similar. The percent removal of MIB in DI water versus the powdered carbon dose of a CO_2 treated, air treated, or an untreated carbon evaluated in the work of Bach (2004) is reproduced in Figure 6-1.

Figure 6-1 indicates that the CO_2 treated carbon had a higher adsorption capacity for MIB than either the air treated or untreated carbon and the air treated carbon had less of an adsorption

capacity for MIB compared to the untreated carbon. Note that MIB removal is not affected by pH change and MIB does not affect pH (Herzing et al., 1977).

The studies of Pendleton et al. (1997) showed the effects of activated carbon surface chemistry on the adsorption of MIB and linked decreased adsorption with an increase in the hydrophilic nature of an oxidized carbon. As MIB will adsorb to both hydrophobic and hydrophilic adsorption sites, direct competition for adsorption sites between water and MIB, the mechanism suggested by Pendleton and coworkers, would not explain the decreased adsorption of MIB with oxygenation of the carbon's surface. Therefore, given the increased acidity of the air treated carbons (Table 6-1) and previous research showing the impact of an oxidized surface on adsorption, the air treated carbon in the study of Bach (2004) did not remove as much MIB as the untreated carbon due to the presence of water clusters on the oxygenated surface of the air treated carbon which impeded MIB adsorption.

While the impact of air treatment and the associated oxidation of the carbon surface on adsorption are well understood, an increase in removal with CO_2 treatment was unexpected given the similar surface acidity of the CO_2 treated carbon compared to the untreated carbon. Bach (2004) proposed that the CO_2 treated carbon delays adsorption of water as the CO_2 is desorbed from the surface thereby leaving the adsorption sites free for MIB adsorption. A slight increase in the adsorption of water vapor following CO_2 treatment, while indicative of a change in the way carbon behaves with water molecules, may not translate to the water based system used in the adsorption study and therefore additional work needs to be done to confirm this hypothesis.

NOM is ubiquitous in surface waters and the concentration of NOM can be 100,000 times that of the trace contaminant MIB and, furthermore, the adsorption of NOM has been shown to decrease the removal of MIB via competitive adsorption (Newcombe et al., 2002;

Tennant, 2004). Therefore, it was of interest to compare the performance of the air treated, CO_2 treated, and untreated carbons for MIB removal in natural water which was done in the work of Bach (2004) and is reproduced for the reader's convenience in Figure 6-2.

Unlike the DI water scenario, the air treated carbon removed more MIB in natural water than did the untreated carbon. NOM can adsorb through electrostatic forces (as well as non-electrostatic forces) wherein the negative charge of the NOM is attracted to a positive charge on the carbon surface (Newcombe, 1999). The pH_{pzc},the pH at the point of zero charge where the surface carries a negligible charge, can be used to determine the charge on a surface (Ravichandran, 1998; Tennant, 2004). In a solution with a pH above the pH_{pzc}, the carbon surface will carry a negative charge and a solution with a pH below the pH_{pzc} will yield a positive surface charge. The untreated carbon with a pH_{pzc} of 10.4 (Table 6-1) in contact with a natural water pH of approximately 7 will have a positive surface charge. Given this difference in surface charge, it was hypothesized that the untreated carbon would adsorb more NOM and, as there are fewer adsorption sites available after NOM adsorption, less MIB adsorption would occur (i.e., competitive adsorption). Bach (2004) also hypothesized that the air treated carbon, with a pH_{pzc} of 8 in contact with a natural water of pH 7, will have less of a positive surface charge than the untreated carbon and will not adsorb as much NOM, leaving more adsorption sites available for MIB. However, the NOM remaining in solution was not evaluated to support the hypothesis of competitive adsorption.

Therefore, the intent of the present work is to bolster the hypotheses made in the work of Bach (2004) concerning differences in adsorption performance of the treated carbons. An additional goal is to evaluate the removal of a compound other than MIB, one that will have different chemical properties, to determine if the pH excursion treatments impact the adsorption

of other compounds. To this end, the removal of phenol by the treated carbons in a column study was also be evaluated.

Impact of Wetting Time on MIB Adsorption for CO_2 Treated Carbon

The CO_2 treated carbon was found to remove more MIB (10%) than the untreated carbon at the lower carbon doses (Figure 6-1), despite the similarity in their total acidity (Table 6-1). A possible explanation for this occurrence is a disparity between the time it takes the CO_2 treated carbon to wet compared to the untreated carbon. To determine if this proposed mechanism is plausible, the adsorption experiments were repeated for the CO_2 treated carbon and the untreated carbon with DI water except that the respective carbons were mixed with DI water for a period of time (i.e., 0, 5, 60, and 150 minutes; wetting time) before the MIB was added, instead of simultaneous water/MIB addition. The results of this experiment are shown in Figure 6-3 with error bars representing one standard deviation of replicate experiments.

As the wetting time increased (i.e., the longer the carbon was in contact with only DI water before addition of MIB) the lower the adsorption capabilities of both the CO_2 and the untreated carbon. This is expected, as the carbons will adsorb water which blocks the adsorption sites available for MIB when it is added after 5, 60, or 150 minutes. The observation that the adsorption capacities of the CO_2 and untreated carbon are equal after 150 minutes wetting indicates that the adsorption advantage of the CO_2 treated carbon is likely related to its temporarily decreased water adsorption. This phenomenon is expected to hold true even in natural waters, where the CO_2 treated carbon also outperformed the air treated and untreated carbons (Figure 6-2).

In separate experiments, CO_2 bubbling of an MIB solution containing the untreated carbon demonstrated no effect on MIB removal when the volatilization of MIB from solution was taken into account. Volatilization under these experimental conditions (i.e., bubbling with

CO_2) yielded an MIB removal of approximately 50%. Therefore, simply the presence of CO_2 in water and any effect it has on pH did not affect MIB adsorption, a finding supported by Herzing et al. (1977).

MIB Adsorption from Natural Water

An increase in removal of MIB with the air treated carbon at low carbon doses compared to the untreated carbon, as shown in Figure 6-2, was hypothesized to relate to competitive adsorption with NOM. The phenomenon of decreased MIB removal with an increase in NOM removal over a range of pH values is supported in the work of Tennant (2004). To substantiate this hypothesis in the work of Bach (2004), Table 6-2 shows the results of the evaluation of the concentration of NOM remaining in solution, represented by dissolved organic carbon (DOC), after 24-hr of contact with a 20 ppm dose of carbon and 153 ng/L MIB. The concentration of NOM remaining in solution is lowest for the untreated carbon and highest with the air treated and CO2 treated carbon, as anticipated by the theory that NOM is attracted to the positive charge on the untreated carbon. Given that fewer adsorption sites are available for MIB once NOM has adsorbed to the surface, it is anticipated that the removal of MIB will decrease as the removal of NOM increases, which is the case when comparing Figure 6-2 to Table 6-2. The CO2 treated carbon outperforms the air treated carbon, despite the similar removal of NOM, due to the CO2 treated carbon's increased wetting time.

Phenol Adsorption from Deionized Water

To determine whether the impact on adsorption performance with treatments to overcome pH excursions is dependant on MIB being the target compound and on batch studies, the performance of an air treated, CO_2 treated, and an untreated commercially available carbon (F400) was evaluated for the removal of phenol in DI water via a column study. The results of

this study are shown in Figure 6-4 where the effluent phenol concentration from the column is shown versus bed volumes (BV) treated.

As with the batch studies, the treatments to overcome pH excursions, performed on a commercially available activated carbon in this case, showed a difference in adsorption performance depending on the treatment used. Not surprisingly, given the dependence of phenol adsorption on the oxygenation of the surface (Bansal et al., 2002; Salame and Bandosz, 2003), the air treated carbon results in fewer bed volumes treated before a measurable concentration of phenol is produced in the effluent. Moreover, the phenol concentration is higher in the effluent of the air treated carbon's column at similar bed volumes treated by the CO_2 and untreated carbons. Again, the impact of the increased surface oxygenation of the air-treated carbon, negatively impacts the performance of the air treated carbon for phenol removal due to an increase in the carbon's surface oxygenation.

Interestingly, Figure 6-4 does not show an increase in the performance of the CO_2 treatment as compared to the untreated carbon as found with MIB removal in batch studies. It is possible that the difference in wetting, which played a role in the batch studies, does not manifest in the column studies due to the difference in adsorption kinetics (e.g., batch versus flow-through systems). More likely, the slight impact on adsorption that results from a difference in wetting time (e.g., approximately 10% improved removal of MIB) in DI water batch studies containing ng/L concentrations of MIB does not manifest in a solution containing mg/L concentrations of the target compound (phenol). In other words, the high concentration of phenol drives the compound onto the carbon's surface via a concentration gradient that overcomes the slight influence of wetting time. Under these conditions, the dominating factor may be the relative

oxygenation of the carbon's surface and, as has been previously discussed, the carbon dioxide and untreated carbon have similar surface acidity.

Conclusions

The adsorption capacity for MIB of two GACs that have undergone two separate treatments to overcome pH excursions, namely air and CO_2 treatments, were compared in a study by Bach (2004). The untreated carbon removed more MIB than the air treated carbon while this trend was reversed when NOM was present. Increase in surface acidity with the air treated carbon created preferential adsorption sites for water, which out-competed MIB in water not containing NOM. When NOM was present, the negatively charged NOM was attracted to the positively charged surface of the untreated carbon via electrostatic forces, thus out-competing MIB for adsorption sites. In addition, the hypothesis that in both water scenarios the CO_2 treated carbon removed the most MIB due to a longer wetting time was confirmed by analysis of MIB removal versus wetting time. Finally, an analysis of the removal of phenol following air and CO_2 treatments on a commercially available carbon showed a decrease in performance with air treatment, as found in batch studies with MIB. However, similar performance of the CO_2 and untreated carbons for removal of phenol was found as compared to the improved performance of the CO_2 carbon versus the untreated carbon in MIB removal. These results reaffirm that treatments to create pH stable reactivated carbons will change the carbon's adsorption capabilities and, thus, use of these treatments should be based on more than their ability to create pH stable carbons.

Table 6-1. Characteristics of sample carbons

Treatment	pH_{pzc}	BET surface area (± 5%)	Total acidity (μeq/g)
Carbon dioxide	8.3	885	170
Air	8.0	927	400
Untreated	10.4	896	160

Table 6-2. DOC remaining in solution after contact with 20 ppm carbon

Treatment	DOC remaining in solution (mg/L)
Carbon dioxide	36.8 ± 0.7
Air	34.8 ± 1.0
Untreated	31.0 ± 1.5

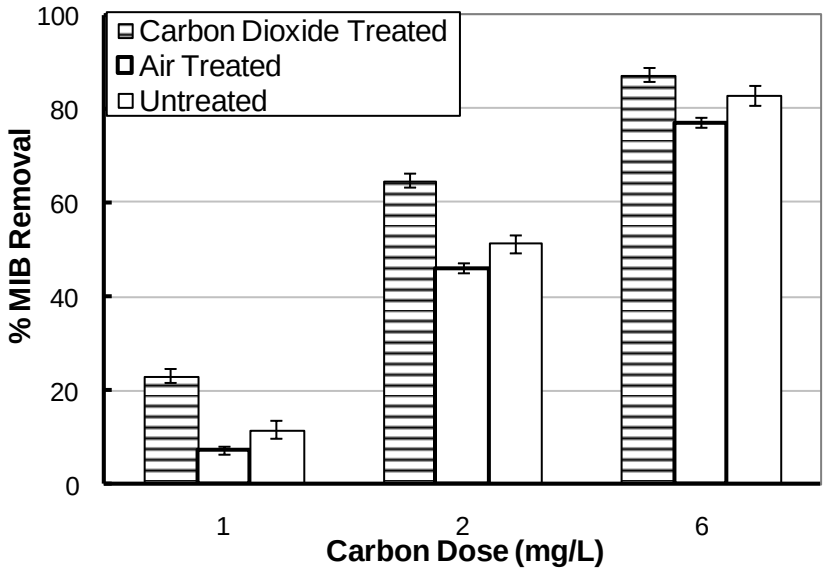

Figure 6-1. Percent removal of MIB in DI water versus dose of carbon (24-hr contact time) (Bach, 2004)

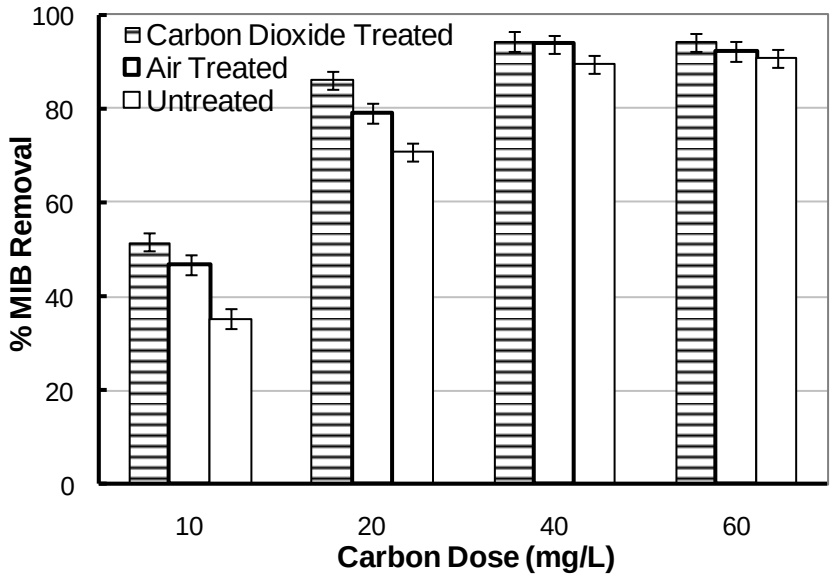

Figure 6-2. Percent removal of MIB in raw water (TOC = 10 mg/L) versus dose of carbon (24-hr contact time) (Bach, 2004).

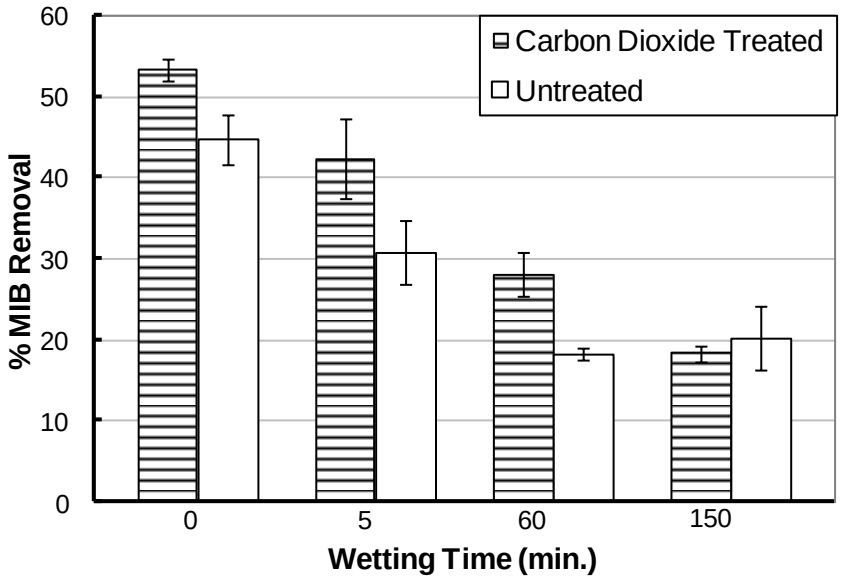

Figure 6-3. Percent MIB removal versus wetting time in DI water with a CO_2 and untreated carbons (carbon dose = 2ppm, contact time = 24 hrs).

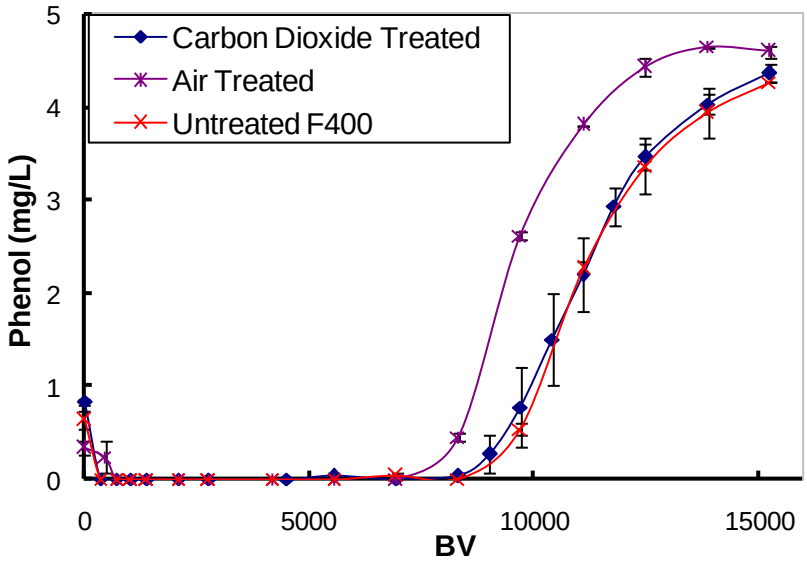

Figure 6-4. Effluent phenol concentration in DI water versus BV treated with a CO2 treated, air treated, and an untreated carbon.

CHAPTER 7
IMPACT OF DISSOLVED OXYGEN ON ACTIVATION OF POWDERED ACTIVATED CARBON

Despite the millenniums over which activated carbon has been used and the centuries of research into the mechanisms behind activated carbon's success, there is currently minimal research effort being put into tailoring the carbon surface to enhance carbon's capacity for specific contaminants. The lack of tailoring means that activated carbon is often not utilized to its full potential. For example, perchlorate, a chemical found in rocket fuel and increasingly discovered in drinking water supplies, had minimal affinity for activated carbon in preliminary studies (Chen et al., 2005a). However, subsequent studies using an ammonia-tailoring process found that the tailored activated carbon removed four times as much perchlorate as a standard activated carbon, indicating that many studies using standard activated carbon may not represent the full capabilities of activated carbon for this particular pollutant (Chen et al., 2005a, 2005b).

As new contaminants are found and existing regulations made more stringent, the ability to efficiently tailor activated carbons for removal of specific compounds, by manipulation of pore size and/or surface chemistry, is crucial. Therefore, the objective of this work is to tailor the thermal activation of a wood-based carbon by changing the dissolved oxygen (DO) content of the water used to create the steam used for activation. Research by Chestnutt et al. (2007) has determined that altering the DO in the water used to create steam for reactivation of carbon can alter the resulting reactivated carbon but it could be possible to modify the activated carbon from its inception using this method rather than during the reactivation process. By developing a method of activation that requires only a shift in DO content to create activated carbons with differing properties, capable of adsorbing a variety of contaminants, activated carbon is thus made adaptable to the changing types of and standards for contaminant removal. To this end, the ability of the DO content of the water used to create steam for activation of a wood-based fly ash

to impact adsorption was evaluated along with the impact on the carbon's chemical and physical properties. In addition, the interaction of the DO and typical tailoring parameters of temperature, time, and oxidant flow rate was evaluated.

Dissolved Gases in Solution

Alteration of the dissolved gases in solution will occur as a result of attempts to change the DO and, therefore, the quantity and possible effects of the change in these dissolved gases should be evaluated. The dissolved gases in solution chosen for evaluation at the individual experimental conditions were those naturally found in the atmosphere at the four highest concentrations, namely, nitrogen, oxygen, argon, and carbon dioxide. The system employed in this work includes a pressure vessel set at 10 psi (gauge) for a total pressure on the system of 24.7 psi (absolute) where the pressuring gas was air, oxygen, or nitrogen. For comparison, the theoretical concentration of dissolved gases in a system at atmospheric pressure was also calculated. Complete purity of the gas above the systems pressurized in nitrogen and oxygen is likely not a realistic condition but, for the purpose of this exercise, it is assumed that any air remaining in the system will contribute only negligibly to the final dissolved gas concentrations. The theoretical dissolved gas concentrations are shown in Table 7-1 along with the measured values for the DO. An example calculation using Henry's law can be found in Appendix A.

A theoretical DO value of 9.1 mg/L at atmospheric pressure fit within expected values, while DO levels under pressurization of the system, even in air, were higher than the measured values. A brief review of industrial techniques shows that utilizing a pressure vessel to increase the DO level is not unique. The purpose of dissolved air flotation (DAF) is to infuse water with a high level of DO so that, when the DO devolves from solution, the oxygen bubbles will lift microscopic particles to the surface which are then removed (Appleton, 2006). DO levels used in DAF technology may be as high as 40 mg/L and may be attained through pressurization. A

patent by Barnett (1999) employs a pressure system to imbue water with DO at five times atmospheric pressure, which is indicated as approximately 50 mg/L, to aid in biological treatment of a wastewater. These findings indicate that the theoretical DO levels found under pressurization are within reason.

However, there is a significant discrepancy between the theoretical DO level, predicted using Henry's law, and the measured DO level. The reason for the failure of Henry's law to fit the experimental data obtained could be one of several. While Henry's law is expected to fail at high pressures (Petrucci and Harwood, 1997), research has shown that the Henry's constant of nitrogen from 14.4 psi to approximately 573 psi only varied by 10% and only 8% in a study of nitrogen with oil at pressures of 14.7 psi to 735 psi (Gerth, 1985). Given that the experiments herein employ pressure not even twice that of atmospheric, it is not considered likely that the system deviates significantly from Henry's law due solely to an increase in pressure.

Henry's law also applies only in systems at equilibrium and, moreover, gas/liquid equilibrium is a very slow process compared to many other reactions involving dissolved species. Equilibrium in gas/liquid systems depends on the interfacial area available for gas transfer, which explains why bubbling a liquid with gas increases the rate of equilibration as the small gas bubbles create higher surface area for water/gas contact compared to gas above a layer of water (Benjamin, 2002). The system employed herein did utilize some form of bubbling, more in the nitrogen system than in others; the system with oxygen easily exceeded the limit of detection of the DO probe (i.e., greater than 20 mg/L) with even seconds of oxygen bubbling. Given the ease with which the DO level can be changed by bubbling the water with oxygen for a short amount of time, it is likely this latter phenomenon is creating the discrepancy between the experimental DO levels and that predicted by Henry's law; namely, the system is not at

equilibrium. The portion of the reaction that progresses over the duration of the experiment leads to the experimentally determined values which, as seen in Table 7-1, are at most half as high as the theoretical values. Of most interest is the difference between theoretical and experimental values for the oxygen pressurization scenario. For the purposes of this experiment's goals (i.e., determination of the effect of a change in oxygen), the gas/liquid system does not need to be at equilibrium as long as the DO level is relatively steady throughout the experiment and uniform between experiments. The DO level throughout experiments was easily held within +/- 1 mg/L.

At high temperatures, as the water turns from liquid to vapor, the dissolved gases will devolve and will be present at higher than atmospheric concentrations inside the furnace. The use of high temperatures in inert environments, such as nitrogen and argon, as a means to remove oxygen-containing functional groups and create a more basic carbon is common (Leon y Leon et al., 1992; Menéndez et al., 1996; Barton et al., 1997; Considine et al., 2001; Lillo-Rodenas et al., 2005). However, it is not expected that the small concentration of inert gas (i.e., nitrogen and argon) (e.g., $8*10^{-6}$ mol at the highest) versus oxidizing gas (i.e., water vapor and oxygen) (e.g., 0.886 mol H_2O) is high enough to qualify as an inert environment where the chemisorption of oxygen would be deterred (See Appendix A for example calculation of moles of dissolved gas versus moles of water vapor). Aside from the possibility of creating an inert environment during the oxidation step, the adsorption of these inert gases during the oxidation step would be negligible as the preceding pyrolysis step would saturate the carbon with as much nitrogen as it could adsorb at that temperature (Puri, 1970).

Given that carbon dioxide in solution can change the pH of the system and its associated alkalinity, it is of interest to calculate the theoretical shift in pH with an increase in carbon

dioxide in solution. Whereas water exposed to the air at atmospheric pressure would be expected to have a pH of 5.7, based solely on carbon dioxide dissolution in water, water exposed to air at 1.68 times atmospheric pressure would be expected to have a pH of 5.59, only slightly less than that at atmospheric pressure (See Appendix A for calculations). It is not expected that this slight shift in pH will cause any significant change in the activation of carbon with this water used as the basis to make steam.

Carbon dioxide is also used as an oxidant in the activation of carbon according to the reactions shown in Chapter 2. However, given that the concentration of carbon dioxide is an order of magnitude less than that of oxygen, which can react with twice as many reactive sites as can carbon dioxide (see Chapter 2), the contribution of carbon dioxide activation in all scenarios seems negligible. Given the discussion of the relative impact of nitrogen, argon, and carbon dioxide, it is clear why changes in dissolved oxygen are taken as the dominant influencing factor in these activations.

Box-Behnken Approach and Mass Loss

In order to evaluate the impact of DO and other activation parameters on the resulting activated carbon, the Box-Behnken approach, an example of a statistical design of experiments, was employed. The first step in the Box-Behnken design process is to determine the levels of each of the four factors to be evaluated (i.e., activation time, activation temperature, steam to carbon ratio (i.e., steam flow), and DO level). Preliminary experiments indicated what levels of the four factors would allow for even spacing of levels, as required by the Box-Behnken approach, be practical to employ, and encompass the broadest range of impact on the carbon. A more detailed discussion of the selection of the levels of these parameters, including results of preliminary tests, can be found in Appendix B. The results of these studies yielded the three levels of the four factors shown in Table 7-2.

Next, 29 separate activated carbons were created according to the Box-Behnken design of experiments. Of these carbons, 25 were unique based on the setting of the activation time, activation temperature, SC, and DO level while four samples were replicates of the center point. A complete list of the activation parameters for each of the 29 carbons can be found in Appendix C.

The initial mass of carbon before activation and the final mass after activation were recorded for each carbon in order to determine the mass lost during activation. The mass loss is a measure of the gasification of the carbon (i.e., the degree of activation) and was the first response evaluated. The mass loss data were input into the Design-Expert software which analyzed the significance of each factor in mass loss and produced a model based on these data to predict the mass loss that would result over the entire range of levels and factors studied. For a complete list of mass loss for each carbon and the entire output from Design-Expert, see Appendix C. Pertinent statistical information and results from the Box-Behnken analysis have been summarized in Table 7-3. Note that a Prob > F (P-value) greater than 0.05 for lack of fit (i.e., insignificant lack of fit) and a low standard deviation, which includes both the lack of fit and random error, are preferred.

The statistically significant factors (Prob > F of less than 0.05) in mass loss were found to be temperature and time with significant interactions between temperature and time and also temperature and SC. The final column of Table 7-3 represents the predicted weighting of each parameter where the summation of the activation parameters, multiplied by their weighting factor, and the intercept would yield the predicted mass loss. Note that a negative weighting factor indicates a detrimental impact of this factor on mass loss. Figure 7-1 shows a 3-D model produced by Design-Expert of the predicted mass loss, in percent of initial mass, versus time and

temperature of activation, both significant factors. The levels of the remaining two factors are set at their medium value.

The model resulting from the Box-Behnken analysis predicts that as the time and temperature of activation increases so will the mass loss of the carbon. The slight curves in the graph are indicative of an interaction where the two factors acting together have an influence greater than the factor acting alone. The statistical significance of the interaction between time and temperature is affirmed by the results of Design-Expert as shown in Table 7-3. Indeed, the predicted model is a quadratic model due to the presence of an interaction between temperature and time and also temperature and SC.

The influence of temperature and time on mass loss during activation, namely an increase in mass loss with an increase in time and temperature, is an expected result as this phenomenon is well-supported in the literature (Gergova et al., 1993; Gonzalez et al., 1994; Rodríguez-Reinoso et al., 1995; Gergova et al., 1996; Martin-Gullon et al., 1996; Tennant and Mazyck, 2003). An increase in temperature will speed gasification reactions, which remove carbon atoms and therefore mass, while an increase in activation time will allow for more gasification. At 623K, the interaction between time and temperature of activation is evident as the increase in mass loss with time is negligible indicating that at this low temperature there is minimal gasification that will occur such that longer treatment times do not impact mass loss. Indeed, an activation temperature of 623 K is low compared to that normally employed in activation (e.g., 1073K) (Kawamura, 2000). The influence of treatment time and temperature on surface area is confirmed in Table 7-4, where there is an increase in surface area with time and temperature except at 623 K where surface area is unaffected by an increase in treatment time.

The interaction between temperature and SC in mass loss can be seen in Figure 7-2 in the curved sides of this 3-D graph. Note, however, that SC alone is not a statistically significant factor influencing mass loss; SC is only significant when interacting with temperature.

An interaction between temperature and SC has been shown in the literature where only at high temperatures does the steam flow influence the gasification of the resulting carbon. Hydrogn is produced as a reaction of the water molecule with the carbon surface and also the water-gas shift reaction (See Chapter 2). The hydrogen may then react with an active site on the carbon surface which prohibits further reaction of the steam with that active site, thus inhibiting gasification (Walker et al., 1959; Puri, 1970; Menéndez et al., 1996; Lussier et al., 1998; Bansal et al., 2002). It has been postulated by Rodríguez-Reinoso et al. (1995) that at higher steam flow and higher temperatures the inhibiting reactant, hydrogen, is less effective. Therefore, an increase in steam (i.e., oxidant) will produce greater gasification and mass loss but only at higher temperatures where the creation of the inhibiting agent hydrogen, which would increase with an increase in steam flow, does not influence gasification. The influence of SC and temperature on surface area is supported in Table 7-4, where there is an increase in surface area with SC except at low temperature.

The Design-Expert results for mass loss, indicating a positive relationship between time and temperature and also an interaction with time and temperature and with SC and temperature, are an affirmation of the reliability of this approach as these results conform to phenomenon found in the literature concerning activation with steam. DO was not found to be a significant parameter in mass loss during activation.

MIB Removal

Following creation of the 29 activated carbons, these carbons were then powdered to create a PAC slurry for use in subsequent batch adsorption studies. The first performance

response of interest was the performance of the activated carbons for removal of the common taste- and odor-causing compound MIB. Preliminary experiments demonstrated that a PAC dose of 10 mg/L in contact with 153 ng/L of MIB for 24 hours would yield a suitable range of removal. The MIB removal data were input into the Design-Expert software which analyzed the significance of each factor in the removal of MIB and produced a quadratic model to predict the performance of the carbons over the entire range of levels studied. For a complete list of the MIB removal of each carbon and the statistical results of Design-Expert, see Appendix C. Pertinent statistical information for the MIB removal response is summarized in Table 7-5.

All parameters were found to be statistically significant factors (Prob > F of less than 0.05) influencing MIB removal, whether acting independently or as an interaction, as expected given that the selection of these factors was based on their influence on adsorption of MIB. While the final column of Table 7-5 contains the weighting factor of each parameter's influence on the predicted MIB removal, Figure 7-3 shows a 3-D model of the predicted removal of MIB versus both time and temperature of activation. As the time and temperature of activation increases, so does the removal of MIB. Note that the shape of the mass loss and MIB removal curves versus time and temperature are similar at higher temperatures. Figure 7-4 shows MIB removal versus SC and DO, the interaction of which was found to be significant, as well as SC alone, in the removal of MIB.

SC acting alone has a significant impact on removal of MIB but the interaction between DO and SC is also significant as demonstrated in Figure 7-4 where the trend in removal changes depending on the level of DO. At low SC, an increase in DO is detrimental while at high SC a change in DO yields negligible change in MIB removal.

The trends in MIB removal with changes in temperature, activation time, SC, and DO relate to chemical and/or physical changes in the carbon caused by these activation parameters. As such, the following sections explore the chemical and physical properties of the activated carbons in order to elucidate the role of each of the four factors on these properties and subsequent adsorption of MIB.

Physical Properties

The mass loss, which can be taken as a general indicator of the gasification of the carbons, was shown to be impacted by temperature and time. It is well known that an increase in mass loss generally correlates to an increase in both surface area and pore volume as gasification removes carbon atoms from the internal surface of the carbon (Gergova et al., 1994; Centeno et al., 1995; Rodríguez-Reinoso et al., 1995; Gergova et al., 1996; Mazyck and Cannon, 2002; Zhang et al., 2003). Therefore, it is expected that the increase in MIB removal with time and temperature, predicted in Figure 7-3, is due in part to the increase in the surface area of the carbons related to temperature and time as found in Table 7-4. An improvement in the removal of MIB with time at low temperature, where the physical structure of the carbon remains similar, may be related to changes in surface chemistry as discussed further in later sections.

In order to evaluate the influence of the extreme levels of SC and DO on the physical properties of the carbon, and to determine if physical properties dominate the observed phenomenon of Figure 7-4, four carbons representing the four corners of Figure 7-4 were evaluated for their BET surface area and pore size distributions. Descriptions of the conditions of activation for these four carbons as well as their BET surface area and their pore volumes are shown in Table 7-6. These carbons were labeled based on a code where SC is designated S with levels at low (L) or high (H) and the same applies for the DO (D) level.

Within standard error for BET surface area measurements, only SHDL and SLDH have different surface area. A similar BET surface area but an increase in mass loss as predicted with an increase in steam flow (Figure 7-2) indicates that the changes in steam flow yield different pore size distributions making up this surface area. A summary of the pore volume is presented in Table 7-6 with the PSD plots shown in Figure 7-5.

Evaluation of the PSDs of these four carbons shows a predominance of micropores with a small volume of mesopores and macropores. In a study by Tennant and Mazyck (2003) for MIB removal using PAC, carbons having a large volume of large micropores and small mesopores (1.2-10 nm) were found to correlate to the highest removal of MIB. Therefore, this range is also presented in Table 7-6 as this gives the range of pore sizes that are expected to most significantly affect MIB removal.

From Table 7-6, it is apparent that an increase in steam flow (SHDL versus SLDL or SHDH versus SLDH) will produce a higher volume of pores in the range of 1.2-10 nm. An increase in the PSD with an increase in steam flow is anticipated based on the correlation between increase in steam flow and mass loss, where a higher concentration of oxidant yields more gasification. However, the similarity in SHDH and SLDL indicates that a decrease in steam flow can still produce a similar pore volume to a higher steam flow if only the DO content were decreased which would have advantages in terms of cost savings of having to pump a lower flow of steam to get the same result. SLDH, having a low steam flow and also high DO, has the lowest volume of pores in the 1.2-10 nm range.

The influence of DO on the pore size distribution, namely the occurrence of a higher volume of 1.2-10 nm with a lower DO may relate to a study of the activation of carbon with oxygen by Tomkow et al. (1977). These authors suggested that only limited micropores are

formed during activation with oxygen due to the formation of oxygen-containing functional groups at the entrance of the micropores which cuts off the micropores from further activation as the oxidant cannot fit into the narrowed entrance created by the functional groups. In the current research, where the DO in the water is expected to devolve upon conversion of the water into steam, the small quantities of free oxygen may react with the carbon surface to create oxygen-containing functional groups which would impede further activation by steam. The influence of DO on the surface chemistry of the carbon will be discussed in the following section.

As the volume of 1.2-10 nm pores are expected to correlate to MIB adsorption, it is anticipated that SLDH, with the lowest volume in the ideal range of pore sizes, would remove the least MIB. In the predicted MIB removal of Figure 7-4 this theory is confirmed in that SLDH is the only carbon to have a significantly different removal of MIB. The similarity in the ideal range volume of SLDL and SHDH explains their similar removal of MIB but one may expect that SHDL would have higher removal as it has a higher volume of ideal pores compared to the other carbons. It is most likely that the small increase in this ideal pore range volume from SLDL and SHDL (i.e., 13%) compared to the large increase in this pore range from SLDH and SHDH (i.e., 39%) is not significant enough to manifest differences in performance outside of the standard deviation.

It is clear that the DO content of the water used to create steam for activation of these carbons influenced the physical structures of these carbons but the influence of the DO on the chemical properties of the carbon must also be investigated.

Surface Chemistry

Following creation of the 29 activated carbons, the samples were then analyzed for their pH at the point of zero charge (pH_{pzc}). The pH_{pzc} is often used as a measure of the carbon's surface acidity where a lower pH_{pzc} indicates a more acidic surface (El-Sayed and Bandosz,

2003; Ania et al., 2004). Furthermore, activated carbon acidity can be related to the content of the oxygen-containing functional groups on the carbon surface which are often acidic (Puri, 1970; Otake and Jenkins, 1993; Barton, 1997; Ania et al., 2004). The pH_{pzc} data was input into the Design-Expert software which analyzed the significance of each factor in the resulting pH_{pzc} of the carbons and produced a linear model to predict the pH_{pzc} of the carbons over the entire range of levels studied. For a complete list of the pH_{pzc} values of each carbon and the statistical results of the Design-Expert process, see Appendix C. Pertinent statistical information for the pH_{pzc} response is shown in Table 7-7.

A linear model best fit the data, which means that no interactions were statistically significant and only temperature and SC were found to be statistically significant factors impacting the pH_{pzc}. Figure 7-6 shows a 3-D model of the predicted pH_{pzc} versus both SC and temperature of activation.

As demonstrated in Figure 7-6, as both the SC and temperature of activation increase so does the pH_{pzc} (i.e., the activated carbon becomes more basic/less acidic). The impact of temperature on pH_{pzc} relates to the decomposition of acidic oxygen-containing functional groups starting at 773K. Removal of oxygen containing-functional groups to create a more basic carbon through the use of high temperatures in inert environments is a common practice (Leon y Leon et al., 1992; Menéndez et al., 1996; Barton et al., 1997; Considine et al., 2001; Lillo-Rodenas et al., 2005). While inert conditions at high temperatures were not deliberately employed for this purpose in the current research, following activation the reactor was allowed to cool to room temperature in a flow of nitrogen gas before the carbon sample was removed. During the cooling of the sample from as high as 973K to less than 373K, the carbon is briefly exposed to high temperatures in an inert environment which may strip the surface of the functional groups

formed during the activation process. A less acidic carbon with increasing activation temperature supports the finding of Figure 7-3, where improved MIB removal was predicted as temperature of activation increases; a less acidic surface would attract fewer water molecules leavings the adsorption sites free to remove MIB (Pendleton et al., 1997; Considine et al., 2001). Though the pH_{pzc} is predicted to be constant regardless of activation time, as activation time was not found to be a significant factor in pH_{pzc}, there may be changes in the quantity of basic groups with time that are not evident in this study of surface chemistry but manifest in improved removal of MIB with activation time at even the lowest temperature employed (Figure 7-3).

The occurrence of an increase in steam flow relating to an increase in pH_{pzc} (i.e., an increase in basicity) may be explained by an associated increase in the formation of hydrogen as the steam flow is increased. Recall that hydrogen is created as a result of the water molecule's reaction with the carbon's surface and/or the water-gas shift reaction. The free hydrogen molecule would then react with active sites to form hydrogen-containing functional groups (Walker et al., 1996). These hydrogen-containing functional groups would occur on sites that could have contained an oxygen-containing functional group, as Bansal et al. (1974) determined that both oxygen and hydrogen adsorb to the same reactive sites, so that the formation of an acidic-oxygen containing functional group is avoided. Aside from possible direct competition of the hydrogen and oxidant for adsorption sites, the hydrogen also blocks active sites from further reactions with atmospheric oxygen to create functional groups following activation. The process of preventing oxygen chemisorption by preadsorption with hydrogen has been proposed by Bansal et al. (1974) and confirmed by Mendendez et al. (1996) where hydrogen exposure was used to create a stable basic carbon.

As a less acidic surface is favorable for the removal of MIB, an increase in steam flow, the creation of hydrogen, and the corresponding increase in pH_{pzc} would be expected to correspond to improved MIB removal. In support of the link between steam, hydrogen, and MIB removal, Nowack et al. (2004) observed similar performance for removal of MIB in a steam treated carbon compared to a carbon treated in hydrogen at a similar temperature. These authors took the similar performance of the steam and hydrogen treated carbons as support of the influence of the water-gas shift's production of hydrogen and subsequent reaction of this hydrogen with the carbon surface on improved removal of MIB. The influence of steam flow on surface chemistry supports the results of Figure 7-4 which shows that at high DO there is an improved removal of MIB with increasing SC.

The expected increase in performance as SC is increased is only significant at high DO, at low DO the performance of the carbons remains the same regardless of steam flow. It is possible that at high DO, the competition provided by hydrogen is more significant as there are more oxidants to compete with (i.e., both steam and O_2). Without this competition from hydrogen, the higher oxygen in contact with the carbon, as the DO devolves from the water upon creation of steam, results in the creation of more acidic functional groups and therefore a more acidic carbon. At low DO, hydrogen is competing with a smaller quantity of oxygen and the resulting impact of competition with hydrogen is less significant and produces negligible results on total acidity. However, the DO level was not found to significantly impact the total acidity of the carbon, which could indicate that, while the impact on the total number of oxygen-containing functional groups remains the same regardless of DO, the type of individual oxygen-containing functional groups changes with the DO level. A change in the dominant type of oxygen-containing functional group would not necessarily change the total acidity.

Activation with oxygen would produce active sites with different energy levels than those produced by steam reactions and these active sites may react to form different functional groups when exposed to the atmosphere. Puri (1970) notes that the activity of the surface may determine the type of group formed, with more active surfaces producing lactones while less active sites produce carbonyls. Otake and Jenkins (1993) and Molina-Sabio et al. (1996) also make note of differences in the thermal stability of surface oxides depending on the method of oxidation (air versus HNO_3 activation and steam versus CO_2 activation, respectively). The findings of these studies, along with the knowledge of the relative stability of functional groups created by oxygen and steam reactions, where the exothermic nature of the $C\text{-}O_2$ adsorption step makes the resulting functional groups short-lived, support a hypothesis that different oxidants can yield different types of functional groups. Therefore, by passifying the surface of the carbon in low DO versus high DO, the formation of different functional groups may be avoided though the total acidity remains unchanged. In other words, if oxygen reacts with the surface in the high DO conditions, different types of individual functional groups may result than if mostly steam reacted with the surface, as in the low DO conditions.

A preliminary analysis of the precursor and activated carbons demonstrated that these carbons are highly basic, as indicated in Figure 7-6, which makes their analysis via the Boehm titration method, a common wet method of evaluating individual acidic functional groups, difficult. In a study by El-Sayed and Bandosz (2003) of individual functional groups using the Boehm titration method, when the total basicity was almost 3 times the measured total acidity the Boehm titration method measured negligible quantities of individual acidic functional groups. Therefore, to evaluate whether surface chemistry is a factor in the observed changes in Figure 7-4, the same four carbons representing the four corners of Figure 7-4 and described in Table 7-6

were evaluated for their removal of MIB in dichloromethane, a nonaqueous solvent. The goal of this experiment is to determine whether MIB removal changes depending on the activation conditions even in a scenario where the acidic surface's interaction with the polar water molecule has been removed. The MIB removal of these four carbons in the dichloromethane solvent, where the carbon dose was increased to 1100 mg/L, is shown in Table 7-8.

The removal of MIB in dichloromethane is low compared to the removal of MIB in water. Considine et al. (2003) also evaluated the removal of MIB from dichloromethane using activated carbon and the decrease in removal of MIB in dichloromethane was explained by the difference in the polarity of the solvents and the way the solvent interacts with the carbon surface. Within standard error, the removals of MIB in dichloromethane with the four corner point carbons are similar. The similar removal supports the theory that a difference in surface chemistry is partly responsible for the difference in removal of the SLDH carbon, as when the water molecules and the hypothesized interaction of the water molecules with the acidic functional groups are removed from the solution SLDH performs just as well as the other three carbons.

Chemical versus Physical Methods of Removing DO

Removal of DO can be accomplished either by physical means (e.g., bubbling with nitrogen gas or passing the water through membranes) or chemical means (e.g., addition of an oxygen scavenger). For use in boiler streams, it has been found that physical methods do not allow for removal of all of the dissolved oxygen and therefore the streams are often polished with an oxygen scavenger (Bizot and Bailey, 1997). Sodium sulfite is a common oxygen scavenger employed in the boiler industry because it is relatively cheap, safe, and effective at removing DO. As this study has so far focused on the removal of oxygen through physical means, it was also of interest to evaluate a chemical means of removing dissolved oxygen to

determine if the results are similar. To this end, the SHDL and SLDL activation scenarios described in Table 7-6 were repeated but with sodium sulfite used to decrease the DO. The carbons which mimic the DO levels used in the Box-Behnken approach (i.e., 3 mg/L DO) are labeled $SHDL_s$ and $SLDL_s$, where the subscript s is used to denote that these conditions were created as a result of sodium sulfite addition. In addition, two carbons were created under the same conditions as SHDL and SLDL except that the DO was reduced to 0 mg/L, which is easily done with sodium sulfite compared to physical removal of DO which cannot remove all DO. The 0 mg/L DO carbons are labeled $SHDL_o$ and $SLDL_o$. The MIB removal and the chemical and physical properties of these four activated carbons are shown in Table 7-9.

Both sets of carbon, comparing low and high SC at a given DO concentration, have similar BET surface area and similar trends in pH_{pzc}, namely a decrease in pH_{pzc} at low steam flow. The removal of MIB with the $SHDL_s$ and $SLDL_s$ also showed similar trends to the removal of MIB with SHDL and SLDL (approximately 62% MIB removal) with no significant change in removal with a change in SC. The MIB removal with $SHDL_o$ and $SLDL_o$, however, showed a decrease in removal with $SHDL_o$ compared to $SLDL_o$. The difference in removal with the 0 mg/L DO activations may relate to the difference in their ideal pore size volume (1.2-10 nm). The PSD plots for these carbons are shown in Figure 7-7.

Of the four carbons created with sodium sulfite as an oxygen scavenger, only $SHDL_o$ had a significantly different pore volume in the ideal range of pores than the other three carbons. The decrease in the volume of this ideal pore range explains the decrease in MIB removal with this carbon. It may be that at this lower DO, where more sodium sulfite was added to reach 0 mg/L of DO, and a higher SC, where a higher volume of water vapor containing sodium sulfite

contacted the carbon, more sodium sulfite interacts with the carbon surface, thus impacting adsorption.

Phenol Removal

The same PAC slurries created from the 29 activated carbons of the Box Behnken where used in a phenol batch adsorption study. The performance of the carbons for removal of phenol is of interest because of the different adsorption mechanism for the adsorption of phenol (i.e, π- π bonding) versus MIB adsorption. In addition, phenol is a common toxic organic compound in surface waters for which activated carbon is used. Preliminary experiments demonstrated that a PAC dose of 50 mg/L in contact with 5 mg/L of phenol for 24 hours would yield a range of removal that was easily detectable. The phenol removal data was input into Design-Expert software which analyzed the significance of each factor in the removal of phenol and produced a linear model, indicating a lack of statistically significant interactions between factors, to predict the performance of the carbons over the entire range of levels studied. For a complete list of the phenol removal of each carbon and the statistical results of the Design-Expert process, see Appendix C. Pertinent statistical information for the phenol removal response is shown in Table 7-10.

Only temperature and time were found to be statistically significant factors influencing phenol removal. Figure 7-8 shows a 3-D model of the predicted removal of phenol versus both time and temperature of activation.

As with MIB removal, where both time and temperature were found to be significant factors, it is likely that increases in surface area and/or pore size distribution associated with increased temperature of activation and treatment time simply yielded more adsorption sites for phenol removal. In addition, the decrease in total surface acidity found with increasing temperature may also play a role in the increased removal of phenol with temperature as an

increase in surface acidity has also been found to be detrimental to phenol adsorption (Bansal et al., 2002; Ania et al., 2004).

Neither steam flow nor DO was found to be a significant factor in phenol removal. It is possible that the influence of surface chemistry and physical changes brought about by DO were overcome by the higher concentrations of phenol employed herein such that the concentration gradient drove the phenol onto the carbon surface despite the obstacles. Furthermore, as it was suggested that the different functional groups may have been created with different levels of DO and this is what impacts MIB removal, the particular acidic functional groups formed in the low SC and high DO carbons may not impact phenol adsorption as it impacts MIB adsorption. For example, in a study by Salame and Bandosz (2003) the decreased removal of phenol by wood-based activated carbons was shown to have a stronger correlation to an increase in the quantity of carboxylic groups than to total surface acidity. Another possibility is that the wood-based activated carbon used herein responds differently than coal-based carbons, as the difference in coal and wood-based carbons has been discussed. Specifically, one adsorption mechanism for phenol onto activated carbon is π- π bonding where the aromatic phenol and the aromatic π-electrons on the carbon surface interact. However, wood and wood-based precursors are seen to have higher H/C elemental ratios, which suggest a lower aromatic structure, than their coal-based counterparts (Buczek et al., 1993; Gergove et al., 1993; Pendleton et al., 1997; El-Sayed and Bandosz, 2003; Fernades et al., 2003). Therefore, the removal of phenol with the wood-based activated carbon used herein may not be impacted by changes in surface chemistry as it may have a low occurrence of π- π bonding in its original form.

Summary and Conclusions

The Box-Behnken approach was employed to evaluate the influence of four factors on the physical and chemical properties and performance of the resulting activated carbons. An

initial evaluation of mass loss following activation using the Box-Behnken design confirmed the validity of this approach as an increase in mass loss with activation time and activation temperatures as well as an interaction between activation temperature and SC are phenomenon supported in the literature.

The Box-Behnken approach also predicted an increase in MIB and phenol removal with activation time and temperature. An increase in the physical properties of the carbon with activation time and temperature, supported by an observed increase in mass loss under these conditions, as well as a decrease in surface acidity with an increase in activation temperature were deemed responsible for an increase in removal of these compounds.

An interaction between SC and DO was also seen with the removal of MIB where only at high DO and low SC did these factors impact MIB removal in the form of decreased removal. Neither DO nor SC was found to be significant in the removal of phenol. The physical properties of the carbon, namely a decrease in the PSDs of the carbons, explained a decrease in removal at the highest DO and lowest SC level. However, a low SC level was also found to correspond to a more acidic carbon which can impact MIB removal. While the total acidity of the carbons treated at low SC remained unchanged regardless of the DO level, the high DO activated carbon had decreased removal of MIB. It was proposed that different groups are formed at high DO, where the free oxygen devolved from the water upon creation of steam, while the total acidity remains unchanged. A lack of difference in removal found in dichloromethane, a nonpolar solvent, supports that the difference in removal found with low SC and high DO may be a combination of both physical and surface chemistry changes, though this theory would need to be confirmed with new techniques to evaluate surface chemistry on the heterogeneous and basic activated carbons used herein.

An additional study of DO removal with sodium sulfite indicated that high levels of sodium sulfite may be detrimental to MIB removal, though the amount required to decrease DO to 3 mg/L did not impact performance.

While the impact of DO on surface chemistry may require further study, it is clear that the DO level in the water used to create steam for activation of carbon does influence the resulting carbon's ability to adsorb certain compounds.

Table 7-1. Concentration of dissolved gases in water at 273 K

Gas (mg/L)	Air (14.7 psi)	Air (24.7 psi)	Oxygen (24.7 psi)	Nitrogen (24.7 psi)
Nitrogen	14.8	25.2	0	32.3
Oxygen	9.1	15.5	73.6	0
Oxygen (measured)	9.0	7-8	12-13	2-3
Argon	0.6	0.9	0	0
Carbon Dioxide	0.5	0.9	0	0

Table 7-2. Levels of four factors employed in the Box-Behnken design

Factor	Low	Medium	High
Temperature (K)	673	823	973
Time (min.)	10	30	50
Steam to carbon ratio (SC) (g H_2O/g carbon)	0.4	1.4	2.4
DO (mg/L)	3	7.5	12

Table 7-3. Box-Behnken statistical results for mass loss

Parameter	F-value	Prob > F-value	Coefficients of Equation	Value
Lack of fit (F-value)	2.90	0.156		
DO (mg/L)	0.82	0.377	0.91	
Temperature (K)	185.0	< 0.0001	-0.14	
Time (min.)	7.54	0.0125	-0.31	
SC (g H_2O/ g carbon)	3.78	0.0662	-7.39	
Temperature^2	39.6	< 0.0001	0.00013	
DO * Temperature	3.63	0.0713	-0.0018	
Temperature * Time	9.53	0.0058	0.00065	
Temperature * SC	12.1	0.0023	0.015	
Intercept			45.79	
Standard deviation				1.27
R-squared				0.93

Table 7-4. Surface area versus treatment time, treatment temperature, and SC (DO = 7.5 mg/L)

Temperature (K)	Time (min.)	SC (g H_2O/g carbon)	BET Surface Area (m^2/g) (± 5%)
973	10	1.4	541
973	50	1.4	615
673	10	1.4	470
673	50	1.4	498
673	30	0.4	468
673	30	2.4	496
973	30	0.4	537
973	30	2.4	606

Table 7-5. Box-Behnken statistical results for MIB removal

Parameter	F-value	Prob > F-value	Coefficients of Equation	Value
Lack of fit (F-value)	2.44	0.2009		
DO (mg/L)	4.12	0.0559	-4.76	
Temperature (K)	73.6	< 0.0001	-0.038	
Time (min.)	39.2	< 0.0001	1.12	
SC (g H_2O/ g carbon)	5.16	0.0344	-10.33	
DO^2	2.25	0.1491	0.2	
$Temperature^2$	14.5	0.0011	0.00046	
DO * Time	2.70	0.1158	-0.064	
DO * SC	6.47	0.0193	1.99	
Intercept			126.7	
Standard deviation				7.0
R-squared				0.88

Table 7-6. BET surface area and total pore volume of four carbons

Activated carbon label	SC (g H_2O/ g carbon)	DO (mg/L)	BET surface area (± 5%)	Micro-pore volume (< 2 nm) (cc/g)	Meso-pore volume (2-50 nm) (cc/g)	Macro-pore volume (>50 nm) (cc/g)	Pore volume (1.2-10 nm) (cc/g)
SHDL	2.4	3	501	0.232	0.021	0.003	0.0371
SLDL	0.4	3	461	0.217	0.021	0.006	0.0327
SHDH	2.4	12	478	0.221	0.022	0.006	0.0356
SLDH	0.4	12	430	0.202	0.020	0.006	0.0257

Table 7-7. Box-Behnken statistical results for pH_{pzc}

Parameter	F-value	Prob > F-value	Coefficients of Equation	Value
Lack of fit (F-value)	0.34	0.9544		
DO (mg/L)	0.83	0.3699	-0.017	
Temperature (K)	143.5	< 0.0001	0.0066	
Time (min.)	2.32	0.1409	0.0063	
SC (g H_2O/ g carbon)	13.4	0.0013	0.30	
Intercept			7.0	
Standard deviation				0.28
R-squared				0.87

Table 7-8. Activation conditions of four carbons and their removal of MIB in dichloromethane (time = 30 min., temperature = 873K)

Activated carbon label	MIB removal (%) (± 1.6%)
SHDL	5.4
SLDL	5.8
SHDH	6.2
SLDH	5.8

Table 7-9. BET surface area and total pore volume carbons treated with sodium sulfite

Activated carbon label	MIB removal (%) (± 2.5%)	pH_{pzc} (± 0.1)	BET surface area (m^2/g) (± 5%)	Micro-pore volume (< 2 nm) (cc/g)	Meso-pore volume (2-50 nm) (cc/g)	Macro-pore volume (>50 nm) (cc/g)	Pore volume (1.2-10 nm) (cc/g)
$SHDL_s$	64	11.67	506	0.227	0.025	0.006	0.0381
$SLDL_s$	59	11.31	484	0.230	0.021	0.006	0.0361
$SHDL_0$	49	11.63	469	0.225	0.019	0.006	0.0305
$SLDL_0$	57	11.37	494	0.236	0.019	0.006	0.0355

Table 7-10. Box-Behnken statistical results for phenol removal

Parameter	F-value	Prob > F-value	Coefficients of Equation	Value
Lack of fit (F-value)	2.64	0.1791		
DO (mg/L)	0.21	0.6517	-0.10	
Temperature (K)	47.8	< 0.0001	0.046	
Time (min.)	4.92	0.0362	0.11	
SC (g H_2O/ g carbon)	1.47	0.2368	1.22	
Intercept			29.8	
Standard deviation				3.47
R-squared				0.69

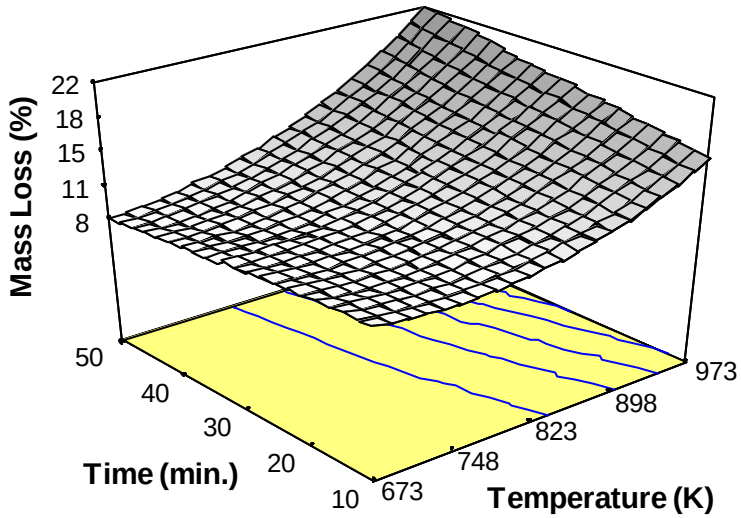

Figure 7-1. Mass loss versus time and temperature (SC = 1.4 g H_2O/g carbon, DO = 7.5 mg/L)

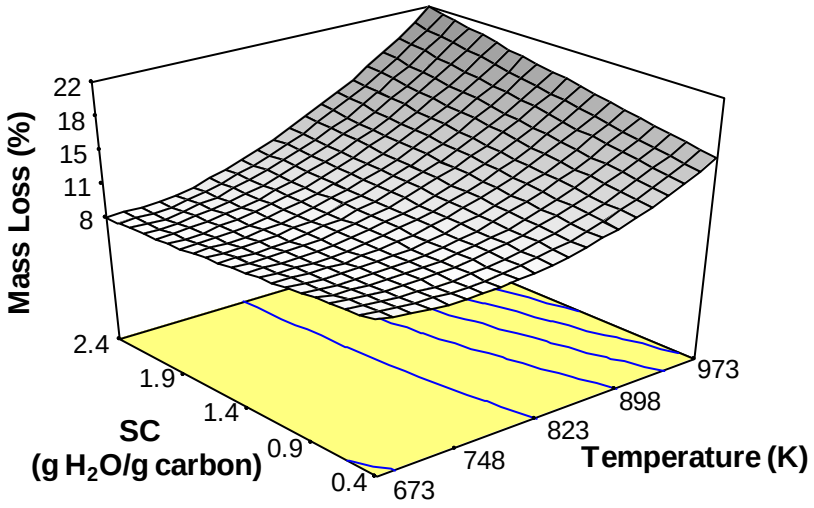

Figure 7-2. Mass loss versus SC and temperature (time = 30 min., DO = 7 mg/L)

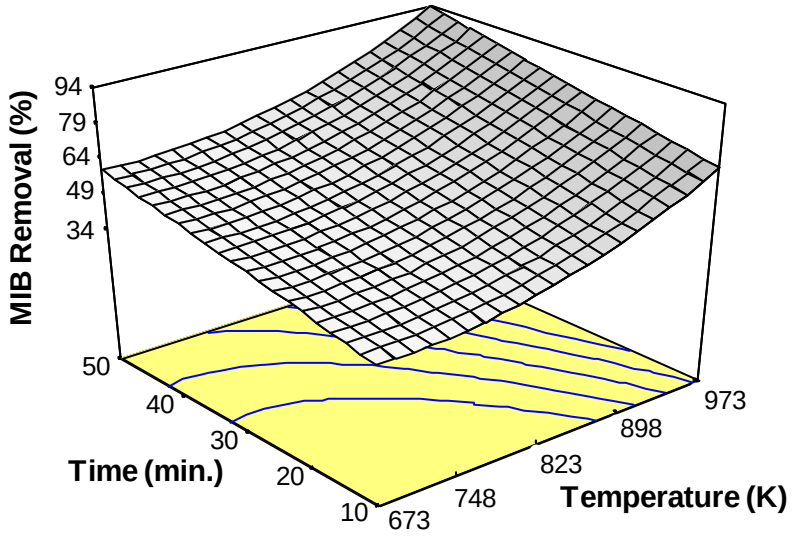

Figure 7-3. MIB removal versus time and temperature (SC = 1.4 g H_2O/g carbon, DO = 7.5 mg/L)

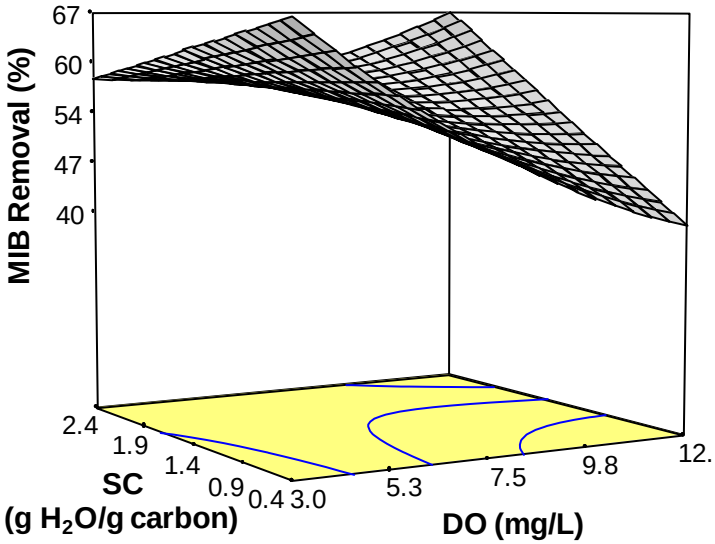

Figure 7-4. MIB removal versus SC and DO (time = 30 min., temperature = 873K)

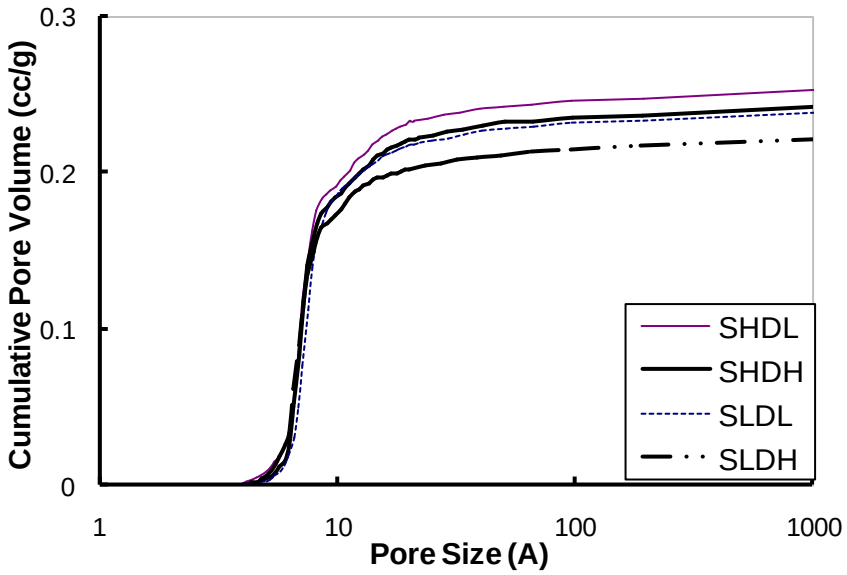

Figure 7-5. Pore size distributions of sample carbons

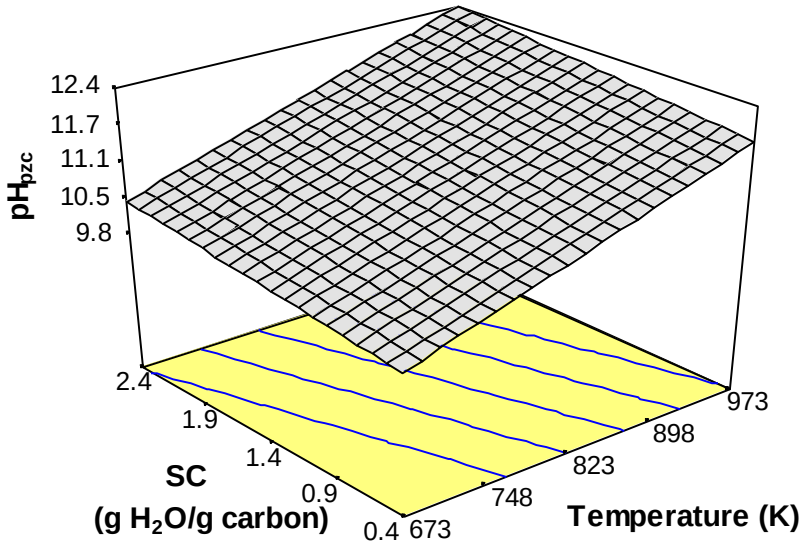

Figure 7-6. pH_{pzc} versus SC and temperature (time = 30 min., DO = 7 mg/L)

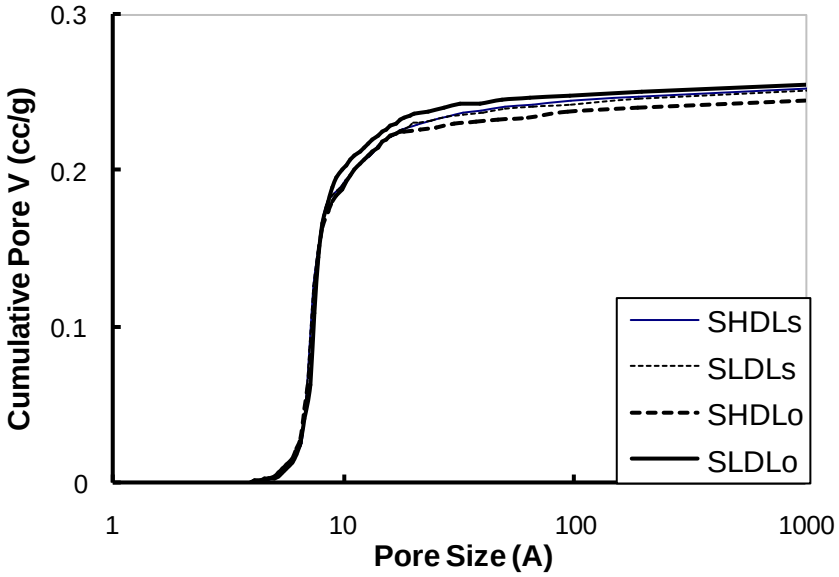

Figure 7-7. PSDs of carbons treated with sodium sulfite

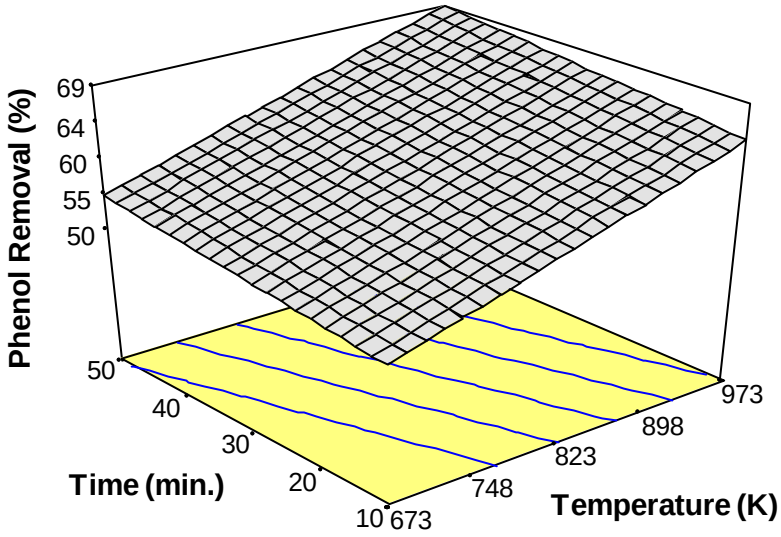

Figure 7-8. Phenol removal versus time and temperature (SC = 1.4 g H_2O/g carbon, DO = 7 mg/L)

CHAPTER 8
CONTRIBUTIONS TO SCIENCE

- First to determine that activated carbon treated with CO_2 yields improved removal of MIB due to a delay in the wetting of the carbon surface;

- Supported the importance of investigating individual acidic functional groups on the surface of activated carbon as not all of the individual acidic functional groups measured were altered following air treatment and yet the water contact pH and the air-treated carbon's performance in the removal of MIB and NOM was altered following air-treatment;

- First to demonstrate that variations in the DO content of water used to create steam for activation of a wood-based carbon alters the subsequent performance of the activated carbon for removal of MIB through a combination of physical and chemical changes in the carbon surface;

- Highlighted the necessity to tailor activated carbon for a specific contaminant as the performance of the activated carbons for removal of phenol, unlike MIB, was unaffected by alterations in the DO content of the water used to create steam for activation.

CHAPTER 9
FUTURE WORK

- Explore the impact of wetting time of activated carbon, as it pertains to the slurries by which PAC and GAC are transported, on the resulting adsorption performance of the activated carbon;

- Investigate the influence of the DO content of water used to create steam for activation of carbon on the subsequent adsorption performance of the activated carbon for removal of MIB and phenol in natural water (e.g., water containing NOM);

- Determine a method to either evaluate the quantity and type of individual acidic oxygen-containing functional groups on the surface of highly basic, heterogeneous carbons or evaluate the influence of the DO content of water used to create steam on the surface chemistry of a more homogenous surface (e.g., silica gel).

APPENDIX A
SAMPLE CALCULATIONS FOR DISSOLVED GASES

Table A-1. Henry's constants (at 273 K) and partial pressure of atmospheric gases

	Bunsen coefficient*	Air (14.7 psi)
Nitrogen	0.01559	7.80E-01
Oxygen	0.03109	2.10E-01
Argon	0.03412	9.00E-03
Carbon Dioxide	0.8981†	3.15E-04

*Weiss (1970) and †Taiz and Zeiger (2006)

Sample calculation of dissolved gas concentration in solution

Scenario: Air, 24.7 psi = 1277 torr

Henry's law expressed using a volumetric solubility coefficient (i.e, the Bunsen Method): $C_{O_2} = \frac{P_{O_2}}{(760/1000/K)} * \beta_{o_2}$, where P_{O2} = partial pressure, B_{O2} = Bunsen coefficient, and K = molecular weight/molecular volume

B_{O2} = 0.03109

P_{O2} = (1277torr – 17.52 torr) * $\frac{0.21 O_2}{torr}$ = 264.5 torr O_2/ torr

$$C_{O_2} = \frac{264.5 torr O_2 / torr}{\frac{760}{1000\, mg/g * (32\, g/mol/22.4 L/mol)}} * 0.03109 = 15.5 \text{ mg/L}$$

Sample calculation of change in pH with change in carbon dioxide in solution

Scenario: Atmospheric pressure

Bunsen Method: $C_{CO_2} = \frac{P_{CO_2}}{760/1000/K} * \beta_{Co_2}$

B_{CO2} = 0.8981

P_{O2} = (760torr – 17.52 torr) * $\frac{0.0003 CO_2}{torr}$ = 0.223 torr O_2/ torr

$$C_{CO_2} = \frac{0.223 torr O_2 / torr}{760/1000\, mg/g/(44\, g/mol/22.4 L/mol)} * 0.8981 = 0.376 \text{ mg/L}$$

$$C_{CO_2} = 0.376 mg/L * mol/44000 mg CO_2 = 9 * 10^{-6} mol/L$$

$$k = \frac{[H^+]*[HCO_3^-]}{[H_2CO_3]} = \frac{[H^+]*[HCO_3^-]}{C_{CO_2}} \xrightarrow{-->} [H^+]*[HCO_3^-] = 9*10^{-6}*10^{-6.35} = 4.02*10^{-12}$$

Charge Balance: $[H^+] = [HCO_3^-] + [CO_3^{2-}] + [OH^-]$, assume $[CO_3^{2-}]$ and [OH-] are negligible in this scenario

$$[H^+] = \frac{4.02*10^{-12}}{[H^+]} \longrightarrow [H^+]^2 = 4.02*10^{-12} \longrightarrow [H^+] = \sqrt{4.02*10^{-12}} = 2.0*10^{-6}\, mol/L$$

$$pH = -\log(2.0*10^{-6}) = 5.70$$

Scenario: 1.68 times atmospheric pressure

Bunsen Method: $C_{CO_2} = \frac{P_{CO_2}}{760/1000/K} * \beta_{Co_2}$

B_{Co2} = 0.8981 mg/L/torr

P_{O2} = (1277torr – 17.52 torr) * $\frac{0.0003\, CO_2}{torr}$ = 0.377 torr O_2/ torr

$$C_{CO_2} = \frac{0.377\, torr O_2/torr}{760/1000\, mg/g/(44\, g/mol/22.4 L/mol)} * 0.8981 = 0.6381 \text{ mg/L}$$

$$C_{CO_2} = 0.6381 mg/L * mol/44000 mg CO_2 = 15*10^{-6}\, mol/L$$

$$k = \frac{[H^+]*[HCO_3^-]}{[H_2CO_3]} = \frac{[H^+]*[HCO_3^-]}{C_{CO_2}} \xrightarrow{-->} [H^+]*[HCO_3^-] = 15*10^{-6}*10^{-6.35} = 6.48*10^{-12}$$

Charge Balance: $[H^+] = [HCO_3^-] + 2[CO_3^{2-}] + [OH^-]$, assume $[CO_3^{2-}]$ and [OH-] are negligible in this scenario

$$[H^+] = \frac{6.48*10^{-12}}{[H^+]} \longrightarrow [H^+]^2 = 6.48*10^{-12} \longrightarrow [H^+] = \sqrt{6.48*10^{-12}} = 3.0*10^{-6}\, mol/L$$

$$pH = -\log(3.0*10^{-6}) = 5.59$$

Scenario: Atmospheric pressure plus calcium chemistry

Bunsen Method: $C_{CO_2} = \frac{P_{CO_2}}{760/1000/K} * \beta_{Co_2}$

B_{CO2} = 0.8981

P_{O2} = (760torr – 17.52 torr) * $\frac{0.0003\,CO_2}{torr}$ = 0.223 torr O_2/ torr

$$C_{CO_2} = \frac{0.223 torr O_2 / torr}{760/1000\, mg/g/(44\, g/mol/22.4 L/mol)} * 0.8981 = 0.376 \text{ mg/L}$$

$$C_{CO_2} = 0.376 mg/L * mol/44000 mg CO_2 = 9*10^{-6} mol/L$$

$$k = \frac{[H^+]*[HCO_3^-]}{[H_2CO_3]} = \frac{[H^+]*[HCO_3^-]}{C_{CO_2}} \xrightarrow{-->} [H^+]*[HCO_3^-] = 9*10^{-6} * 10^{-6.35} = 4.02*10^{-12}$$

Charge Balance: $[H^+] + 2[Ca^{2+}] = [HCO_3^-] + 2[CO_3^{2-}] + [OH^-]$, assume $[CO_3^{2-}]$ and [OH-] are negligible in this scenario and the calcium in solution (as measured) is 2.5 mg/L or $8*10^{-4}$ M.

$$[H^+] = \frac{4.02*10^{-12}}{[H^+]} - 2*(8*10^{-4}) \longrightarrow [H^+] = 2.51*10^{-9} M$$

$$pH = -\log(2.51*10^{-9}) = 8.60$$

Moles of dissolved gases versus moles of steam and sample calculation

Table A-2. Moles of dissolved gases and water vapor versus treatment scenario

		Level of O_2 (mol O_2)		
SC (g H_2O/ g carbon)	mol H_2O	3 mg/L	7.5 mg/L	12 mg/L
0.4	0.111	$1.88*10^{-7}$	$4.69*10^{-7}$	$7.50*10^{-7}$
1.4	0.389	$6.56*10^{-7}$	$1.64*10^{-6}$	$2.63*10^{-6}$
2.4	0.667	$1.13*10^{-6}$	$2.81*10^{-6}$	$4.50*10^{-6}$

Scenario: 1.4 g H_2O/g carbon and 3 mg/L oxygen

1.4 g H2O/ g carbon * 5 g carbon = 7g H_2O
7 g H_2O / (18 g/mol) (molecular weight of H_2O) = 0.389 moles of H_2O

7 g H_2O / (1000 g/L) (density of water) = 0.007 L H_2O
3 mg/L Oxygen * 0.007 L / (32000 mg/mol) = $6.56*10^{-7}$ moles of oxygen

APPENDIX B
PRELIMINARY STUDIES FOR DETERMINATION OF LEVELS FOR BOX BEHNKEN

To begin any experiment, one must first determine the levels (or settings) of the variables to be evaluated. In this study, the variables of activation time, activation temperature, steam to carbon ratio (SC), and the dissolved oxygen (DO) content in the water used to create steam were evaluated to determine the impact of these parameters on the adsorption performance of the resulting carbons for MIB and also the impact of these parameters on both the chemical and physical properties of the resulting carbons. The following section discusses how the levels were determined for the Box-Behnken approach. Note that no attempt is made to explain observed phenomenon as that is outside the scope of this section.

For the latter variable, DO content, it was decided to use the same demarcations used in a previous study on the impact of DO content on reactivation of carbon (Chesnutt et al., 2007). In a study by Chestnutt et al. (2007), the DO contents were characterized as being low (less than 4 mg/L), medium (between 7-8 mg/L), and high (greater than 10 mg/L). In order to use the Box-Behnken approach, there must be three levels for each variable and these levels must be evenly spaced. Therefore, the DO content levels in this study were set at 3 mg/L, 7.5 mg/L, and 12 mg/L and where achieved by pressuring the water vessel with either nitrogen, air, or oxygen gas.

Given that activations are typically carried out at high temperatures (1173 K), preliminary experiments were performed at 1023 K and also a lower temperature, as low temperatures are known to manifest differences in surface chemistry, of 823 K. The activation time, 30 min., and SC, 0.68 g H_2O/g carbon, for these studies were based on steam activations used in a previous study of steam activation by Tennant and Mazyck (2003). The results of the first experiment varying both temperature and DO and evaluating MIB removal in batch studies are shown in Figure B-1.

Activations at 1023 K did not manifest a difference in MIB removal but the activations at 823K demonstrated that higher DO in the water used to create steam for activation does alter the carbons performance for MIB removal. It was also noted that in the study of Chesnutt et al. (2007) a very low temperature (648 K) was employed which manifested significant difference in MIB removal with altered DO. Therefore, in order to encompass the range of results where DO impacts MIB and conditions where it does not, the temperatures employed for the Box-Behnken approach were 673 K, 823 K, and 973 K.

Next, to shorten activation time and thereby cut experiment time in half, an activation time of 15 minutes was evaluated at the same steam flow as Figure B-1 (0.68 SC) and an activation temperature of 823 K. The performance of these carbons for removal of MIB is shown in Figure B-2.

From Figure B-2, it is apparent that there is a change in MIB removal depending on the activation time employed. As 15 and 30 minutes of treatment create different removals of MIB, and in order to create evenly spaces treatment times that represent extreme conditions, treatment times of 10, 30, and 50 minutes were employed in the Box-Behnken study.

Finally, an analysis of flow was performed where the steam flow was raised to the highest possible in the system (2.84 g H2O/g carbon) and compared to the previously employed flow based on Tennant and Mazyck (2003). The performance of these carbons for removal of MIB is shown in Figure B-3.

There is a change in MIB removal depending on the SC employed. As 0.68 g H_2O/g carbon and 2.84 g H_2O/g carbon create different removals of MIB, and in order to create evenly spaces treatment times that represent extreme conditions, SC of 0.4 g H_2O/g carbon, 1.4 g H_2O/g carbon, and 2.4 g H_2O/g carbon were employed in the Box-Behnken study.

These preliminary studies highlight the importance of studying interactions between factors, as clearly DO is not an influencing factor under all conditions and this underlines why the Box-Behnken statistical design of experiments was employed in this study.

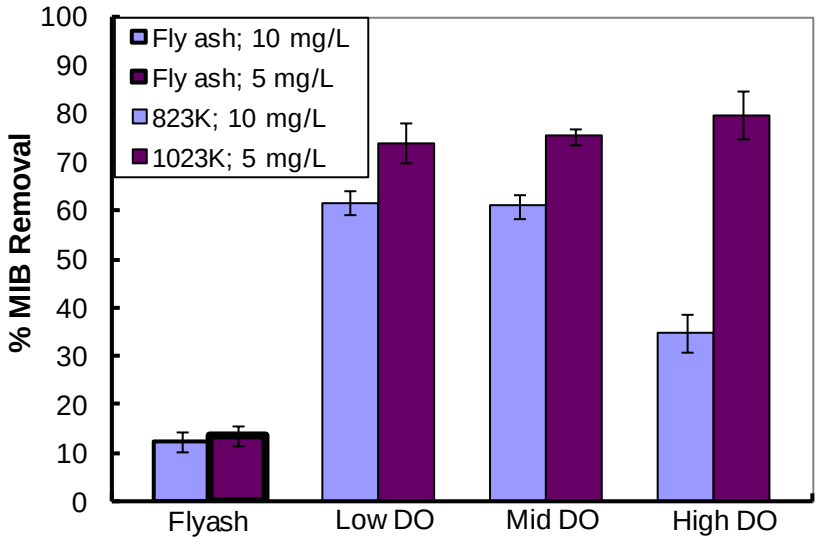

Figure B-1. MIB removal versus activation temperature and DO (SC = 0.68 g H_2O/g carbon, activation time = 30 min.).

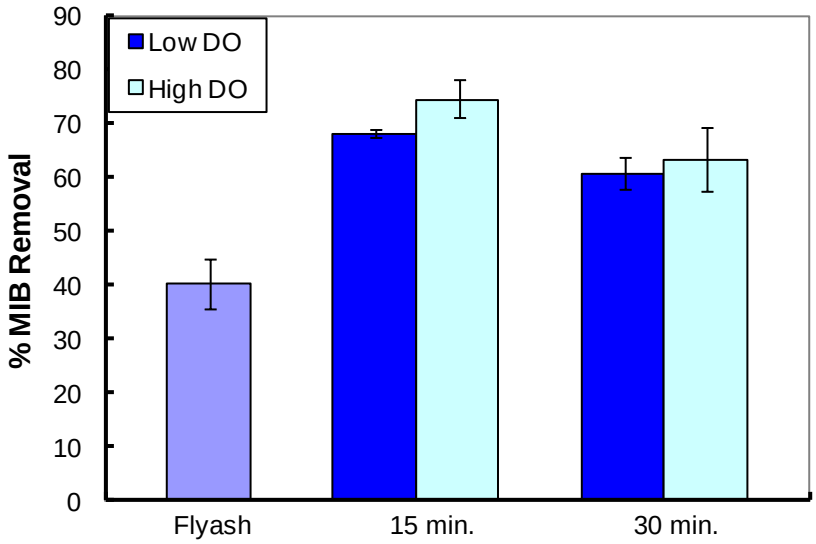

Figure B-2. MIB Removal versus time and DO (temperature = 823 K, SC = 0.68 g H_2O/g carbon).

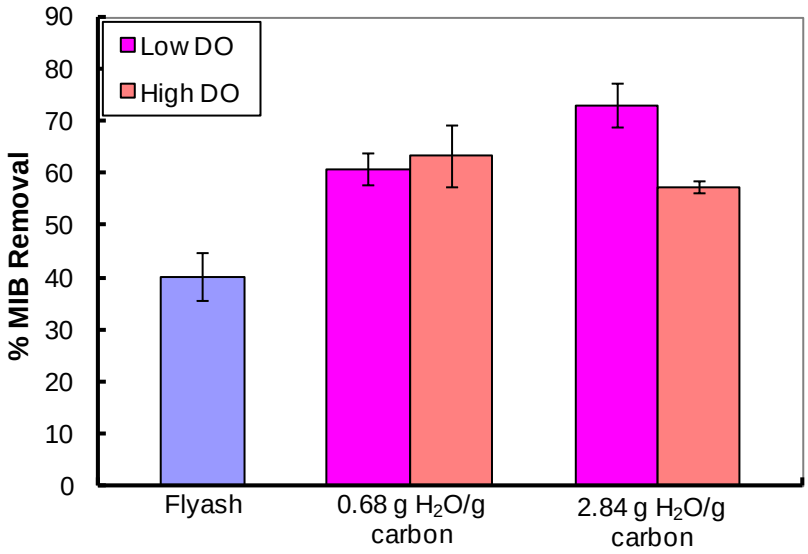

Figure B-3. MIB removal versus steam flow and DO (temperature = 823 K, time = 30 min.).

APPENDIX C
BOX-BEHNKEN RESULTS

Table C-1. Box-Behnken carbons activation conditions, MIB removal, mass loss, pH_{pzc}, phenol removal

	Factor A	Factor B	Factor C	Factor D	Response 1	Response 2	Response 3	Response 4
Std.	Dissolved oxygen (mg/L)	Temperature (K)	Time (min.)	Steam/ Carbon (g H_2O/g carbon)	MIB removal (%)	Mass loss (%)	pzc (pH)	Phenol removal (%)
1	3	673	30	1.4	56.5	8	9.9	56.8
2	12	673	30	1.4	42.4	9	10.0	49.6
3	3	973	30	1.4	94.7	21	11.8	65.9
4	12	973	30	1.4	66.9	17	12.1	67.4
5	7.5	823	10	0.4	37.1	11	10.5	52.6
6	7.5	823	50	0.4	65.7	10	11.0	59.4
7	7.5	823	10	2.4	42.4	10	11.0	54.8
8	7.5	823	50	2.4	62.9	12	11.4	62.7
9	3	823	30	0.4	72.6	11	11.0	63.2
10	12	823	30	0.4	49.2	11	10.4	61.6
11	3	823	30	2.4	56.8	11	11.5	62.4
12	12	823	30	2.4	69.3	11	11.7	63.0
13	7.5	673	10	1.4	30.5	10	9.9	45.9
14	7.5	973	10	1.4	75.4	15	12.0	68.1
15	7.5	673	50	1.4	58.7	10	10.1	54.4
16	7.5	973	50	1.4	95.9	23	11.9	68.8
17	3	823	10	1.4	37.3	10	11.2	53.6
18	12	823	10	1.4	50.5	10	10.9	55.6
19	3	823	50	1.4	76.5	12	11.6	56.4
20	12	823	50	1.4	66.5	11	11.0	55.6
21	7.5	673	30	0.4	38.5	8	9.7	50.7
22	7.5	973	30	0.4	71.1	14	12.0	64.8
23	7.5	673	30	2.4	63.0	8	10.5	59.2
24	7.5	973	30	2.4	95.3	22	12.1	64.8
25	7.5	823	30	1.4	55.3	9	11.2	63.2
26	7.5	823	30	1.4	57.0	11	10.7	59.0
27	7.5	823	30	1.4	56.2	11	11.2	59.0
28	7.5	823	30	1.4	45.2	11	11.8	63.6
29	7.5	823	30	1.4	52.4	11	11.6	62.3

Table C-2. Analysis of variance (ANOVA) results for mass loss (Prob > F of less than 0.05 are significant factors)

Source	Sum of squares	DF	Mean square	F-value	Prob > F	
Model	422.83	8	52.85	32.80	< 0.0001	significant
A	1.32	1	1.32	0.82	0.3769	
B	298.75	1	298.75	185.42	< 0.0001	significant
C	12.15	1	12.15	7.54	0.0125	significant
D	6.08	1	6.08	3.78	0.0662	
B^2	63.80	1	63.80	39.60	< 0.0001	significant
AB	5.84	1	5.84	3.63	0.0713	
BC	15.35	1	15.35	9.53	0.0058	significant
BD	19.55	1	19.55	12.13	0.0023	significant
Residual	32.22	20	1.61			
Lack of fit	29.66	16	1.85	2.90	0.1565	not significant
Pure error	2.56	4	0.64			
Cor total	455.05	28				

Table C-3. Statistical data for mass loss

Parameter	Values
Std. dev.	1.26
Mean	12.0
C.V.	10.5
PRESS	99.5
R-squared	0.929
Adj R-squared	0.900
Pred R-squared	0.781
Adeq precision (ratio greater than 4 desired)	20.4

Table C-4. Data for coefficient of parameters for mass loss

Factor	Coefficient estimate	DF	Standard error	95% CI low	95% CI high	VIF	Actual factors
Intercept	10.82	1	0.31	10.17	11.46		45.79
A-DO	-0.33	1	0.37	-1.10	0.43	1	0.91
B-Temperature	4.99	1	0.37	4.23	5.75	1	-0.14
C-Time	1.01	1	0.37	0.24	1.77	1	-0.31
D-Steam to carbon ratio	0.71	1	0.37	-0.05	1.48	1	-7.39
B^2	3.01	1	0.48	2.01	4.01	1	0.00013
AB	-1.21	1	0.63	-2.53	0.12	1	-0.0018
BC	1.96	1	0.63	0.63	3.28	1	0.00065
BD	2.21	1	0.63	0.89	3.53	1	0.015

Table C-5. Diagnostic case studies for mass loss

Standard order	Actual value	Predicted value	Residual	Leverage	Student residual	Cook's distance	Outlier t
1	8	7.96	-0.17	0.50	-0.19	0.00	-0.18
2	9	9.72	-1.15	0.50	-1.28	0.18	-1.30
3	21	20.36	0.89	0.50	0.99	0.11	0.99
4	17	17.28	-0.09	0.50	-0.10	0.00	-0.10
5	11	9.10	1.82	0.23	1.63	0.09	1.70
6	10	11.11	-0.79	0.23	-0.71	0.02	-0.70
7	10	10.52	-0.27	0.23	-0.25	0.00	-0.24
8	12	12.53	-0.86	0.23	-0.77	0.02	-0.76
9	11	10.44	0.56	0.23	0.51	0.01	0.50
10	11	9.77	1.63	0.23	1.46	0.07	1.51
11	11	11.86	-0.75	0.23	-0.68	0.01	-0.67
12	11	11.20	-0.60	0.23	-0.54	0.01	-0.53
13	10	9.79	0.06	0.50	0.06	0.00	0.06
14	15	15.85	-0.83	0.50	-0.92	0.09	-0.92
15	10	7.89	2.35	0.50	2.62	0.76	3.15
16	23	21.78	1.47	0.50	1.63	0.30	1.71
17	10	10.14	0.17	0.23	0.15	0.00	0.15
18	10	9.48	0.52	0.23	0.47	0.01	0.46
19	12	12.15	-0.54	0.23	-0.49	0.01	-0.48
20	11	11.49	-0.16	0.23	-0.14	0.00	-0.14
21	8	10.34	-1.97	0.50	-2.20	0.54	-2.46
22	14	15.90	-2.14	0.50	-2.39	0.63	-2.75
23	8	7.34	0.89	0.50	0.99	0.11	0.99
24	22	21.74	0.71	0.50	0.79	0.07	0.79
25	9	10.82	-1.57	0.06	-1.27	0.01	-1.29
26	11	10.82	0.29	0.06	0.24	0.00	0.23
27	11	10.82	0.23	0.06	0.19	0.00	0.18
28	11	10.82	0.26	0.06	0.21	0.00	0.21
29	11	10.82	0.06	0.06	0.05	0.00	0.05

Table C-6. ANOVA results for MIB removal

Source	Sum of squares	DF	Mean square	F-value	Prob > F	
Model	7306	8	913	18.35	< 0.0001	significant
A	205	1	205	4.12	0.0559	
B	3665	1	3665	73.62	< 0.0001	significant
C	1951	1	1951	39.19	< 0.0001	significant
D	257	1	257	5.16	0.0344	significant
A^2	112	1	112	2.25	0.1491	
B^2	724	1	724	14.54	0.0011	significant
AC	135	1	135	2.70	0.1158	
AD	322	1	322	6.47	0.0193	significant
Residual	996	20	50			
Lack of fit	903	16	56	2.44	0.2009	not significant
Pure error	92	4	23			
Cor total	8302	28				

Table C-7. Statistical data for MIB removal

Parameter	Values
Std. dev.	7.05
Mean	60.0
C.V.	11.7
PRESS	2380.4
R-squared	0.880
Adj R-squared	0.832
Pred R-squared	0.713
Adeq precision (ratio greater than 4 desired)	15.3

Table C-8. Data for coefficient of parameters for MIB removal

Factor	Coefficient estimate	DF	Standard error	95% CI low	95% CI high	VIF	Actual factors
Intercept	54.16	1	2.127	49.72	58.59		126.7
A-DO	-4.13	1	2.037	-8.38	0.12	1	-4.76
B-Temperature	17.48	1	2.037	13.23	21.72	1	-0.038
C-Time	12.75	1	2.037	8.50	17.00	1	1.12
D-Steam to carbon ratio	4.63	1	2.037	0.38	8.87	1	-10.33
A^2	4.03	1	2.685	-1.57	9.63	1.019	0.2
B^2	10.24	1	2.685	4.64	15.84	1.019	0.00046
AC	-5.80	1	3.528	-13.16	1.56	1	-0.064
AD	8.98	1	3.528	1.62	16.33	1	1.99

Table C-9. Diagnostic case studies for MIB removal

Standard order	Actual value	Predicted value	Residual	Leverage	Student residual	Cook's distance	Outlier t
1	56.5	55.09	1.41	0.31	0.24	0.00	0.24
2	42.4	46.82	-4.42	0.31	-0.76	0.03	-0.75
3	94.7	90.04	4.66	0.31	0.80	0.03	0.79
4	66.9	81.77	-14.87	0.31	-2.55	0.33	-3.02
5	37.1	36.78	0.32	0.26	0.05	0.00	0.05
6	65.7	62.28	3.42	0.26	0.56	0.01	0.55
7	42.4	46.03	-3.63	0.26	-0.60	0.01	-0.59
8	62.9	71.53	-8.63	0.26	-1.42	0.08	-1.46
9	72.6	66.67	5.93	0.52	1.21	0.17	1.22
10	49.2	40.45	8.75	0.52	1.78	0.38	1.89
11	56.8	57.97	-1.17	0.52	-0.24	0.01	-0.23
12	69.3	67.65	1.65	0.52	0.34	0.01	0.33
13	30.5	34.17	-3.67	0.27	-0.61	0.01	-0.60
14	75.4	69.12	6.28	0.27	1.04	0.04	1.04
15	58.7	59.67	-0.97	0.27	-0.16	0.00	-0.16
16	95.9	94.62	1.28	0.27	0.21	0.00	0.21
17	37.3	43.77	-6.47	0.52	-1.32	0.21	-1.34
18	50.5	47.10	3.40	0.52	0.69	0.06	0.68
19	76.5	80.87	-4.37	0.52	-0.89	0.09	-0.89
20	66.5	61.00	5.50	0.52	1.12	0.15	1.13
21	38.5	42.30	-3.80	0.27	-0.63	0.02	-0.62
22	71.1	77.25	-6.15	0.27	-1.02	0.04	-1.02
23	63.0	51.55	11.45	0.27	1.89	0.14	2.04
24	95.3	86.50	8.80	0.27	1.46	0.09	1.50
25	55.3	54.16	1.14	0.09	0.17	0.00	0.17
26	57.0	54.16	2.84	0.09	0.42	0.00	0.41
27	56.2	54.16	2.04	0.09	0.30	0.00	0.30
28	45.2	54.16	-8.96	0.09	-1.33	0.02	-1.36
29	52.4	54.16	-1.76	0.09	-0.26	0.00	-0.25

Table C-10. ANOVA results for pH_{pzc}

Source	Sum of Squares	DF	Mean square	F-value	Prob > F	
Model	12.94	4	3.23	40.01	< 0.0001	significant
A	0.07	1	0.07	0.83	0.3699	
B	11.60	1	11.60	143.53	< 0.0001	significant
C	0.19	1	0.19	2.32	0.1409	
D	1.08	1	1.08	13.36	0.0013	significant
Residual	1.94	24	0.08			
Lack of fit	1.22	20	0.06	0.34	0.9544	not significant
Pure error	0.72	4	0.18			
Cor total	14.88	28				

Table C-11. Statistical data for pH_{pzc}

Parameter	Values
Std. dev.	0.284
Mean	11.0
C.V.	2.56
PRESS	2.57
R-squared	0.869
Adj R-squared	0.847
Pred R-squared	0.826
Adeq precision (ratio greater than 4 desired)	21.7

Table C-12. Data for coefficient of parameters for pH_{pzc}

Factor	Coefficient estimate	DF	Standard error	95% CI low	95% CI high	VIF	Actual factors
Intercept	11.09	1	0.053	10.984	11.202		7.01
A-DO	-0.08	1	0.082	-0.244	0.094	1	-0.017
B-Temperature	0.98	1	0.082	0.814	1.153	1	0.0066
C-Time	0.13	1	0.082	-0.044	0.294	1	0.0063
D-Steam to carbon ratio	0.30	1	0.082	0.131	0.469	1	0.30

Table C-13. Diagnostic case studies for pH_{pzc}

Standard order	Actual value	Predicted value	Residual	Leverage	Student vesidual	Cook's distance	Outlier t
1	8	7.96	-0.17	0.50	-0.19	0.00	-0.18
2	9	9.72	-1.15	0.50	-1.28	0.18	-1.30
3	21	20.36	0.89	0.50	0.99	0.11	0.99
4	17	17.28	-0.09	0.50	-0.10	0.00	-0.10
5	11	9.10	1.82	0.23	1.63	0.09	1.70
6	10	11.11	-0.79	0.23	-0.71	0.02	-0.70
7	10	10.52	-0.27	0.23	-0.25	0.00	-0.24
8	12	12.53	-0.86	0.23	-0.77	0.02	-0.76
9	11	10.44	0.56	0.23	0.51	0.01	0.50
10	11	9.77	1.63	0.23	1.46	0.07	1.51
11	11	11.86	-0.75	0.23	-0.68	0.01	-0.67
12	11	11.20	-0.60	0.23	-0.54	0.01	-0.53
13	10	9.79	0.06	0.50	0.06	0.00	0.06
14	15	15.85	-0.83	0.50	-0.92	0.09	-0.92
15	10	7.89	2.35	0.50	2.62	0.76	3.15
16	23	21.78	1.47	0.50	1.63	0.30	1.71
17	10	10.14	0.17	0.23	0.15	0.00	0.15
18	10	9.48	0.52	0.23	0.47	0.01	0.46
19	12	12.15	-0.54	0.23	-0.49	0.01	-0.48
20	11	11.49	-0.16	0.23	-0.14	0.00	-0.14
21	8	10.34	-1.97	0.50	-2.20	0.54	-2.46
22	14	15.90	-2.14	0.50	-2.39	0.63	-2.75
23	8	7.34	0.89	0.50	0.99	0.11	0.99
24	22	21.74	0.71	0.50	0.79	0.07	0.79
25	9	10.82	-1.57	0.06	-1.27	0.01	-1.29
26	11	10.82	0.29	0.06	0.24	0.00	0.23
27	11	10.82	0.23	0.06	0.19	0.00	0.18
28	11	10.82	0.26	0.06	0.21	0.00	0.21
29	11	10.82	0.06	0.06	0.05	0.00	0.05

Table C-14. ANOVA results for phenol removal

Source	Sum of squares	DF	Mean square	F-value	Prob > F	
Model	656.55	4	164.14	13.60	< 0.0001	significant
A	2.52	1	2.52	0.21	0.6517	
B	576.85	1	576.85	47.80	< 0.0001	significant
C	59.41	1	59.41	4.92	0.0362	significant
D	17.76	1	17.76	1.47	0.2368	
Residual	289.60	24	12.07			
Lack of fit	269.20	20	13.46	2.64	0.1791	not significant
Pure error	20.41	4	5.10			
Cor total	946.15	28				

Table C-15. Statistical data for phenol removal

Parameter	Values
Std. dev.	3.47
Mean	59.4
C.V.	5.84
PRESS	434.2
R-squared	0.693
Adj R-squared	0.642
Pred R-squared	0.541
Adeq precision (ratio greater than 4 desired)	12.6

Table C-16. Data for coefficient of parameters for phenol removal

Factor	Coefficient estimate	DF	Standard error	95% CI low	95% CI high	VIF	Actual factors
Intercept	59.46	1	0.65	58.13	60.79		29.76
A-DO	-0.46	1	1.00	-2.53	1.61	1	-0.10
B-Temperature	6.93	1	1.00	4.86	9.00	1	0.046
C-Time	2.23	1	1.00	0.16	4.29	1	0.11
D-Steam to carbon ratio	1.22	1	1.00	-0.85	3.29	1	1.22

Table C-17. Diagnostic case studies for phenol removal

Standard order	Actual value	Predicted value	Residual	Leverage	Student residual	Cook's distance	Outlier t
1	56.8	52.99	3.81	0.20	1.23	0.08	1.24
2	49.6	52.07	-2.47	0.20	-0.80	0.03	-0.79
3	65.9	66.85	-0.95	0.20	-0.31	0.00	-0.30
4	67.4	65.94	1.46	0.20	0.47	0.01	0.46
5	52.6	56.02	-3.42	0.20	-1.10	0.06	-1.11
6	59.4	60.47	-1.07	0.20	-0.34	0.01	-0.34
7	54.8	58.45	-3.65	0.20	-1.18	0.07	-1.19
8	62.7	62.90	-0.20	0.20	-0.07	0.00	-0.06
9	63.2	58.70	4.50	0.20	1.45	0.11	1.48
10	61.6	57.79	3.81	0.20	1.23	0.08	1.24
11	62.4	61.14	1.26	0.20	0.41	0.01	0.40
12	63.0	60.22	2.78	0.20	0.90	0.04	0.89
13	45.9	50.30	-4.40	0.20	-1.42	0.10	-1.45
14	68.1	64.17	3.93	0.20	1.27	0.08	1.28
15	54.4	54.75	-0.35	0.20	-0.11	0.00	-0.11
16	68.8	68.62	0.18	0.20	0.06	0.00	0.06
17	53.6	57.70	-4.10	0.20	-1.32	0.09	-1.34
18	55.6	56.78	-1.18	0.20	-0.38	0.01	-0.37
19	56.4	62.15	-5.75	0.20	-1.85	0.17	-1.96
20	55.6	61.23	-5.63	0.20	-1.81	0.17	-1.91
21	50.7	51.31	-0.61	0.20	-0.20	0.00	-0.19
22	64.8	65.18	-0.38	0.20	-0.12	0.00	-0.12
23	59.2	53.75	5.45	0.20	1.76	0.16	1.84
24	64.8	67.61	-2.81	0.20	-0.91	0.04	-0.90
25	63.2	59.46	3.74	0.03	1.10	0.01	1.10
26	59.0	59.46	-0.46	0.03	-0.14	0.00	-0.13
27	59.0	59.46	-0.46	0.03	-0.14	0.00	-0.13
28	63.6	59.46	4.14	0.03	1.21	0.01	1.22
29	62.3	59.46	2.84	0.03	0.83	0.00	0.83

LIST OF REFERENCES

Albers, P.W., Pietsch J., Krauter, J., Parker, S.F., 2003. Investigations of activated carbon catalyst supports from different natural sources. Phys. Chem. Chem. Phys. 5, 1941-1949.

Alcaniz-Monge, J., Cazorla-Amoros, D., Linares-solano, A., 1994. Effect of the activating gas on tensile strength and pore structure of pitch-based carbon fibres. Carbon 32 (7), 1277-1283.

Ania, C.O., Parra, J.B., Pis, J.J., 2004. Oxygen-induced decrease in the equilibrium adsorptive capacities of activated carbons. Adsorption Science and Technology 22 (4), 337-351.

Appleton, Wisconsin, 2006. Wastewater treatment facility: Treatment plant tour. Accessed: July 9. <http://www.appleton.org/departments/utilities/wastewater/plant_tour/>.

Arriagada, R., Garcia, R., MolinaSabio, M., RodriguezReinoso, F., 1997. Effect of steam activation on the porosity and chemical nature of activated carbons from Eucalyptus globulus and peach stones. Microporous Materials 8 (3-4), 123-130.

Bach, M.T., 2004. The role of calcium in and methodologies for overcoming pH excursions for reactivated granular activated carbon. Thesis (M.E.). University of Florida.

Benjamin, M.M., 2002. Water Chemistry. McGraw-Hill; New York.

Bansal, R.C., Aggarwall, D., Goyal, M., Kaistha, B.C., 2002. Influence of carbon-oxygen surface groups on the adsorption of phenol by activated carbons. Ind. Journal of Chem. Tech. 9, 290.

Bansal, R.C., Donnet, J.B., Stoeckli, F., 1988. Active Carbon. Marcel Dekker, Inc.; New York.

Bansal, R.C., Vastola, F.J., Walker, P.L., 1974. Influence of hydrogen chemisorption on the subsequent chemisorption of oxygen on activated graphon. Carbon 12, 355.

Barnett, K.E., 1999. Wastewater treatment method and plant. United States Patent Number 5,961,830.

Barton, S.S., Evans, M.J.B, Halliop, E., MacDonald, J.A.F., 1997. Acidic and basic sites on the surface of porous carbon. Carbon 35 (9), 1361-1366.

Bizot, P.M., Bailey, B.R., 1997. Sodium sulfoxylate formaldehyde as a boiler additive for oxygen scavenging. United States Patent Number 5,660,736.

Boehm, H., 1966. Functional groups on the surfaces of solids. Angewandte Chemie Inernational Edition 5, 533-522.

Box, G.E.P., Behnken, D.W., 1960. Some new three level designs for the study of quantitative variables. Technometrics 2 (4), 455-475.

Buczek. B., 1993. Development of properties within particles of active carbons obtained by a steam activation process. Langmuir 9, 2509-2512.

Bull, R.J., Robinson, M., Meier, J.R., Stober, J., 1982. Use of biological assay systems to assess the relative carcinogenic hazards of disinfection by-products. Environmental Health Perspectives 46, 215-227.

Campbell, A.G., Folk, R.L., Tripepi, R.R., 1997. Wood ash as an amendment in municipal sludge and yard waste composting processes. Compost Science & Utilization 5 (1), 62-73.

Cannon, F.S., Snoeyink, V.L., Lee, R.G., Dagois, G., DeWolfe, J.R., 1993. Effect of calcium in field-spent GACs on pore development during regeneration. JAWWA 85 (3), 76-89.

Cannon, F.S., Snoeyink, V.L., Lee, R.G., Dagois, G., 1994. Reaction mechanism of calcium-catalyzed thermal regeneration of spent granular activated carbon. Carbon 32 (7), 1285-1301.

Carr, S., Farmer, R.W., 1995. React-pH^{TM} improves pH in carbon effluent. The National Environmental Journal 5 (2), 54.

Centeno, T.A., Stoeckli, F., 1995. The oxidation of an asturian bituminous coal in air and its influence on subsequent activation by steam. Carbon 33 (5), 581-586.

Chen ,W.F., Cannon, F.S., Rangel-Mendez, J.R., 2005a. Ammonia-tailoring of GAC to enhance perchlorate removal. I: Characterization of NH_3 thermally tailored GACs. Carbon 43 (3), 573-580.

Chen, W.F., Cannon, F.S., Rangel-Mendez, J.R., 2005b. Ammonia-tailoring of GAC to enhance perchlorate removal. II: Perchlorate adsorption. Carbon 43 (3), 581-590.

Chestnutt, T.E., Bach, M.T., Mazyck, D.W., 2007. Improvement of thermal reactivation of activated carbon for the removal of 2-methylisoborneol. Water Res. 41, 79-86.

Clark, R.M., Lykins, B.W., 1989. Granular Activated: Design, Operation and Cost. Lewis Publishers; Chelsea, MI.

Considine, R., Denoyel, R., Pendleton, P., Schumann, R., Wong, S.H., 2001. The influence of surface chemistry on activated carbon adsorption of 2-methylisoborneol from aqueous solution. Colloids and Surfaces A: Physicochemical and Engineering Aspects 179 (2-3), 271-280.

Crittenden, J.C., Berrigan, J.K., Hand, D.W., 1986. Design of rapid small-scale adsorption tests for a constant diffusivity. Journal of Water Pollution Control Federation 58 (4), 312-319.

Crittenden, J.C., Reddy, P.S., Arora, H., Trynoski, J., Hand, D.W., Perram, D.L., Summers, RS., 1991. Predicting GAC performance with rapid small-scale column tests. JAWWA 83 (1), 77-87.

Das, K.C., Melear, N.D., Kastner, J.R., Buquoi, J.Q., 2003. Influence of ash amendment on odor emissions and aerobic biodegradation of biosolids mixes. Transactions of the ASAE 46 (4), 1185-1191.

Dussert, B.W., Farmer, R.W., Hayden, R.A., 1995. Oxidized activated carbon for the control of pH and alkalinity in water treatment applications. United States Patent 5,466,378.

El-Sayed, Y., Bandosz, T.J., 2003. Effect of increased basicity of activated carbon surface on valeric acid adsorption from aqueous solution activated carbon. Phys. Chem. Chem. Phys 5 (21), 4892-4898.

Farmer, R.W., Dussert, B.W., Kovacic, S.L., 1996. Improved granular activated carbon for the stabilization of wastewater pH. American Chemical Society, Division of Fuel Chemistry 41 (1), 456-460.

Farmer, R.W., Kovacic, L., Matviya, M., Wadhwa, N.P., 1998. Activated carbon treated by carbon dioxide for the stabilization of treated water pH. United States Patent Number 5,714,433.

Fernandes, M.B., Skjemstad, J.O., Johnson, B.B., Wells, J.D., Brooks, P., 2003. Characterization of carbonaceous combustion residues. I. Morphological, elemental, and spectroscopic features. Chemosphere 51, 785-795.

Frederick, H.T., Cannon, F.S., Dempsey, B.A., 2001a. Calcium and TOC loading: Effect of hydroxyl and carboxyl substituents. Colloids and Surfaces A: Physicochemical and Engineering Aspects 191 (1-2), 161-177.

Frederick, H.T., Cannon, F.S., Dempsey, B.A., 2001b. Calcium loading onto granular activated carbon with salicylate or phthalate. Colloids and Surfaces A: Physicochemical and Engineering Aspects 177 (2-3), 157-168.

Frederick, H.T., Cannon, F.S., 2001. Calcium-NOM loading onto GAC. JAWWA 93(12), 77-89.

García-García, A., Gregório, A., Franco, C., Pinto, F., Boavida, D., Gulyurtlu, I., 2003. Unconverted chars obtained during biomass gasification on a pilot-scale gasifier as a source of activated carbon production. Bioresource Technology 88, 27-32.

Garten, V.A., Weiss, V.E., 1957. The ion and electron exchange properties of activated carbon in relation to its behavior as a catalyst and adsorbent. Rev Pure Appl Chem 7, 69-122.

Gerber, N.N., 1968. A volatile metabolite of actinomycetes, 2-methylisoborneol. Journal of Antibiotics 22 (10), 508.

Gergova, K., Eser. S., 1996. Effects of activation method on the pore structure of activated carbons from apricot stones. Carbon 34 (7), 879-888.

Gergova, K., Petrov, N., Eser, S., 1994. Adsorption properties and microstructure of activated carbons produced from agricultural by-products by steam pyrolysis. Carbon 32 (4), 693-702

Gergova, K., Petrov, N., Butuzova, L., Minkova, V., Isaeva, L., 1993. Evolution of the active surface of carbons produced from various raw-materials by steam pyrolysis activation. Journal of chemical technology and biotechnology 58 (4), 321-330.

Gerth, W.A., 1985. Applicability of Henry's law to hydrogen, helium, and nitrogen solubilities in water and olive oil at 37 °C and pressures up to 300 atmospheres. Archives of Biochemistry and Biophysics 241 (1), 187-199.

Gillogly, T., Sneoyink, V., Elarde, J., Wilson, C., Royale, E., 1998. ^{14}C-MIB adsorption on PAC in natural water. JAWWA 90(1), 98-108.

Gonzalez, M.T., Molina-Sabio, M., Rodriguez-Reinoso, F., 1994. Steam activation of olive stone chars, development of porosity. Carbon 32 (8), 1407-1413.

Hammer, M.J., Hammer, M.J., Jr., 2001. Water and Wastewater Technology. Prentice Hall; Upper Saddle River, NJ.

Hassler, J.W., 1974. Purification with activated carbon: industrial, commercial, environmental. Chemical Pub. Co.; New York.

Herzing, D., Snoeyink, V., Wood, N., 1977. Activated carbon adsorption of the odorous compounds 2-methylisoborneol and geosmin. JAWWA 69, 223.

Heschel, W., Klose, E., 1995. On the suitability of agricultural by-products for the manufacture of granular activated carbon. Fuel 74 (12), 1786-1791.

Jung, M.W., Ahn, K.H., Lee, Y., Kim, K.P., Rhee, J.S., Park, J.T., Paeng, K.J., 2001. Adsorption characteristics of phenol and chlorophenols on granular activated carbons (GAC). Microchemical Journal 70 (2), 123-131.

Karanfil, T., Kitis, M., 1999. Role of granular activated carbon surface chemistry on the adsorption of organic compounds. 2. Natural Organic Matter. Environ. Science and Technology 33 (18), 3225-3233.

Kastner, J.R., Das, K.C., Buquoi, Q., Melear, N,D., 2003. Low temperature catalytic oxidation of hydrogen sulfide and methanethiol using wood and coal fly ash. Environ. Sci. Technol. 37 (11), 2568-2574.

Kawamura, S., 2000. Integrated design and operation of water treatment facilities. John Wiley & Sons; New York.

Khezami. L., Chetouani, A., Taouk, B., Capart, R., 2005. Production and characterisation of activated carbon from wood components in powder: Cellulose, lignin, xylan. Powder Technology 157, 48-56.

Kipling, J.J., Gassser, C.G., 1960. Adsorption from liquid mixtures at solid surfaces. J. Phys.Chem 64 (6), 710.

Kirk-Othmer, 1977. Encyclopaedia of Chemical Technology, Third Edition, Wiley; New York.

Knappe, D.R.U., Snoeyink, V.L., Dagois, G., DeWolfe, J.R., 1992. Effect of calcium on thermal regeneration of GAC. JAWWA 84 (8), 73-80.

Kruyt, H.R., De Kadt, G.S., 1929. Die ladung der kohle. Kolloid Chem. Beihefte 47, 44.

Laine, N.R., Vastola, F.J., Walker, P.L., 1963. Importance of active surface area in carbon-oxygen reaction. Journal of Physical Chemistry 67 (10), 2030.

Leon y Leon, C.A., Solar, J.M., Calemma, V., Radovic, L.R., 1992. Evidence for the protonation of basal plane sites on carbon. Carbon 30 (5), 797-811.

Lillo-Rodenas, M.A., Cazorla-Amoros, D., Linares-Solano, A., 2005. Behaviour of activated carbons with different pore size distributions and surface oxygen groups for benzene and toluene adsorption at low concentrations. Carbon 43 (8), 1758-1767.

Lussier, M.G., Zhang, Z., Miller, D.J., 1998. Characterizing rate inhibition in steam/hydrogen gasification via analysis of adsorbed hydrogen. Carbon 36 (9), 1361-1369.

MacKenzie, J.A., Tennant, M.F., Mazyck, D.W., 2005. Tailored GAC for the effective control of 2-methylisoborneol. JAWWA 97 (6), 76-87.

Martin-Gullon, I., Asensio, M., Font, R., Marcilla ,A., 1996. Steam-activated carbons from a bituminous coal in a continuous multistage fluidized bed pilot plant. Carbon 34 (12), 1515-1520.

Mazyck, D.W., Cannon, F.S., 2000. Overcoming calcium catalysis during the thermal reactivation of granular activated carbon: Part I. Steam-curing plus ramped-temperature N_2 treatment. Carbon 38 (13), 1785-1799.

Mazyck, D.W., Cannon. F.S., 2002. Overcoming calcium catalysis during the thermal reactivation of granular activated carbon. Part II. Variation of steam-curing reactivation parameters. Carbon 40, 241-252.

Mazyck, D.W., Cannon, F.S., Bach, M.T., Radovic, L.R., 2005. The role of calcium in high pH excursions with reactivated GAC. Carbon 43, 511-518.

Menéndez, J.A., Phillips, J., Xia, B., Radovic, L.R., 1996. On the modification and characterization of chemical surface properties of activated carbon: In the search of carbons with stable basic properties. Langmuir 12 (18), 4404-4410.

MolinaSabio, M., Gonzalez, M.T., RodriguezReinoso, F., Sepulveda-Escribano, A., 1996. Effect of steam and carbon dioxide activation in the micropore size distribution of AC. Carbon 34 (4), 505-509.

Montgomery, D.C., 1991. Design and analysis of experiments. Wiley; New York.

Myers, M.H., 1995. Response surface methodology. Wiley; New York.

Newcombe, G., Morrison, J., Hepplewhite, C., Knappe, D.R.U., 2002. Simultaneous adsorption of MIB and NOM onto activated carbon. II. Competitive effects. Carbon 40, 2147.

Newcombe, G., 1999. Charge vs. porosity-some influences on the adsorption of natural organic matter (NOM) by activated carbon. Water Science & Technology 40 (9): 191-198.

Nowack, K.O., Cannon, F.S., Arora, H., 1999. Ferric chloride plus GAC for removing TOC. J AWWA 91 (2), 65-78.

Nowack, K.O., Cannon, F.S., Mazyck, D.W., 2004. Enhancing activated carbon adsorption of 2-methylisoborneol: Methane and steam treatments. Environ. Sci. Technol. 38, 276-284.

Nowack, K.O., Cannon, F.S., 1997. Control of calcium buildup in GAC: Effect of iron coagulation. Carbon 35 (9), 1223-1237.

Otake, Y., Jenkins, R.G., 1993. Characterization of oxygen-containing surface complexes created on a microporous carbon by air and nitric-acid treatment. Carbon 31 (1), 109-121.

Pelekani, C., Snoeyink, V.L., 1999. Competitive adsorption in natural water: Role of activated carbon pore size. Water Research 33 (5), 1209-1219.

Pendleton, P., Wong, S.H., Schumann, R., Levay, G., Denoyel, R., Rouquerol, J., 1997. Properties of activated carbon controlling 2-methylisoborneol adsorption. Carbon 35, 1141.

Petrucci, R.H., Harwood, W.S., 1997. General chemistry: principles and modern applications. Prentice Hall; New Jersey.

Pereira, M.F.R., Soares, S.F., Órfão, J.J.M., Figueiredo, J.L., 2003. Adsorption of dyes on activated carbons: influence of surface chemical groups. Carbon 41 (4), 811-821.

Puri, B.R, 1970. Surface Complexes on Carbon in Chemistry and Physics of Carbon, Vol. 6, ed. P.L. Walker, Jr., Marcel Dekker; New York.

Quirilivan, P.A., Li, L., Knappe, D.R.U., 2005. Effects of activated carbon characteristics on the simultaneous adsorption of aqueous organic micropollutants and natural organic matter. Water Research 39 (8), 1663-1673.

Rangel-Mendez, J.R., Cannon, F.S., 2005. Improved activated carbon by thermal treatment in methane and steam: Physicochemical influences on MIB sorption capacity. Carbon 43, 467.

Rashash, D.M.C., Dietrich, A.M., Hoehn, R.C., 1997. FPA of selected odorous compounds. JAWWA 89 (4), 131-141.

Ravichandran, M., Aiken, G.R., Reddy, M.M., Ryan, J.N., 1998. Enhanced dissolution of cinnabar (mercuric sulfide) by dissolved organic matter isolated from the Florida Everglades. Env. Sci.& Tech. 32, 3305.

Rio, S., Faur-Brasquet, C., Le Coq, L., Le Cloirec, P., 2005. Production and characterization of adsorbent materials from an industrial waste. Adsorption 11, 793-798.

Rodríguez-Reinoso, F., Molina-Sabio, M., González, M.T., 1995. The use of steam and CO_2 as activating agents in the preparation of activated carbons. Carbon 33 (1), 15-23.

Rosenfeld, P.E., Henry, C.L., 2000. Wood ash control of odor from biosolids application. Journal of Environmental Quality 29 (5), 1662-1668.

Ryu, S.K., Jin, H., Gondy, D., Pusset, N., Ehrburger, P., 1993. Activation of carbon-fibers by steam and carbon-dioxide. Carbon 31 (5), 841-842.

Salame, I.I., Bandosz, T.J., 2001. Surface chemistry of activated carbons: Combining the results of temperature-programmed desorption, Boehm, and potentiometric titrations. J. Colloid and Interface Sciences 240, 252-258.

Salame, I.I., Bandosz, T.J., 2003. Role of surface chemistry in adsorption of phenol on activated carbons. Journal of Colloid and Interface Science 264 (2), 307-312.

Sarkar, M., Acharya, P.K., 2006. Use of fly ash for the removal of phenol and its analogues from contaminated water. Waste Management 26,559-570.

Smith, W.R., Polley, M.H., 1956. The oxidation of graphitized carbon black. Journal of Physical Chemistry 60 (5), 689-691.

Snoeyink, V., Summers, R.S., 1999 "Chapter 13. Adsorption of organic compounds." Water Quality and Treatment, AWWA; Denver, CO.

Souza-Macedo, J., Costa-Júnior, N.B., Almeida, L.E., Silva-Vieira, E.F., Cestari, A.R., Fátima-Gimenez, I., Carreño, N.L.V., Barreto, L.S., 2006. Kinetic and calorimetric study of the adsorption of dyes on mesoporous activated carbon prepared from coconut coir dust. Journal of Colloid and Interface Science 298, 515-522.

Speitel, G.E., Dvorak, B.I,. Morley, M.C., 2001. Rapid small-scale column test. AEESP Environmental Engineering Processes Laboratory Manual. Association of Environmental Engineering and Science Professors; Champaign, Illinois.

Streat, M., Patrick, J.W., Perez, M.J.C., 1995. Sorption of phenol and para-chlorophenol from water using conventional and novel activated carbons. Wat. Res. 29 (2), 467-472.

Summers, R.S., Haist, B., Koehler, J., Ritz, J., Zimmer, G., Sontheimer, H., 1989. The influence of background organic matter on GAC adsorption. JAWWA 81 (5), 66-74.

Suzuki, M., 1990. Adsorption engineering. Elsevier; New York.

Szymański, G.S., Karpiński, Z., Biniak, S., Świątkowski, A., 2002. The effect of the gradual thermal decomposition of surface oxygen species on the chemical and catalytic properties of oxidized activated carbon. Carbon 40 (14), 2627-2639.

Taiz, L., Zeiger, E., 2006. Plant Physiology, Fourth Edition. Sinauer Associates, Inc.; Sunderland, MA.

Tennant, M.F., Mazyck, D.W., 2003. Steam-pyrolysis activation of wood char for superior odorant removal. Carbon 41, 2195.

Tennant, M.F., 2004. Activation and use of powdered activated carbon for removing 2-methylisoborneol in water utilities. Dissertation (Ph.D.). University of Florida.

Tomków, K., Siemieniewska, T., Czechowski, F., Jankowska, A., 1977. Formation of porous structures in activated brown-coal chars using O_2, CO_2, and H_2O as activating agents. Fuel 56 (2), 121-124.

Walker, P.L., Rusinko, F., Austin, L.G., 1959. Gas reactions of carbon. Advan. Catal. 11, 133-221.

Walker, P.L., 1996. Production of activated carbons: Use of CO_2 versus H_2O as activating agent. Carbon 34 (10), 1297-1299.

Weiss, R.F., 1970. The solubility of nitrogen, oxygen, and argon in water and seawater. Deep Sea Research 17, 721-735.

Wiegand, W.B., 1937. pH properties of colloidal carbon. Ind. Eng. Chem. 29, 953.

Wigmans, T., 1989. Industrial-aspects of production and use of activated carbons. Carbon 27 (1), 13-22.

Zhang, Y.Z., Lu, Z., Maroto-Valer, M.M., Andresen, J.M., Schobert, H.H., 2003. Comparison of high-unburned-carbon fly ashes from different combustor types and their steam activated products. Energy & Fuels 17 (2), 369-377.

Zou, Y., Han, B.X., 2001. High-surface area activated carbon from Chinese coal. Energy & Fuels 15, 1383-1386.

BIOGRAPHICAL SKETCH

Morgana Bach was born in St. Petersburg, Florida, where she was raised by her mother. She graduated from Gibbs High School in June 1998. From there, she traveled to Gainesville, Florida, to attend the University of Florida where I received she received her bachelor of science degree with highest honors and her Master of Engineering in Environmental Engineering Sciences.

She stayed on at the University of Florida to work on her doctor of philosophy degree with Dr. David W. Mazyck in the field of environmental engineering sciences with a focus on water treatment. She looks forward to working towards the betterment of mankind through research into the technologies which provide clean water and air.